Facies analysis and chemostratigraphy of the Chattanooga Formation in Tennessee and Alabama

by

Chinyere Eunice Eme

B.Tech., Federal University of Technology Owerri, Imo, Nigeria, 2017

A THESIS

submitted in partial fulfillment of the requirements for the degree

MASTER OF SCIENCE

Department of Geology
College of Arts and Sciences

KANSAS STATE UNIVERSITY
Manhattan, Kansas

2023

Approved by:

Major Professor
Karin Goldberg

Copyright

Abstract

The black shales of the Late Devonian to Early Mississippian are known for their rich organic concentrations, serving as source rock and housing unconventional reservoirs. The primary driving mechanism for the high organic matter content of these mudstones is yet to be fully understood. Interpretation of the complex factors controlling deposition of these mudrocks is facilitated by an integration of sedimentologic and chemostratigraphic analysis. Facies analysis, coupled with hand-held X-ray fluorescence (HHXRF), inductively-coupled plasma mass spectrometry (ICP-MS), X-ray diffraction (XRD), tipping point and total organic carbon (TOC) analyses were performed to construct sedimentologic-chemostratigraphic logs that allowed the establishment of a stratigraphic framework, and evaluation of depositional parameters such as detrital input, primary productivity, and degree of oxygenation during the accumulation of the studied succession. The ultimate goal was to identify the controls on sedimentation and main switches in organic matter content of the Chattanooga Formation (Devonian of the Appalachian Basin) in outcrops in Tennessee (TN-1) and Alabama (AL-1). The facies associations indicate that these successions were deposited in deep-marine environments varying from hemipelagic-lower shoreface to pelagic settings. Three sequences were identified in the sedimentary successions at each location (sequences 1 through 3, from base to top). The succession at TN-1 shows an oxic to anoxic environment of deposition with TOC values increasing upward from 3.49-17.80 wt%, while AL-1 shows an anoxic to oxic depositional environment from base to the top of the succession, with decreasing TOC values from 13.3-5.32 wt%. The stratigraphic framework shows incomplete system tracts, which can be attributed to poor preservation of the sedimentary succession resulting from low subsidence rates, typical of epicontinental basins. The only complete sequence, with lowstand, transgressive and highstand

system tracts, is sequence 1 at AL-1. The integration between sedimentological data and chemical indices suggests that high organic content (TOC>10%) is found in settings where high primary productivity coincides with bottom-water anoxia.

KEYWORDS: Sedimentology, Chemostratigraphy, Sequence Stratigraphy, Facies Analysis, Depositional Environment

Table of Contents

List of Figures

List of Tables

Acknowledgements

Dedication

This research is dedicated to the loving memory of my mother, Lolo Nmecha Victoria Eme, who notwithstanding gave me the best. You may not be here, but your legacy lives on.

Chapter 1 - Introduction

Facies analysis, the study of textures, sedimentary structures, fossil content and lithological associations in a sedimentary succession (Miall, 2022), is useful to interpret depositional processes and environments. Chemostratigraphy, the study of chemical variations to determine stratigraphic relationships, may be used to identify the depositional mechanisms controlling sedimentation and the chemical composition. Most of the sedimentary record contains mudrocks, dominated by grains smaller than 62.5 µm; these rocks serve as sources, unconventional reservoirs, and seals of hydrocarbons; they influence the flow of groundwater; and they can be rich in metals (e.g., Picard, 1971; Wedepohl, 1971; Stow, 1981; Blatt, 1982; Lazar et al., 2015). As a result, there has been high interest in the oil and gas industry to understand their deposition. The Chattanooga Formation in Tennessee and Alabama is a unit that houses unconventional hydrocarbon reservoirs; this epicontinental black shale was deposited across the Midcontinent Basin (from the Williston to the Black Warrior Basins), bearing different names at different locations. For instance, it is equivalent to the Woodford Shale in Oklahoma and the Barnett Shale in Texas. Outcrops of this unit can be found in the southern section of the Appalachian Basin in Alabama, Georgia, Mississippi, Tennessee, Kentucky, and Virginia (de Witt, 1981; Over, 2007).

This research aimed at integrating sedimentologic and chemostratigraphic analysis to identify the controls on sedimentation and main switches in organic matter content of the Chattanooga Formation in representative outcrops in Alabama and Tennessee (Fig. 1.1). Our primary objectives were as follows: (1) to employ sedimentological and geochemical analyses to study the Chattanooga Formation in Alabama and Tennessee, (2) to define the stratigraphic framework and evaluate depositional environments for the sedimentary succession, (3) to

1

understand the controls on sedimentation and their influence in the heterogeneity of mudrocks, (4) to identify the main switches in organic matter content.

The two outcrops where this study was carried out were AL-1, comprising a 38-foot succession located behind the United Grocery Outlet in Fort Payne, Alabama (latitude 34° 25' 59" N and longitude -85° 44' 8" W), and TN-1, a 23-foot succession along Enigma Road, Chestnut Mound, Tennessee (latitude 36° 12' 28" N and longitude 85° 48' 53" W) (Fig. 1.1). These outcrops were logged, and a detailed mm-cm facies description was made. A total of 157 samples were collected from both locations at an interval of 4 inches (10 cm) along each outcrop section for chemical analysis.
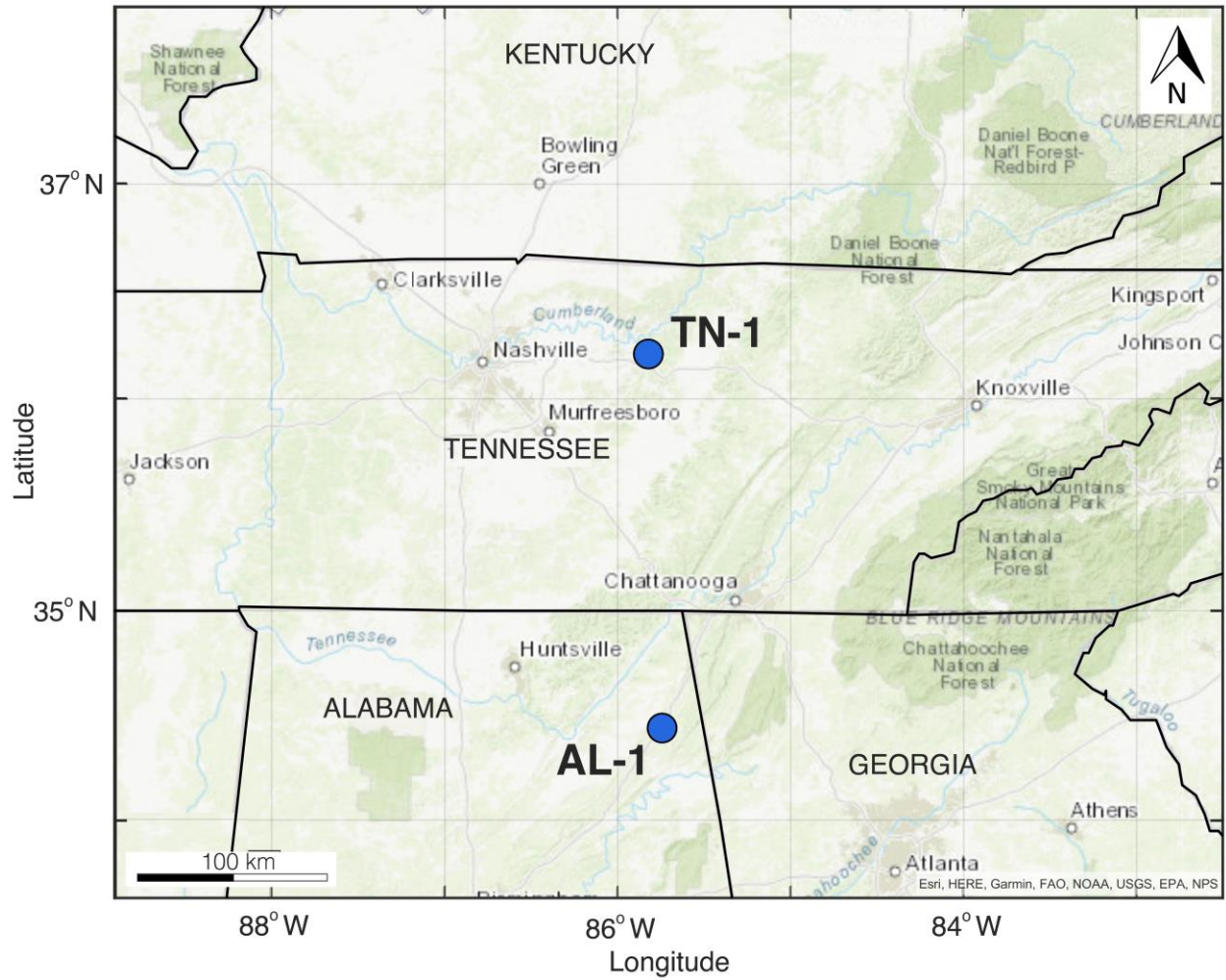
Figure 1.1 Location of the studied outcrops in Tennessee (TN-1) and Alabama (AL-1). Black lines are state boundaries. Image from Google Earth.

Chapter 2 - Geological Setting

The Appalachian Basin is a foreland basin formed as a result of four orogenic events occurring from Ordovician to Silurian, Early to Late Devonian, Late Devonian to Early Mississippian and Late Mississippian to Pennsylvanian periods (Taconic, Potomac, Acadian and Antler Orogenies, respectively). These events resulted from the collision of the passive Appalachian region in the North American continental plate with the Iapetus oceanic plate, suddenly becoming active during the Taconic orogeny in the early Paleozoic. This gave rise to a subduction zone that started receiving shallow marine sediments. During the Middle to Late Devonian, the sedimentation occurred due to folding and thrust faulting during the Acadian orogeny, which resulted in the closing of the Iapetus Ocean (Fig. 2.1). This event gave rise to the Appalachian Basin migrating westward towards Alabama, where the Chattanooga Formation was deposited as part of the westward-thinning Acadian clastic wedge (Woodrow et al., 1988; Lu et al., 2015).

The sedimentary deposits in the Appalachian Basin reflect an interplay between eustatic, climatic and tectonic processes that controlled the development of the major petroleum system, Devonian in age (Ryder, 2001). The Appalachian system is sourced from the Devonian shales deposited in foreland and intrashelfal basins. The Devonian Chattanooga Formation (Frasnian to Famennian age) crops out in the southern part of the Appalachian Basin in northeastern Alabama, Georgia, Mississippi, eastern Tennessee, Kentucky, and Virginia (de Witt, 1981; Over, 2007) (Fig. 2.1).

This unit is part of a thin, epicontinental black shale sequence of Late Devonian age deposited over large portions of the North American craton (de Witt et al., 1993; Schieber, 1998; Li et al., 2015). It is analogous to the New Albany Shale in Illinois, the Ohio Shale in central and

northern Appalachia, and the Woodford Shale in the southern Midcontinent Basin. It has

thickness variations, with Oklahoma (OK) and Kansas (KS) having the thickest parts, whereas

Kentucky (KY) and Tennessee (TN) have sections that are about 10 meters thick, possibly linked

to paleotopographic and paleoceanographic variations (Over, 2007). The petroleum system of the

Appalachian Basin shows that the Chattanooga shales serve as both source rocks and seals for

conventional and basin-center accumulation (Lu, 2015).
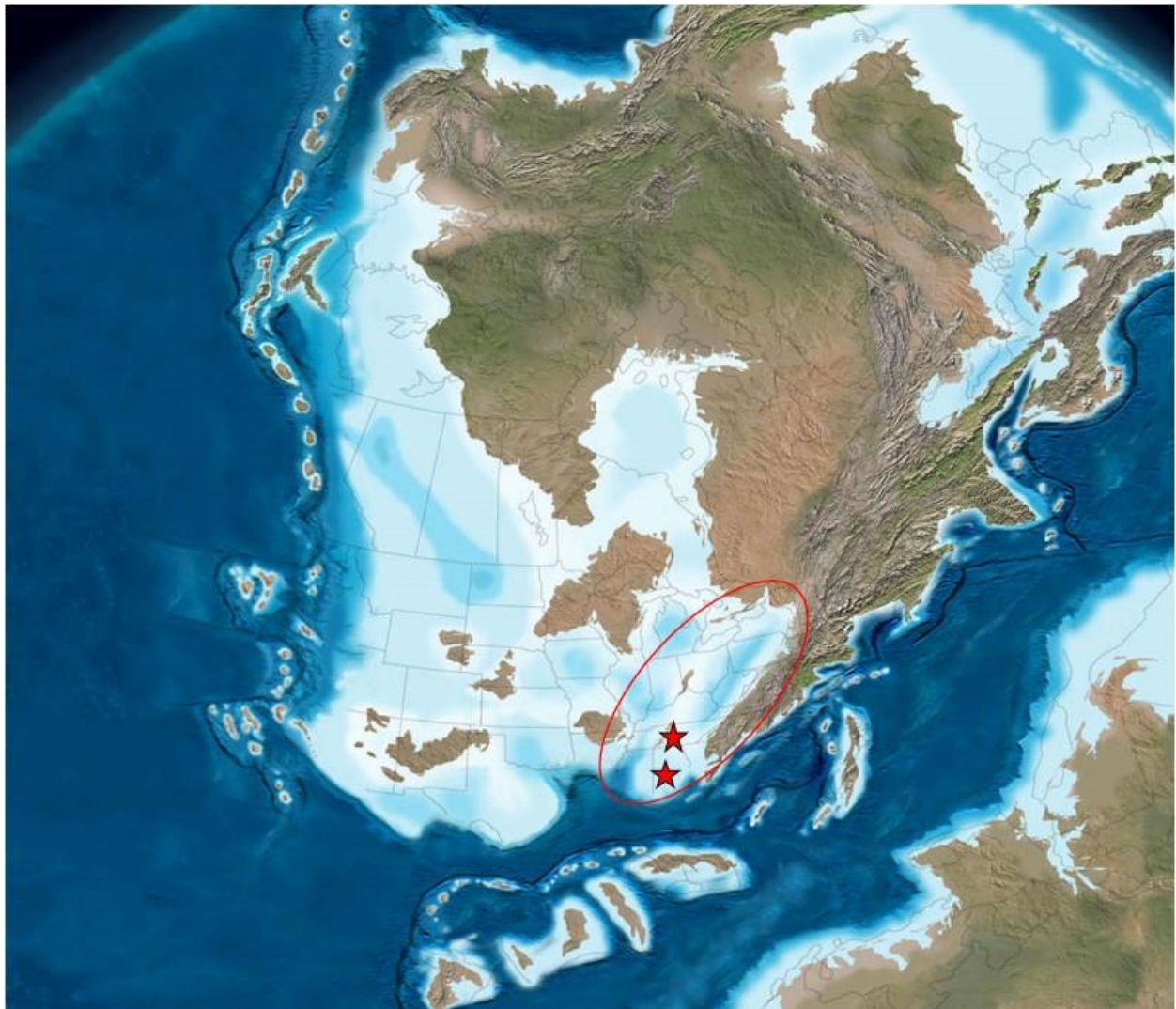
Figure 2.1 Paleogeographic reconstruction of North America during the Late Devonian (350
Ma) overlain by the present-day map of North America. The oval shape indicates the
Appalachian Basin while the red stars indicate the location of the studied outcrops.
Paleogeographic map from Blakey (2013)

The stratigraphy of the Chattanooga Formation in Alabama and Tennessee shows contact with different formations of the Middle Ordovician to Early Mississippian (Figs. 2.2 and 2.3). In Alabama, it is unconformably underlain by the Silurian Red Mountain Formation and overlain by the Maury Shale (Fig. 2.2), while in Tennessee, it is underlain by the Leipiers Formation and overlain by the Maury Formation (Fig. 2.3) (Over, 2007).

In Tennessee and Alabama, the Chattanooga comprises of three units; the lowermost Hardin Sandstone, the Dowelltown Member, and the uppermost Gassaway Member (Conant and Swanson, 1961; Li et al., 2015). The Hardin Sandstone is composed of fine-grained, thick and evenly bedded sandstones with remnants of horizontal lamination and truncated tops overlain by beds of heavily bioturbated sandstones; the Dowelltown Member comprises interbedded black, brown and grey shales with variable degrees of bioturbation and a resistant black shale deposit at the base; the Gassaway Member comprises of dense, bluish, finely laminated black shales with alternating bioturbations, pyrite enriched layers, and an erosional surface which shows a sharp contact with the Dowellton Member at the base due to the presence of a regional, erosional unconformity (Connant and Swanson, 1961; Ettenshon et al., 1989; Scheiber, 1998; 2003; 2009). The lowermost unit only occurs in southwestern Tennessee, while the two members occur in Central Tennessee (Fig. 2.3), with the Dowelltown Member absent in many localities of northern Alabama due to regional erosion (Fig. 2.2) (Robeck and Brown, 1950; Lu, 2015).
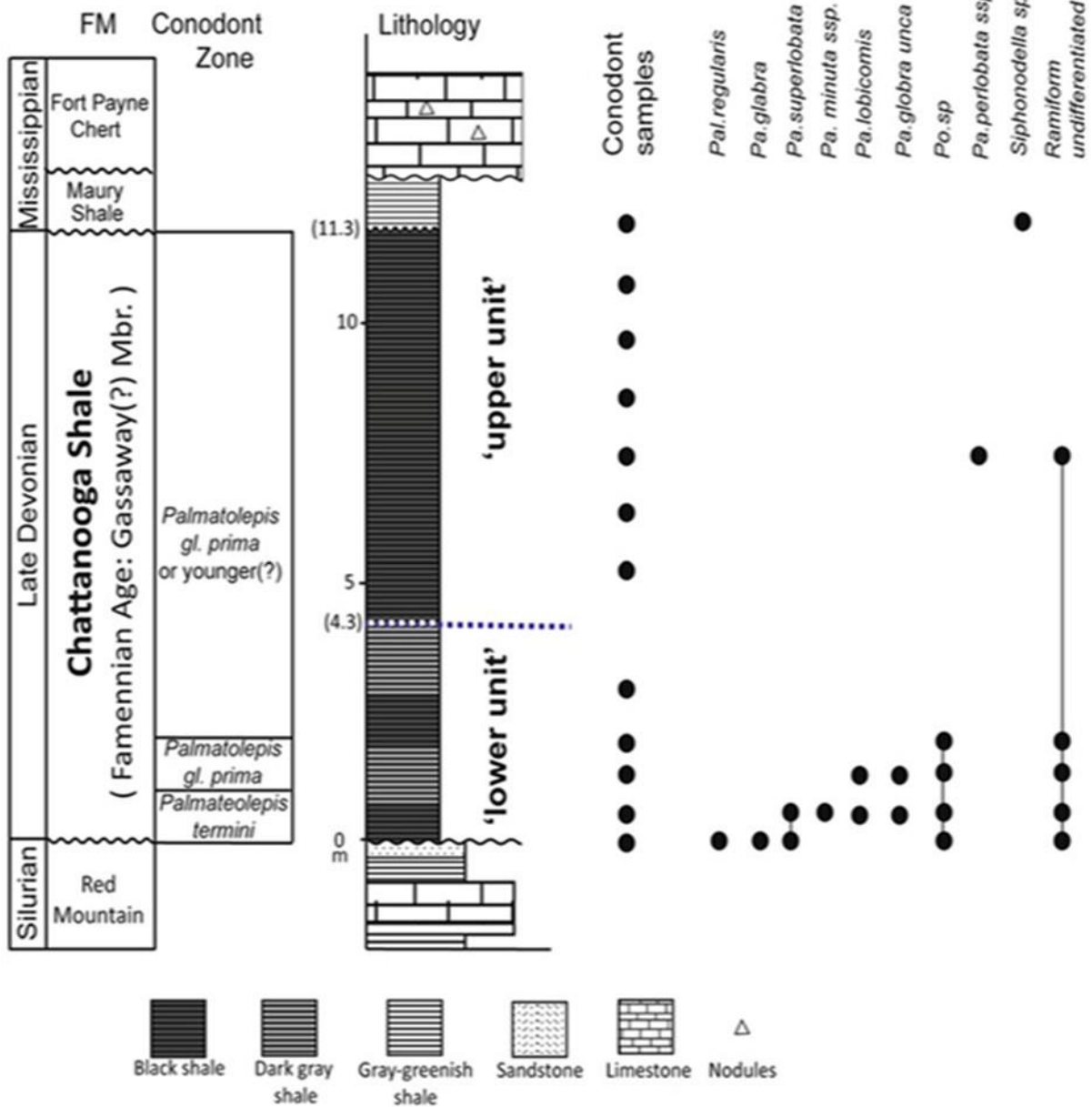
Figure 2.2 Stratigraphic column of the Chattanooga Formation in northeastern Alabama (Schieber; 1998; Hansma et al., 2015; Lu et al., 2019).
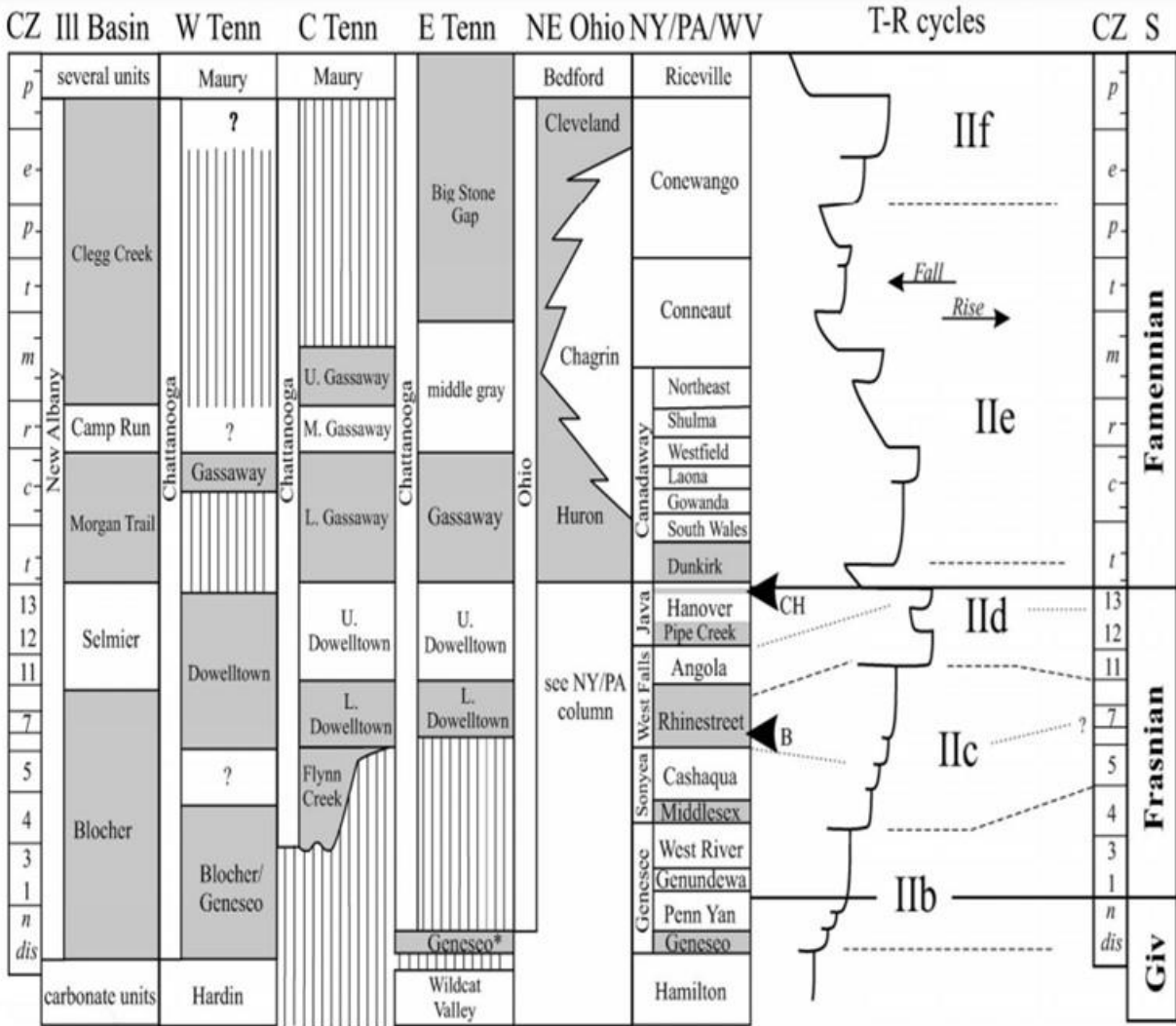
Figure 2.3 Stratigraphic column of the Chattanooga Formation in Western, Central, Eastern Tennessee (Over, 2007).

Paleography and Paleoclimate

The Appalachian Basin dates back about 358.9 to 382.7 million years ago. The present North American plate straddled the equator, forming the Gondwana continent with present day South America, Africa, Australia, Antarctica, India and Asia until the middle Ordovician, when the once quiet Appalachian passive margin changed to a very active plate boundary along which a neighboring oceanic plate, the Iapetus, collided, causing the oceanic plate to sink beneath the North American craton. This gave rise to a new subduction zone, and the Appalachians

orogenies. The succession in this research was formed as a result of the Arcadian orogeny in the Late Devonian and deposited towards the western part of the Appalachian Basin. The Frasnian and Famennian ages of the Late Devonian period marked the end of extinction events. Sea levels were high, and much of the land lay under shallow seas, where tropical reef organisms lived. It represented a warm and drier period, with low temperature gradient from the equator to the poles compared to present day. Reconstruction of tropical seas from conodont data shows that the Late Devonian warmed up to an average value of 30 °C (86 °F) with no corresponding increase in CO_2 concentrations, and continental weathering increased as a result of warmer temperatures (Over et al., 2007, Joachimski et al., 2009).

Chapter 3 - Methodology

To carry out this research, we conducted facies analysis of the studied outcrops, integrated with geochemical analyses. Handheld X-ray fluorescence (HHXRF) was used to measure the concentration of major and trace elements in samples collected every 4 inches (10 cm) along the two sections. LECO analyzer was used to obtain the total organic carbon (TOC %) and inductively coupled plasma mass spectrometry (ICP-MS) to measure the U, Mo and Zr concentration in 20 samples (10 from TN-1 and 10 from AL-1). X-ray diffraction (XRD) was performed in six samples (4 from TN-1 and 2 from AL-1) to determine the clay mineralogy and presence of bentonite. Tipping point analysis helped with defining the stratigraphic framework and identifying the major shift in the environment of deposition.

Facies Analysis

A template from Lazar et al. (2015) (Fig. 3.1) was used for a detailed sedimentological description of the outcrops, including textural and compositional features, sedimentary structures, degree of bioturbation, fossil content and diagenetic features. Samples were collected every four inches (10 cm) along the outcrop section in both locations. The outcrop AL-1 in Alabama totalized one hundred (100) samples collected along an outcrop section about thirty-seven feet (37 ft) thick; in Tennessee at TN-1 a total of fifty-seven (57) samples were collected along a section about twenty-two feet (22 ft) thick. These outcrops were chosen due to their display of the entire section of the Chattanooga Formation and easy access.

The facies description was carried out on a mm-cm scale, and a sedimentary log was constructed bed by bed according to Miall (2022), with grain size on the x-axis and bed thickness on the y-axis, complemented with the location of collected samples, facies codes, and facies associations (Bohacs, 1990; Lazar et al., 2010; Bohacs, 2014). The facies identified were

organized in a facies table that includes facies code, description, interpretation, and a representative photo. These facies were then grouped into facies associations, a group of facies genetically related to each other, and which represent environments of deposition within a depositional system (Collinson, 1996; James and Dalrymple, 2010).

Figure 3.1 Template from Lazar et al., (2015) used for construction of the sedimentary log

12

Handheld X-ray fluorescence (HHXRF) and Chemostratigraphy

X-ray fluorescence is an elemental analysis that quantifies the concentration of different elements in a sample, and it aids in the chemostratigraphic analysis of mudrock successions because it is capable of highlighting shifts with greater precision than is possible through visual facies analysis (Turner et al., 2015; Turner et al., 2016). This technique can detect heterogeneity inside mudrocks that seem homogeneous (Turner et al., 2016). A Bruker Trace III Hand-Held X-Ray Fluorescence (HHXRF) instrument was used to measure the major (Al, Ti, Si, Fe, P) and trace (Ba, Cu, Ni, U, Mo, Zr) elemental concentrations in 57 samples collected from TN-1 and 100 samples from AL-1 outcrops in Tennessee and Alabama, respectively.

For the HHXRF analysis, a sample fragment was prepared by polishing one side with sandpaper grit (which ranged from 120 to 320 depending on how weathered the sample was); to create a smooth surface perpendicular to the lamination. These samples were thoroughly washed under running water to avoid cross contamination and air-dried on a clean surface before further processing. The dried, polished samples were analyzed using the method described by Rowe et al. (2012). The machine was set to run under vacuum with no filter for 180 seconds per sample at voltage of 15kV at 25µA for the major element analysis, while for the trace element analysis, a yellow filter with no vacuum was used to run each sample for 120 seconds using a voltage of 40kV at 12.5µA. A Woodford Standard (RTC-W-220) was analyzed after every five measurements to check for the possibility of drift from the machine. Each sample was measured five times; the elemental concentration for each sample was the average of the five runs. The results from the standard and the sample runs are attached in Appendix A. To assure that the elemental concentrations were accurate, the obtained value (average of five runs for each sample) for both major and trace elements were normalized by comparing with the Woodford

standard (RTC-W-220) accepted values from Rowe et al. (2012). The normalization factor for each element was obtained by dividing the average elemental concentration from the standard runs by the accepted value of each element measured by Rowe et al. (2012). The normalization factor was then multiplied by the results gotten from the sample analysis for both major and trace elements (see Appendix A). To check the precision of the measurements, the standard deviation for the standard runs for each element and the standard error were calculated; the latter by dividing the standard deviation by the number of standard runs.

These corresponding results from the calculations above were used to generate chemostratigraphic logs that allowed the study of elemental variation along the outcrop sections. The major and trace elemental concentration were normalized to aluminum to account for variations in sedimentation rates and continental input (Tribovillard et al., 2006), and then used to calculate chemical indices to serve as proxies for local depositional and environmental conditions during sedimentation (Pearce & Jarvis, 1992; Pearce et al., 1999; Tribovillard et al., 2006; Nance & Rowe, 2015; Turner et al., 2015, Turner et al., 2016). For this study, Ti, Zr and Si were used as proxies for detrital input (Bhatia and Crook, 1986; Pearce and Jarvis, 1992; Pearce et al., 1999; Sageman and Lyons, 2003); Ba, Ni, Cu and P were used as proxies for primary productivity (Tribovillard et al., 2006); U, Mo and Fe were used as proxies for degree of oxygenation (Lyons and Severmann, 2006; Morford et al., 2005; Tribovillard et al. 2006; Arnaboldi and Meyers, 2007; Algeo and Maynard, 2008). Variations in these parameters were also evaluated through the calculation of the enrichment factors of certain elements, which measure the richness of those in the samples compared to an average shale. The enrichment factors (EF): $EF_{element\ X} = X/Al_{sample}/\ X/Al_{average\ shale}$ were calculated for Cu and Ni to evaluate primary productivity and U and Mo to evaluate redox conditions. If EF_X is greater than

1, then element X is enriched relative to average shales and, if EFX is less than 1, it is depleted (Tribovillard et al., 2006).

Total Organic Carbon (TOC) Content

Ten samples from each studied location were analyzed by LECO C/S analyzer to measure the TOC content. In this method, the LECO carbon analyzer measures the TOC by combusting the organic carbon and measuring the resulting carbon dioxide produced. The samples were analyzed at GeoMark Research.

Inductively Coupled Plasma Mass Spectrometry (ICP-MS)

A total of twenty (20) samples, ten per outcrop section were selected and analyzed using the inductively coupled plasma mass spectrometry (ICP-MS) to measure U and Mo concentration, since these elements cannot accurately be measured using HHXRF, and other traces elements (Ni, Cu) to check the accuracy of HHXRF. The analysis was carried out at the Peter Hooper GeoAnalytical Lab (Washington State University). The result of the analysis is attached in Appendix B.

X-ray Diffraction (XRD)

The PANalytical Empyrean multipurpose series 2 X-ray diffractometer equipped with pre-aligned PreFIX modules was used to perform bulk and clay fraction analysis on six samples from the study locations. Six samples (4 from TN-1 and 2 from AL-1) were selected for clay mineralogy and presence of bentonite. Out of the six samples, one sample was chosen from each member of the Chattanooga formation at TN-1 and AL-1 (making a total of four samples from the two locations). The remaining two samples collected from TN-1 were analyzed to determine the presence of bentonite. This analysis was carried out at the Department of Geology, Kansas State University X-ray Laboratory. The purpose of the XRD analysis was to identify mineral

phases that could not be identified through optical microscopy (e.g., clay minerals) and determine the mineralogical/chemical composition of mudrocks.

For the bulk analysis, the samples were washed and filed to remove weathered section before being powered in a clean mortar. This mortar was cleaned with alcohol between each sample to avoid cross contamination of the samples. The powdered samples were then pressed into a cylindrical container of about 27 mm and examined in the diffractometer between two theta values of 5 and 70 degrees. The results were interpreted using the Profex software package using the Speakman (2012) procedure.

For the clay fraction analysis, a modified procedure by Kübler and Jaboyedoff (2000) was used to process the samples. The detailed procedure for this analysis is attached in Appendix C. The samples were measured in the diffractometer using the 2-16 µm and less than 2 µm. The clay fraction data were analyzed using the MacDiff 4.2.5 software because of its extensive clay mineral database with interpretations aided by Moore and Reynolds (1997).

Tipping Point Analysis

Tipping point analysis was incorporated into the methodology to identify critical transitions in the sedimentary succession of the Chattanooga Formation. This analysis helped in the determination of the threshold at which small changes in environmental conditions triggered significant and rapid changes in the sedimentary system. The research applied the statistical framework developed by Dakos et al. (2015), which is based on the detection of early warning signals (EWS) of critical transitions. The EWS analysis involves calculating statistical indicators such as variance, autocorrelation, and skewness with python, which can indicate the proximity to a tipping point. This approach was applied to the geochemical data to identify potential tipping

points in the sedimentary system, and to test whether these correspond to key stratigraphic surfaces. The geochemical indices were plotted as a function of the height of the entire section.

Data Integration

Integration of the results was done by displaying the sedimentological log (with facies and facies associations) and chemostratigraphic logs (with the various indices) side by side in a single figure for each study location. The integrative view aided on establishing the stratigraphic framework, with identification of different sequences based on the facies associations and behavior of chemical indices, and in the interpretation of observed changes along the stratigraphic succession, providing a better understanding of the succession in terms of physical-chemical conditions of the water body, stratigraphic evolution, and controlling mechanisms for the accumulation of organic-rich rocks.

Chapter 4 - Results

The results of the analyses carried out in the study locations are presented below. The implications of these results will be discussed in Chapter 5.

Facies Analysis

In the two outcrop sections studied (Fig. 4.1 and 4.2), five lithofacies were identified based on field description, augmented by identification of their composition under the microscope. The observed facies are listed in a facies table that includes a facies code, facies description and interpretation, and a representative photo displaying the main facies characteristics (Table 1).

The shales (Bsh, Gsh and Sb) and chert were formed by fall-out of detrital mud, organic matter and siliceous biogenic material under low energy, with varying degrees of primary productivity (Loucks and Ruppel, 2007; Stow and Smillie, 2020). Vertical sediment fall-out was episodically interrupted by horizontal oscillatory flow (Sb) (Stow and Smillie, 2020) and biological reworking (Gsh). The sandstone facies (Sst) are interpreted as resulting from influx of fine-grained sediments by density and/or bottom currents. The proportion of facies in the two studied sections (TN-1 and AL-1) is displayed in figure 4.3. The dominant facies are Sb and Bsh, with Chert occurring only at AL-1, and Sst at TN-1.

Figure 4.1 Studied section of the TN-1 outcrop on Enigma Road, Chestnut Mound, Tennessee. The lowermost two feet of the section was exposed only along a ditch, requiring the construction of a composite section. The person for scale is about 6' 3" tall.

Figure 4.2 Studied section of the AL-1 outcrop, located behind United Grocery Store in Fort Payne, Alabama.

Table 1 Description and interpretation of the facies identified in the studied outcrops in Tennessee and Alabama.

Facies Code	Description	Interpretation	Representative Outcrop
Bsh (Black Shale)	Fine to medium grained black	Sediment fall-out under low energy, with	

	shale, very organic rich, with very fine (<1 mm thick), "papery" fissility; may be massive, bioturbated or deformed by folds, with scattered pyrite crystals and nodules and sparse vertical fractures.	accumulation of organic matter and biological reworking	
Gsh (Grey Shale)	Fine to medium grained greenish grey to dark brown mudstone	Sediment fall-out under low energy, with biological reworking	

	bioturbated; may contain massive or laminated.		
Chert	Coarse grained, black chert, with closely spaced vertical fractures; may be massive or laminated	Accumulation of siliceous biogenic material (radiolarians) and organic matter	
Sb (Siliceous Black Shale)	Fine to coarse grained black shale (with fissility) and abundant siliceous bioclasts; May have (2"-3" thick)	Sediment fall-out under low energy, with weak oscillatory flow	

	hummocky cross stratification or discontinuous lamination. May also be massive with sparse vertical fractures, rare pyrite and/or phosphate nodules.		
Sst (Sandstone)	Very fine to fine, well-sorted yellowish to white sandstone, weathered; may be pyritized	Influx of fine-grained sediments by density and/or bottom currents	
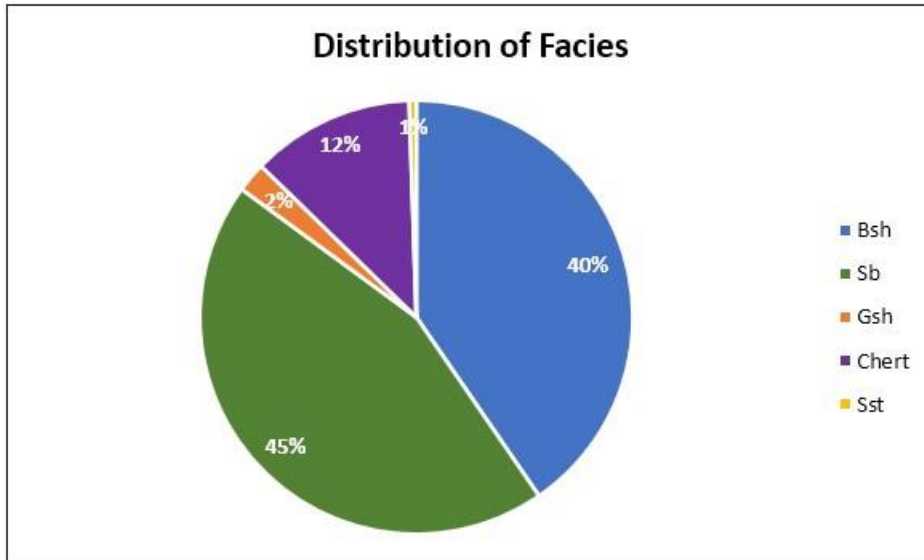
Figure 4.3 Pie chart showing the distribution of facies in the studied locations (TN-1 and AL-1)

The facies identified in the studied sections (TN-1 and AL-1) were grouped into two facies associations (F.A.), which represent a group of genetically related facies. They were assigned based on vertical facies successions that show a progressive change in one or more parameters, such as grain size, bed thickness, sedimentary structures, faunal composition, and/or facies abundance. The facies associations (F.A.) identified in the study area are Pelagic and Hemipelagic-Lower Shoreface, both of which represent deposition in a relatively deep marine environment. The Pelagic F.A., composed of dominantly facies Bsh and Chert, subordinately Gsh and Sb, represents deposition in a distal, deep marine setting below the storm wave base, characterized by sediment fall-out under low energy and high primary productivity, with abundant accumulation of organic matter and siliceous biogenic material, and infrequent biological reworking. The Hemipelagic-Lower Shoreface F.A, comprised of dominantly facies Sb, Gsh and Sst (subordinately Bsh and Chert), represents deposition in the transition from a lower shoreface in a wave-dominated shelf to a deep marine environment, characterized by vertical sediment fall-out with occasional reworking by oscillatory flow and distal

24

density/bottom currents (Stow and Smillie, 2020). Except for Sst, which occurs only in the Hemipelagic-Lower shoreface F.A., the other facies are interbedded in both facies associations, but in different proportions.

The proportion of the facies found at TN-1 is displayed in figure 4.4. The succession in this outcrop comprises mostly of facies Sb, and it is the only location where facies Sst occurs. The base of the succession (up to about 7 ft high) at TN-1 was deposited in a hemipelagic-lower shoreface setting (Fig. 4.5), above which occurred an alternation between pelagic and hemipelagic-lower shoreface settings (up to about 11 ft high). The top half of the succession is dominated by pelagic deposits (up to about 20 ft), overlain by hemipelagic-lower shoreface deposits in the topmost 3 ft.
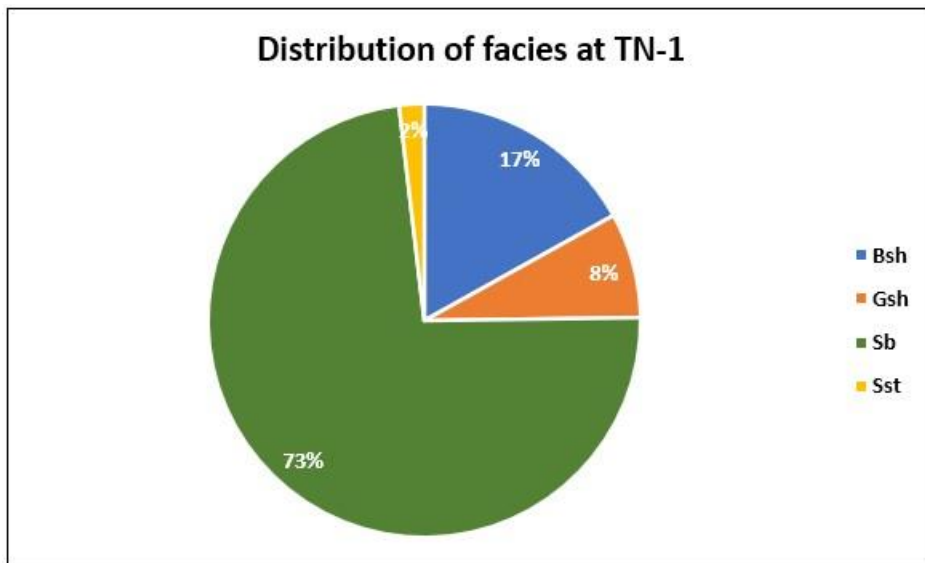
Figure 4.4 Pie chart showing the distribution of facies found at TN-1.
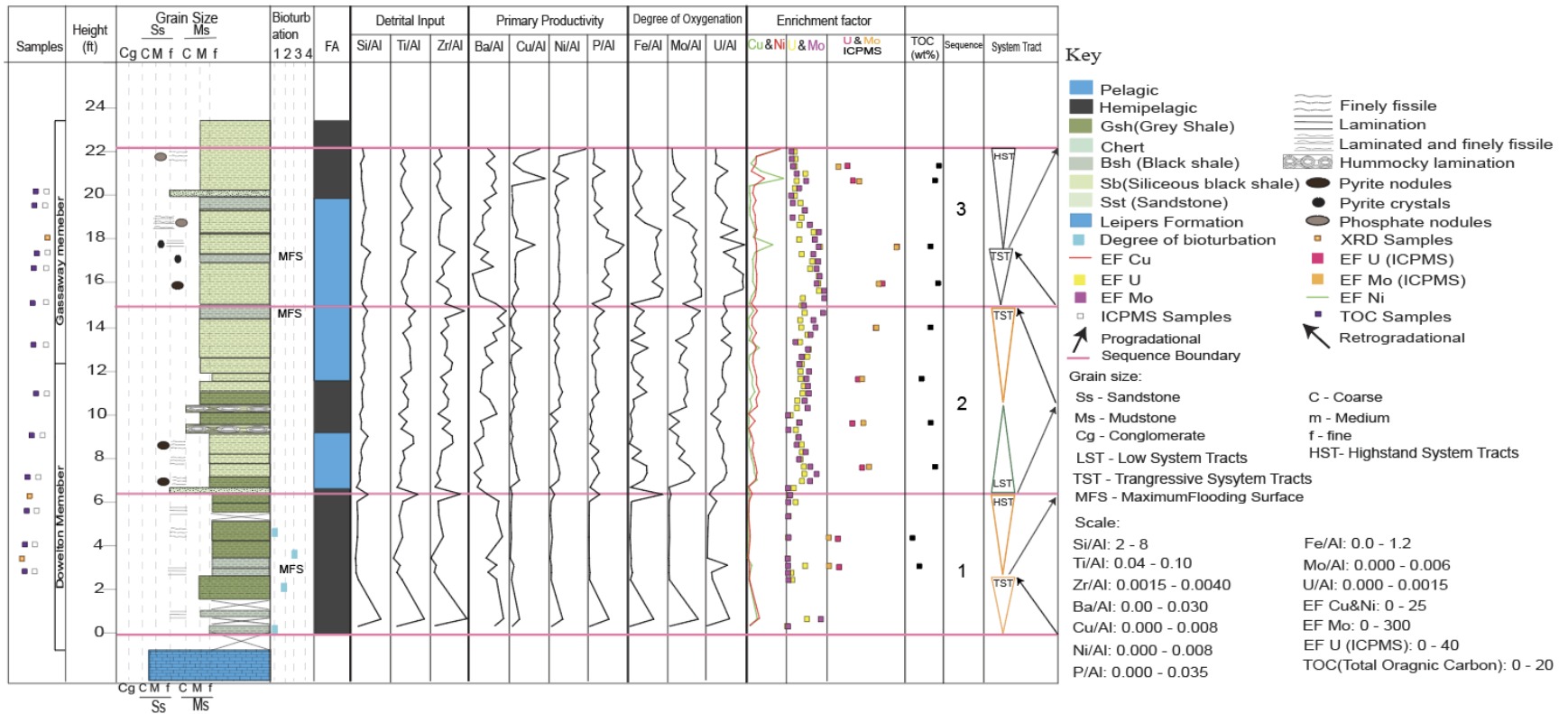
Figure 4.5 Integration between facies analysis and chemostratigraphy of outcrop section at TN-1, showing the stratigraphic framework and system tracts (Van Wagoner et al., 1988; Catuneanu et al., 2011).

At AL-1 the proportion of the facies is very different (Fig. 4.6), with dominance of Bsh and the occurrence of Chert (the latter absent from TN-1). The succession in this outcrop comprises mostly of facies Sb, and it is the only location where facies Sst occurs. At AL-1, the bottom 16 ft of the succession accumulated in a pelagic setting (Fig. 4.7). Above it, about 4 ft were deposited in a hemipelagic-lower shoreface setting, before returning to pelagic conditions (up to 28 high). The topmost 9 ft at AL-1 were deposited in hemipelagic-lower shoreface settings.

The different proportion of facies in the two locations, where the succession at AL-1 is dominated by pelagic deposits, suggests that AL-1 was deposited in overall deeper waters, hence representing a more distal position in comparison with TN-1.
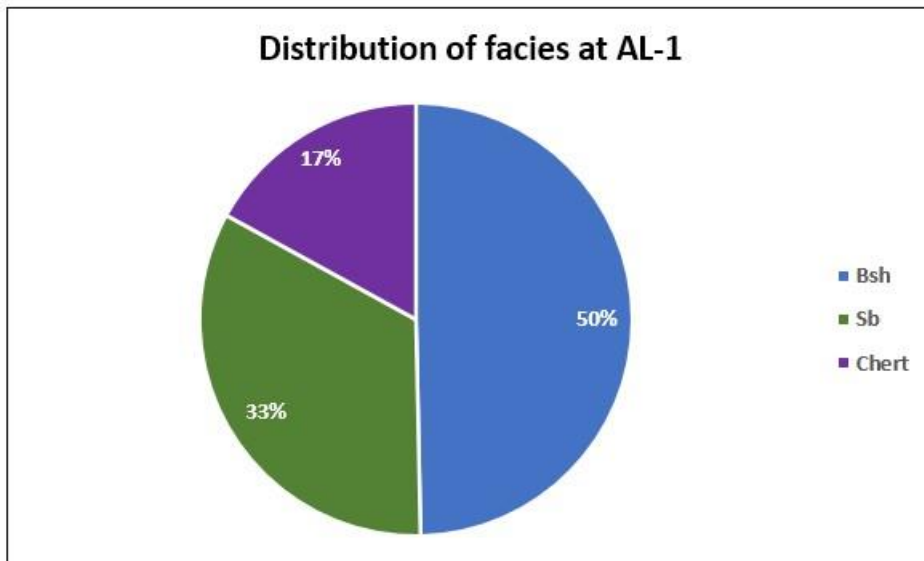
Figure 4.6 Pie chart showing the distribution of facies found at AL-1.
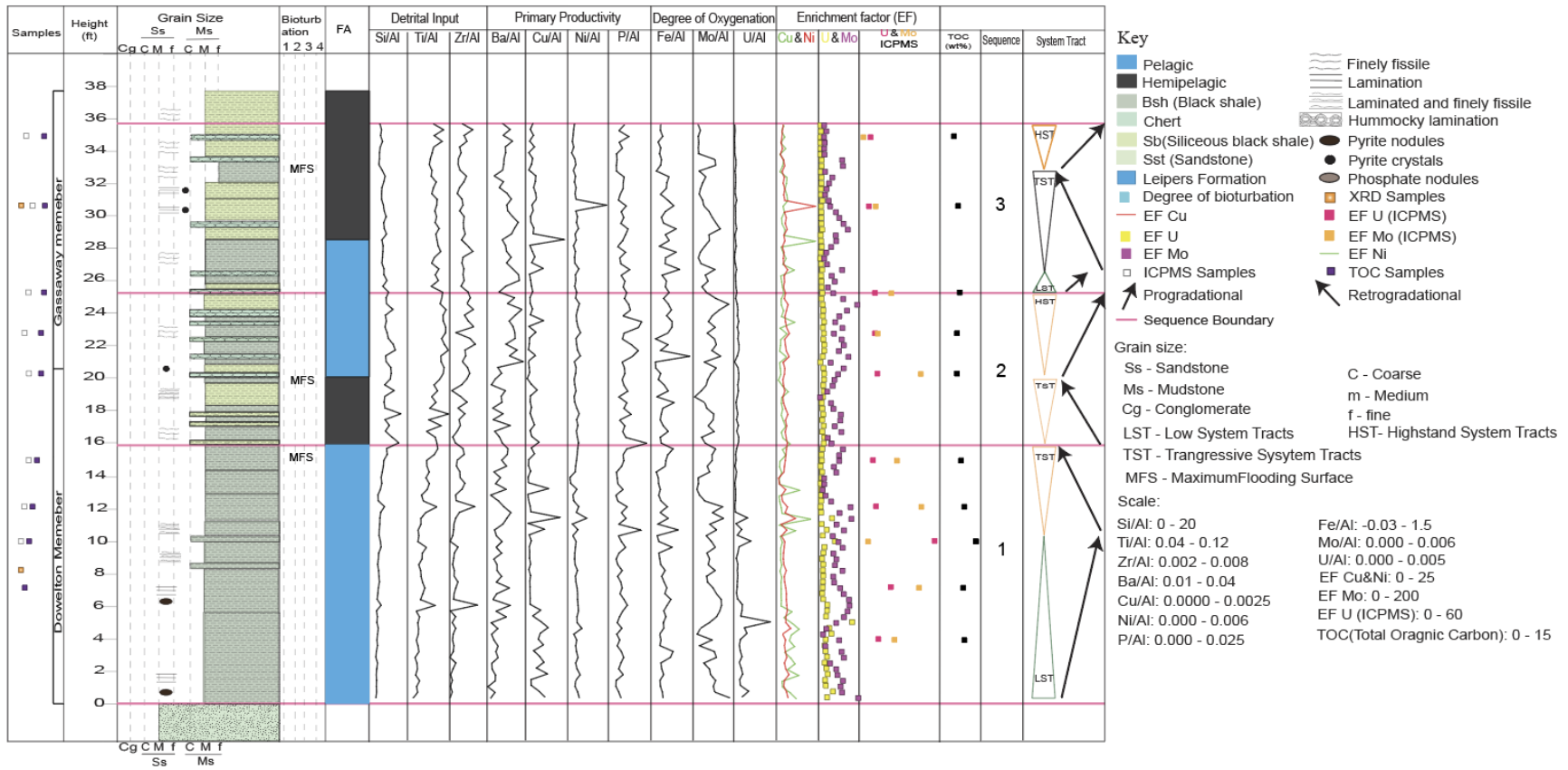
Figure 4.7 Integration between facies analysis and chemostratigraphy of outcrop section at AL-1, showing the stratigraphic framework and system tracts (Van Wagoner et al., 1988; Catuneanu et al., 2011).

Chemostratigraphic Analysis

The chemostratigraphic logs for TN-1 and AL-1 are displayed in Figures 4.5 and 4.7, respectively. The calculated indices are proxies for detrital input (Si/Al, Ti/Al and Zr/Al), primary productivity (Ba/Al, Cu/Al, Ni/Al and P/Al) and degree of oxygenation (Fe/Al, Mo/Al and U/Al). Enrichment factors for Cu, Ni U and Mo are also displayed, along with total organic carbon (TOC, in wt%). These logs, along with the sedimentologic log, were used to interpret changes in the depositional conditions and define a stratigraphic framework for the studied areas. The last two tracks in each figure display the stratigraphic framework, described below along with the chemostratigraphic logs for each location.

TN-1

Three main sequences were identified along this succession, based on the sedimentologic characteristics and behavior of the chemical indices (Fig. 4.5) Sequence 1, from the base of the succession up to about 7 ft high, is characterized by the Hemipelagic-Lower Shoreface F.A. and overall low and constant values of all chemical indices and enrichment factors. The detrital input proxies Ti/Al and Zr/Al show a slight increase toward the top of Sequence 1. The primary productivity proxies (excluding Ba/Al) and proxies for the degree of oxygenation remained very low. The enrichment factors for Cu, Ni, U and Mo are lower than in Sequence 2.

Sequence 2, from 7 to 15 feet high, is characterized by an alternation of Pelagic and Hemi-Pelagic F.A., and higher, more variable chemical indices and enrichment factors in relation to Sequence 1. The values of proxies for detrital input (except Si/Al) show an increase, remaining high throughout Sequence 2. The values of all chemical indices that serve as proxies for primary productivity are slightly higher and much more variable than in Sequence 1.

29

Chemical indices proxies for the degree of oxygenation and enrichment factors for Cu, Ni, U and Mo remain higher than in Sequence 1 through the entire Sequence 2.

Sequence 3 (between 15 and 23 ft high), is distinguished by a Pelagic F.A. at the base, overlain by a Hemipelagic-Lower shoreface F.A. Generally, the chemical indices in this sequence are the most variable compared to the other sequences. The indices for detrital input are high, except for Si/Al, not substantially higher than in the underlying sequences. Proxies for primary productivity display some peaks, except for P/Al, which drops in the top half of Sequence 3, along with the proxies for degree of oxygenation. Enrichment factors for U and Mo display a progressive decline toward the top.

Chemical indices proxies for detrital input, primary productivity and degree of oxygenation display low and constant values in Sequence 1, and higher and variable in Sequences 2 and 3, with the highest values in Sequence 3. This behavior suggests a stable environment during the deposition of Sequence 1, with low detrital input, low primary productivity and mostly oxic bottom waters. Toward the end of this sequence, an increase in sediment influx is indicated by an increase in all the proxies for detrital input at the boundary with Sequence 2. The higher variation in the values of chemical indices in Sequences 2 and 3 suggests a more dynamic depositional environment, with frequent variations in the detrital input, primary productivity and degree of oxygenation. Primary productivity was the highest in Sequence 3, with a couple of peaks in Cu/Al coinciding with peaks in P/Al, what points to sporadic upwelling-driven nutrient input. Proxies for degree of oxygenation suggest the bottom waters were suboxic to anoxic in Sequence 2, and fully anoxic at the base of Sequence 3, changing to suboxic in the second half of this sequence.

AL-1

Three sequences were identified in this location, based on sedimentologic characteristics and behavior of the chemical indices (Fig. 4.7). Sequence 1, from the base of the succession up to 15.8 ft high, is characterized by Pelagic F. A. and overall low values for chemical indices proxy for detrital input and primary productivity, except for localized peaks (e.g., at a height of ~5 ft and ~12 ft) within the section. Except U/Al, the other proxies for degree of oxygenation are highly variable; some peaks (including U/Al) coincide with peaks in proxies for primary productivity and detrital input. This behavior suggest that Sequence 1 was deposited in an environment with sporadic high influx of sediments that likely triggered high productivity and bottom-water anoxia. Enrichment factors for Cu, Ni, Mo and U are relatively high and variable.

Sequence 2, from 15.8 ft to 25.3 ft high, has the highest, more varied values of chemical indices proxies for detrital input and degree of oxygenation, as well as Hemipelagic-Lower shoreface F.A. at the base and Pelagic F.A. above it. Proxies for detrital input and P/Al are the highest in the entire succession. Compared to Sequence 1 (below) and Sequence 3 (above), the chemical indices proxies for primary productivity display the lowest values. Proxies for the degree of oxygenation are lower and more constant than in Sequence 1, but higher and more variable than in Sequence 3. The enrichment factors displayed less variation in comparison to sequences 1 and 3. The behavior of the chemical indices suggest Sequence 2 was deposited in a dynamic environment with variable conditions, with high detrital input and likely in a setting with upwelling, but these conditions did not seem to result in high productivity. The degree of oxygenation in bottom waters was highly variable, mostly suboxic.

Sequence 3 starts at about 25.3 ft high to the top of the succession. It is characterized by Pelagic F.A. overlain by Hemipelagic-Lower shoreface F.A., and generally lower values and

variability of the chemical proxies for detrital input and degree of oxygenation compared to Sequence 2. Chemical indices proxies for primary productivity are more variable, with isolated peaks in Cu/Al and Ni/Al around 28 and 30 ft high, respectively. P/Al is lower and less variable than in Sequence 2. Enrichment factors for Cu and Ni are more variable, and for Mo and U lower than in Sequence 2. U and Mo concentrations are the lowest in the entire succession. The behavior of these indices suggest that Sequence 3 was deposited in a relatively stable environment, with constant detrital input and overall oxic bottom waters. Primary productivity was variable and apparently not influenced by sediment influx or upwelling.

Even though three sequences were identified in each of the studied outcrops, there is no correspondence between the sequences; meaning, Sequence 1 in TN is not the same as Sequence 1 in AL. The comparison between the two study areas, and the possible implications for the paleogeographic context and stratigraphic framework will be discussed in Chapter 5.

Total Organic Carbon (TOC) Content

Total organic carbon ranged between 5 and 13 wt% at AL-1, and from 4 to 18 wt% at TN-1 (Table 2). The higher TOC were observed in samples within the Bsh facies at AL-1 (Sequence 1) and Sb facies at TN-1 (Sequence 3). At AL-1, TOC decreases upward, from 8-13 wt% in Sequence 1 to 6-7 wt% in Sequence 2, and 5-7 wt% in Sequence 3. Conversely, at TN-1, TOC increases from 4-7 wt% in Sequence 1 to 9-16 wt% in Sequence 2, and 13-17% in Sequence 3.

Table 2 Total organic carbon in twenty samples from the studied sections at TN-1 and AL-1.

Sample ID	TOC (wt%)	Sequence
AL-1-11	9.10	1

AL-1-20	8.66	1
AL-1-28	13.30	1
AL-1-34	9.07	1
AL-1-42	7.85	1
AL-1-57	6.35	2
AL-1-64	6.38	2
AL-1-71	7.19	2
AL-1-86	6.81	3
Al-1-98	5.32	3
TN-1-5	7.41	1
TN-1-7	3.69	1
TN-1-14	15.80	2
TN-1-20	13.40	2
TN-1-26	8.61	2
TN-1-33	13.30	2
TN-1-39	17.40	3
TN-1-44	13.30	3
TN-1-53	15.80	3
TN-1-55	17.80	3

Inductively Coupled Plasma Mass Spectrometry (ICP-MS)Analysis

The results of ICP-MS analysis can be found in Appendix B. Mo, U, and Zr

concentrations obtained in the ICP-MS analysis were compared with results obtained from

HHXRF to test the precision of the HHXRF measurements. The results for the studied sections are displayed in figure 12 a-c for TN-1 and figure 13 a-c for AL-1. The R2 calculated in TN-1 for Mo, U, and Zr are 0.916, 0.59, and 0.49, respectively (Fig. 4.8, 4.9 and 4.10), while the R2 in AL-1 for Mo, U, and Zr are 0.53, 0.87, and 0.73 (Fig. 4.11,4.12 and 4.13).
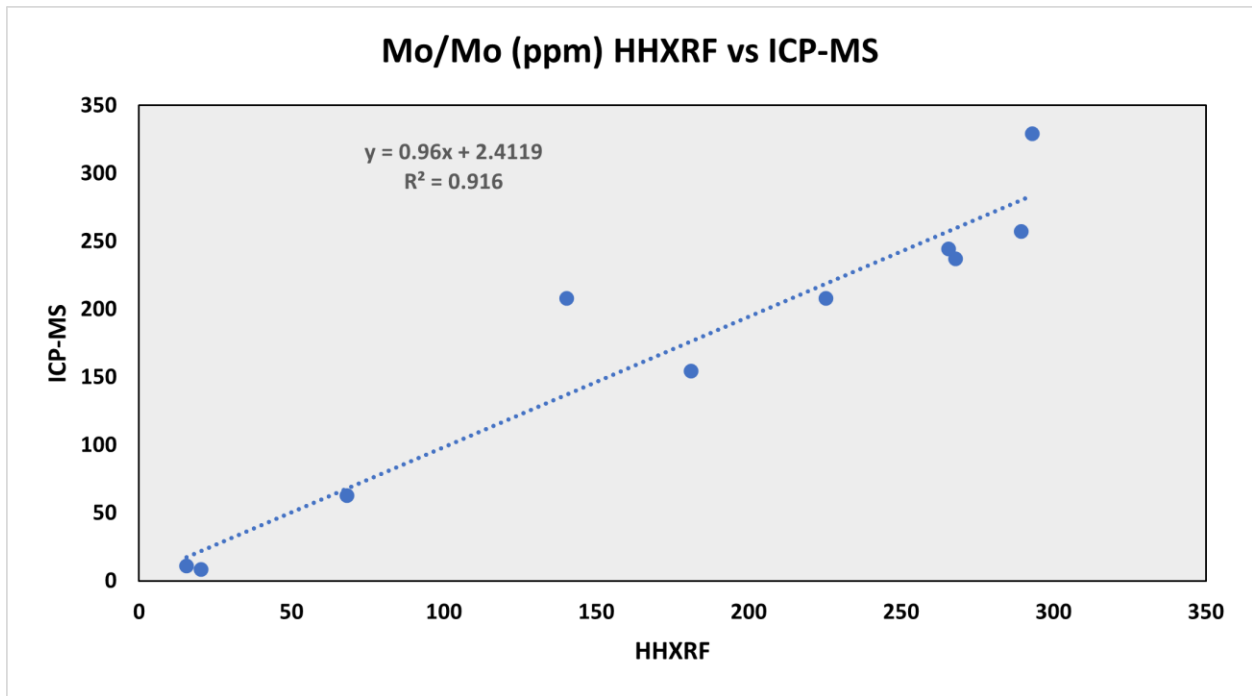
Figure 4.8 Graph of Mo/Mo (ppm) HHXRF vs ICP-MS data from the ten TN-1 samples.
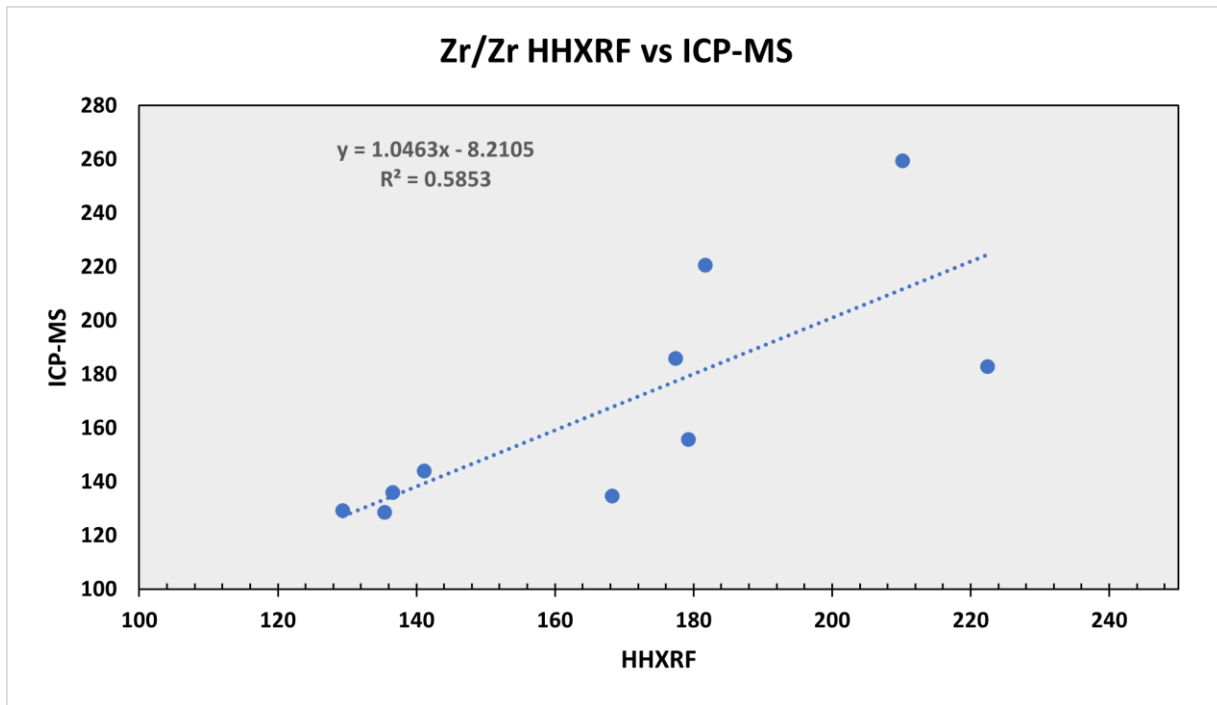
Figure 4.9 Graph of Zr/Zr (ppm) HHXRF vs ICP-MS data from the ten TN-1 samples.
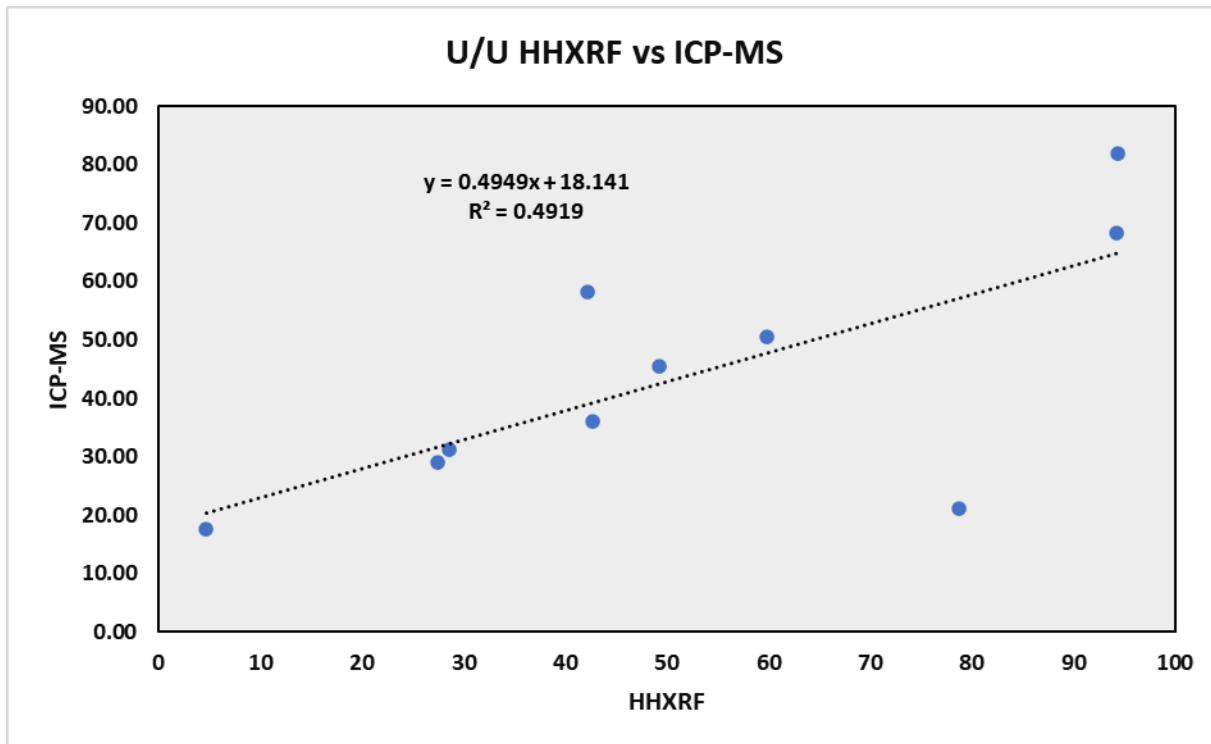
Figure 4.10 Graph of U/U (ppm) HHXRF vs ICP-MS data from the ten TN-1 samples.
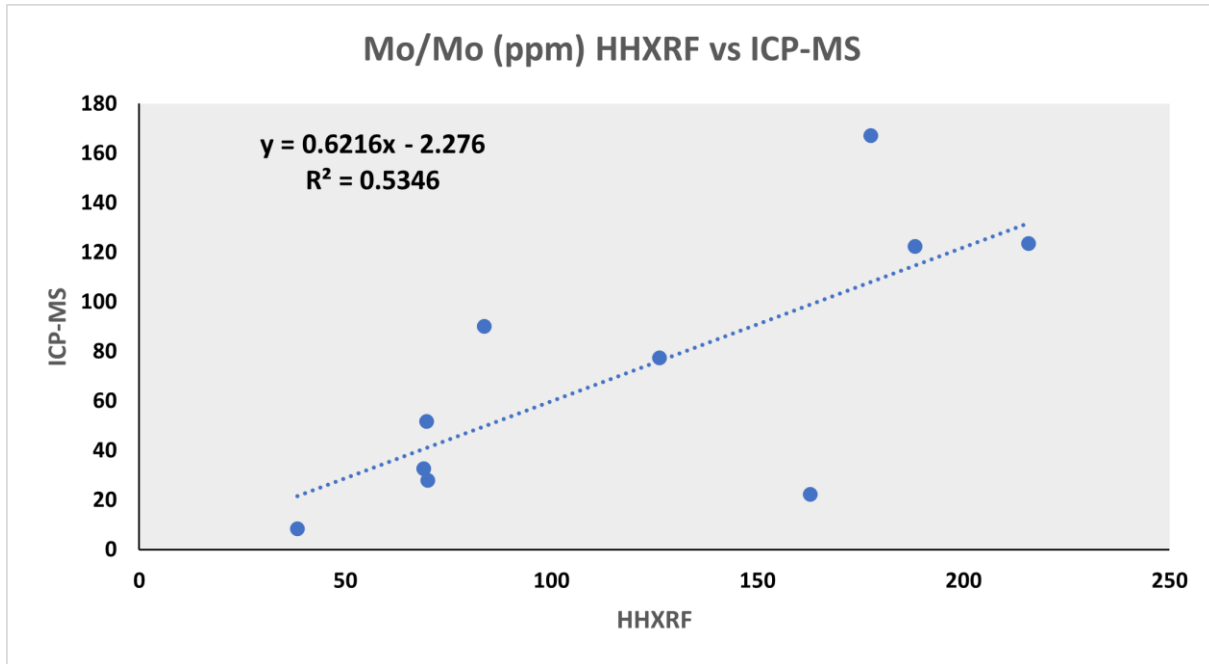
Figure 4.11 Graph of Mo/Mo (ppm) HHXRF vs ICP-MS data from the ten AL-1 samples.
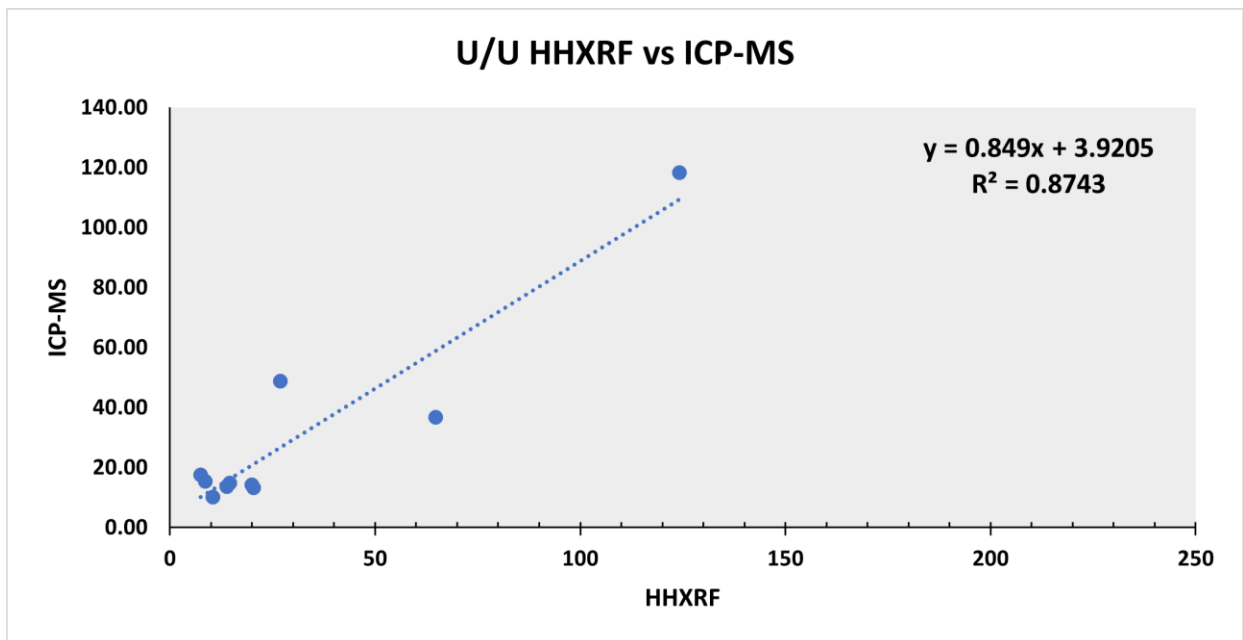
Figure 4.12 Graph of U/U (ppm) HHXRF vs ICP-MS data from the ten AL-1 samples.
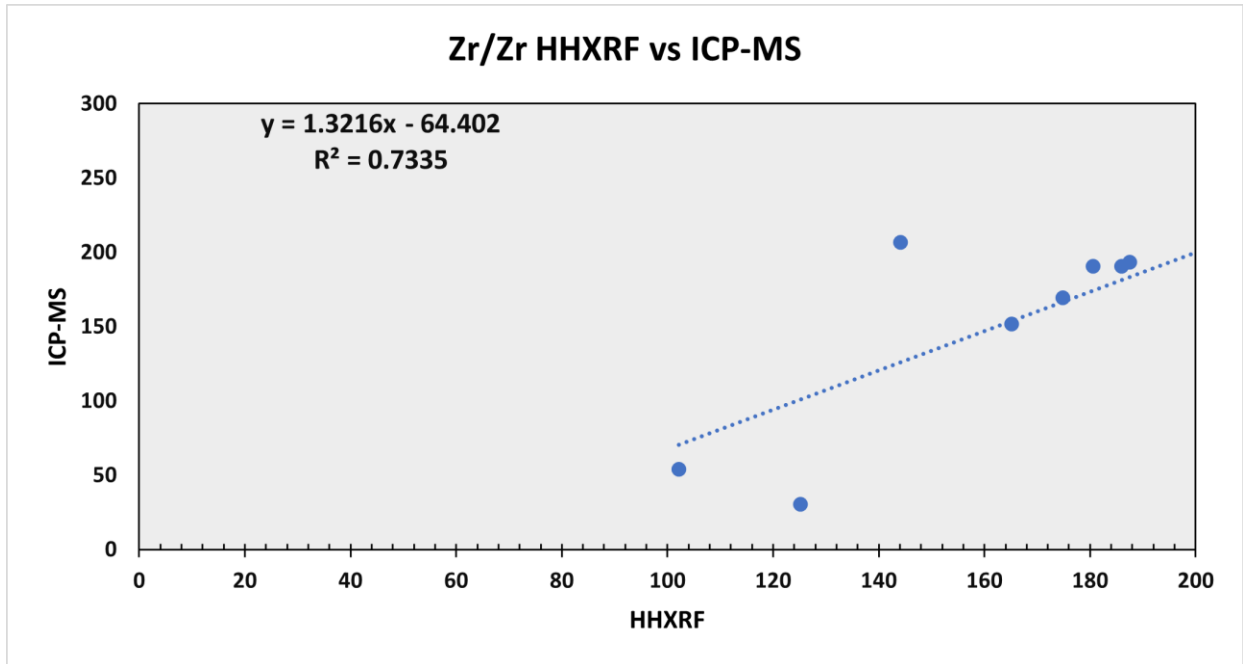
Figure 4.13 Graph of Zr/Zr (ppm) HHXRF vs ICP-MS data from the ten AL-1 samples.

XRD Analysis

The XRD bulk and clay fraction analysis results for samples TN-1-6, TN-1-10, TN-1-16, TN-1-46, AL-1-22, and AL-1-86 can be found in Appendix C. The diffractograms indicate that the samples have similar compositions, exemplified by the diffractogram for TN-1-16 (Fig. 4.14).

In the bulk analyses, the most common mineral is quartz (SiO2). In the clay fraction, illite, muscovite, montmorillonite, illite-montmorillonite, and biotite were identified at both studied locations, with their proportions varying between TN-1 and AL-1, as well as vertically within a single location, as shown in Tables 3-6. AL-1 has more biotite and muscovite (and less illite and illite-montmorillonite) than TN-1. At AL-1, the succession displays an increase in muscovite in relation to biotite at the top.
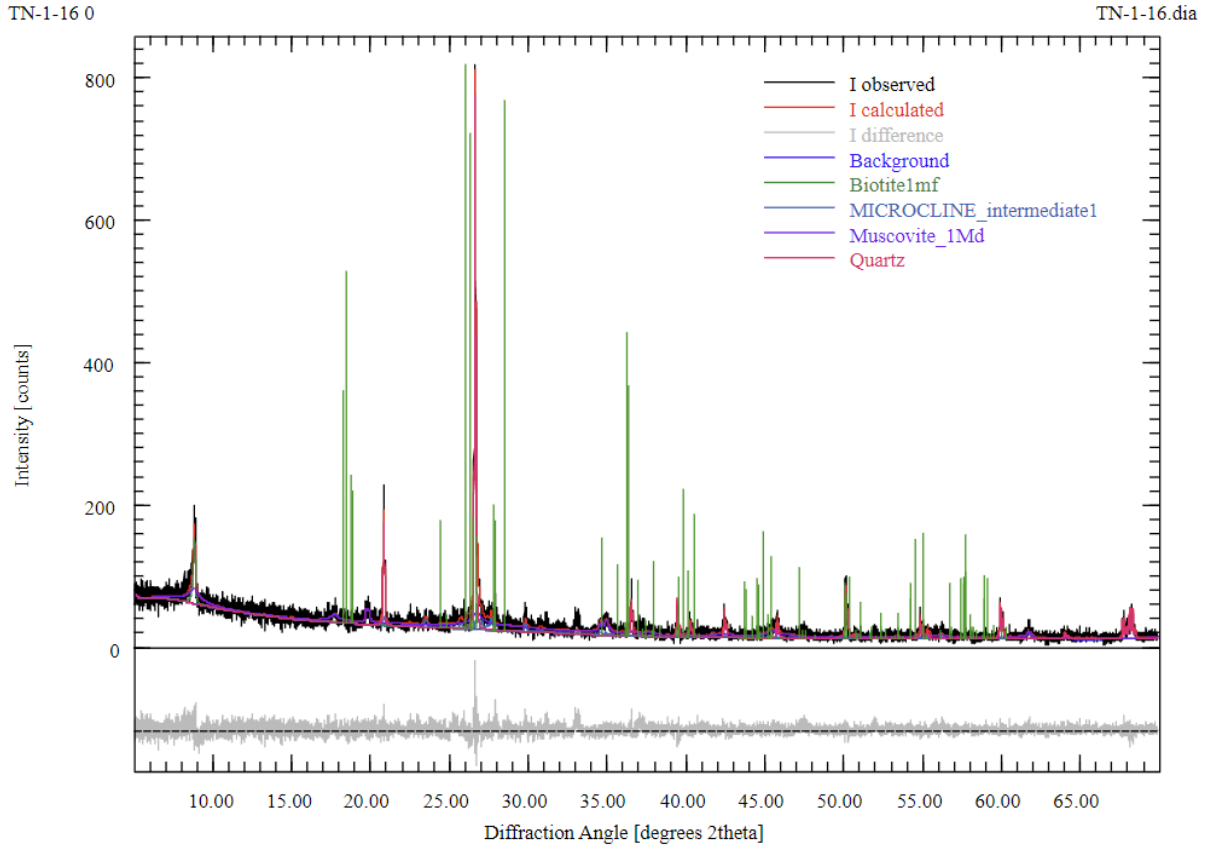
Figure 4.14 Diffractogram (bulk analysis) for sample TN-1-16. Major peaks include biotite, microcline, muscovite, and quartz.

Table 3 Mineralogical composition of the clay fraction (2-16 µm) in samples from TN-1.

Sample ID	Biotite	Muscovite	Montmorillonite	Illite-montmorillonite	Illite
TN-1-6					
TN-1-10					
TN-1-16					
TN-1-46					

Table 4 Mineralogical composition of the clay fraction (<2 µm) in samples from TN-1.

Sample ID	Biotite	Muscovite	Montmorillonite	Illite-montmorillonite	Illite
TN-1-6					
TN-1-10					
TN-1-16					
TN-1-46					

Table 5 Mineralogical composition of the clay fraction (2-16 µm) in samples from AL-1.

Sample ID	Biotite	Muscovite	Montmorillonite	Illite-Montmorillonite	Illite
AL-1-22					
AL-1-86					

Table 6 Mineralogical composition of the clay fraction (<2 µm) in samples from AL-1.

Sample ID	Biotite	Muscovite	Montmorillonite	Illite-montmorillonite	Illite
AL-1-22					
AL-1-86					

Table 7 Key

	>80%
	55-80%
	30-55%

39

	10-30%
	<10%

Tipping Point Analysis

The results for the tipping point analysis are attached in Appendix D. The most useful

statistical tool to mark critical transition points was skewness. It helped in identifying

stratigraphic surfaces by pointing to the position of sudden changes in the behavior of the

individual chemical indices. One recent study by Dai et al. (2021) demonstrated the usefulness of

EWS in identifying tipping points in sedimentary systems. Their study showed that EWS

analysis of sedimentary records can help to identify critical transitions in sedimentary systems,

such as changes in sedimentation rate, sedimentary facies, and sediment provenance (discussed

in Chapter 5).

Chapter 5 - Discussion

The interpretation of complexities in deposition, lithology, and elemental concentration in mudrocks requires geochemical analysis because it is hard to see these changes from macro-observations (Tribovillard et al., 2005; Loucks and Ruppel, 2007; Rowe et al., 2008, Hammes et al., 2011). An integration of sedimentologic and geochemical analysis aids an informed decision as to what is contributing to deposition and the main switches in the organic matter concentration of these mudrocks. The analysis of sedimentologic and chemostratigraphic logs of the Chattanooga Formation in Tennessee and Alabama allowed the identification of three sequences in the sedimentary successions at each location (sequences 1 through 3, from base to top) (Figures 4.5 and 4.7). These sequences were subdivided based on their facies associations and behavior of chemical indices, as presented in Chapter 4. In this chapter, we will present the stratigraphic framework in each of the areas and discuss the controls in the succession, followed by a comparison between the two areas and the implications for the paleogeographic context.

The establishment of a stratigraphic framework (or the partition of a sedimentary succession in units) allows the interpretation of depositional settings and the investigation of the possible drivers of basin evolution. The sequence stratigraphic framework is based on the identification of sequences, stratigraphic units composed of relatively conformable successions of genetically related strata bounded at their top and base by surfaces of erosion or non-deposition (unconformities) (Mitchum et al., 1977; Posamentier et al., 1988; Van Wagoner et al., 1988). A sequence is formed during a complete base level cycle (fall and rise). The fundamental control on the formation of a sequence is changing accommodation (i.e., the space available for sediments to accumulate), which is governed by tectonics and eustasy. The ratio between

41

accommodation and the rate of sediment supply (mostly controlled by climate) will determine

the water depth and the shoreline trajectory (transgression or regression). The stratigraphic

framework is established by identifying key stratigraphic surfaces, marked by changes in

stacking patterns (progradational, aggradational or retrogradational). Key stratigraphic surfaces

include the sequence boundaries, the transgressive surface, and the maximum flooding surface,

which limit the systems tracts (sedimentary succession deposited in particular parts of the cycle).

The stratigraphic system in the two locations is related to the basin history. The

Appalachian Basin, a foreland basin within the Midcontinent Basin, is characterized by four

orogenic events (Taconic, Potomac, Acadian and Antler Orogenies) that occurred in the

Ordovician to Silurian, Early to Late Devonian, Late Devonian to Early Mississippian, and Late

Mississippian to Pennsylvanian periods (Woodrow et al., 1988; Lu et al., 2015). The

Chattanooga Formation was deposited during and after the Acadian Orogeny in an epicontinental

sea (Scheiber, 1994). Evidence of the deformation and volcanism related to this event is found in

the studied sections in the form of volcanic ash beds at TN-1 and folding of the succession in

Sequence 1 at AL-1.

Epicontinental seas are partially enclosed, shallow seas within continental areas, with a

depth of approximately 100m (Johnson and Baldwin, 1996; Schieber 2016). They form mostly

when there is a rise in sea level, causing the oceans to flood the continent (Schieber, 1994, 2016).

Sea level rise causes an increase in accommodation, but sediment deposits are thin and laterally

widespread due to low subsidence and essentially nonexistent bathymetric relief; yet these seas

may have dome- and basin-shaped zones of uplift or subsidence (Shaw, 1964). Thrust loading,

particularly during orogenies, cause the formation of foreland basins with much greater sediment

thickness (high rates of subsidence and eventual sediment accumulation), which eventually

merged laterally into extensive thin sediment blankets that accumulate in the continents' more slowly subsiding regions (DeCelles and Giles, 1996). In contrast to the tens of meters of silt in the heart of the continent, the Appalachian Basin has many kilometers of sediment (Conant and Swanson, 1961, Schieber, 2016). The much thicker and deeper sediments are found within the foredeep (deeper troughs from thrusting), while the thinner sediments could be slightly away from the foredeep (Milici and Swezey, 2006).

In the studied successions, the sequence boundaries are characterized by peaks in detrital proxies (Ti/Al, Zr/Al), compatible with the high rates of sediment supply associated with the formation of unconformities, but, contrary to what was expected, the Lowstand Systems Tracts (LST) are not characterized by high detrital proxies. As a matter of fact, at AL-1 the detrital proxies are the lowest in the LST (the highest in the Highstand Systems Tracts – TST). The Transgressive Systems Tracts (TST) display the highest values for redox proxies (Mo/Al and U/Al), compatible with anoxic bottom waters more easily developed in this systems tract. The Highstand Systems Tract (HST) is characterized by the highest Ti/Al and Zr/Al but intermediate Mo/Al and U/Al. Chemical proxies for primary productivity do not seem to follow particular systems tracts; for instance, the paleoproductivity indices are lower in the LST at TN-1 and higher at AL-1. The various cycles of sea level rise and fall, as seen at both locations is explained below.

TN-1

At TN-1, Sequence 1 is characterized by a more proximal setting of hemipelagic-lower shoreface, with the lowest TOC values (between 4 and 7 wt%) in the entire section. The paleoredox indices suggest oxic to suboxic bottom waters, with short-lived intervals of anoxia and very low primary productivity. The absence of a Lowstand Systems Tract (LST) might be

due to the epicontinental setting of the basin, characterized by low rates of subsidence and accommodation. The lesser preservation of organic matter in this sequence is a result of more oxic bottom waters that allowed reworking by bottom dwellers, since this is the sequence with the highest amount of bioturbation.

Sequence 2, with TOC between 9 and 16 wt%, was formed under alternating pelagic and hemipelagic-lower shoreface conditions. Chemical proxies suggest that this unit was deposited in an anoxic environment. The stratigraphic framework shows a LST overlain by TST. In the absence of a HST, the maximum flooding surface coincides with the erosional surface that marks the sequence boundary. This is possibly the result of the epicontinental setting and distal position, which does not favor the development of well-preserved sequences. At the base of this sequence, the occurrence of Sst facies coinciding with a peak in the chemical proxies for detrital input, paleoproductivity and redox indices suggest that riverine input of nutrients triggered higher primary productivity and anoxia. This sequence has more organics than Sequence 1, possibly because it has received more detrital input (and nutrients) to increase primary productivity. The coincidence between paleoproductivity and redox proxies suggests that anoxia resulted from increased organic flux.

Sequence 3 comprises pelagic environments at the base, followed by hemipelagic-lower shoreface at the top, representing a shallowing-upward cycle that starts under anoxic and grades upward to more oxic conditions.. The presence of phosphate nodules at the upper part of the sequence suggest the presence of upwelling waters , increasing primary productivity and driving anoxia. The highest TOC values in the succession (13-18 wt%) are found in this sequence, thus indicating that high primary productivity and anoxia drove accumulation of organic matter. The absence of a LST might be due to the distal basinal position.

In summary, the stratigraphic section at TN-1 shows that this location was recorded variations in the depositional environments from hemipelagic-lower shoreface to pelagic and back to hemipelagic-lower shoreface settings. All chemical proxies suggest increasing variations from Sequence 1 to 3, and a transition from oxic to suboxic, and anoxic environments. The organic content also increased from Sequence 1 to 3, affirming that accumulation of organic matter was favored by high primary productivity and high preservation under anoxic conditions in a dynamic environment. The stratigraphic framework shows an incomplete sequences, with only the TST preserved in all the sequences, possibly due to the epicontinental nature of the basin. LST was preserved only in Sequence 2 and HST in sequences 1 and 3. Sea level rise and fall might be reflecting eustatic changes associated with the Late Devonian glaciation. In comparison with AL-1, TN-1 was deposited closer to the shoreline, according with the Late Devonian paleogeographic map by Blakey (2013). TN-1 would be in a shallow marine shelf where the continental influx would come from the west.

AL-1

At AL-1, Sequence 1 was deposited in a pelagic environment, where the highest TOC (between 8 and 13 wt%) was preserved. The chemical proxies suggest a depositional environment with anoxic bottom waters, with sporadic high influx of detrital sediment which triggered increased primary productivity. The LST is very thick, possibly being deposited in the foredeep thrust of the foreland basin. Like Sequence 2 at TN-1, the HST was not preserved and therefore the maximum flooding surface coincides with the upper sequence boundary.

Sequence 2 is characterized by a change from hemipelagic-lower shoreface settings at the base to pelagic above it. Shallowing of the depositional setting is accompanied by lower TOC (ranging from 7 to 10 wt%) in comparison with Sequence 1. The behavior of the chemical

indices suggests a dynamic environment with highly variable conditions, and overall high detrital input and episodic upwelling, but these conditions did not seem to result in higher productivity. Like Sequence 3 at TN-1, the LST was not preserved in this sequence, possibly due to its distal location, far removed from the shorelines.

Sequence 3 shows a shallowing-upward trend, deposited under pelagic conditions at the base and hemipelagic-lower shoreface at the top. The lowest TOC in the succession (5 - 7 wt%) are found in this unit, perhaps due to the presence of oxic-suboxic bottom waters. This sequence was the only complete one (in both studied locations), preserving the three systems tracts, although the LST is thin, possibly due to the distal basinal position of this section. Despite the indication of episodic upwelling (e.g., abundance of chert layers and isolated peaks in proxies for primary productivity), the presence of oxygen in the bottom waters seems to have been deleterious to the preservation of organic matter.

Even though three sequences (named 1 through 3, from base to top) were identified in the two studied locations, Sequence 1 at TN-1 is not the same as Sequence 1 at AL-1. Based on the behavior of chemical indices, Sequence 1 at AL-1 is similar to Sequence 2 at TN-1. Moreover, both sequences are composed of a LST and a TST and overlain by a sequence with a TST and a HST (Sequence 2 at AL-1 and Sequence 3 at TN-1).

The facies associations in these successions reflect the different paleogeographic positions of the two locations, with TN-1 accumulated in more proximal settings than AL-1, but the correlative sequences respond to the same allogenic controls. The variations in the accommodation-to-supply ratios recorded at TN-1 and AL-1 was likely controlled by eustatic sea level. At AL-1, a cycle of larger order (represented by the overall shallowing trend from Sequence 1 to Sequence 3) might be pointing to the superposition of a tectonic control, given

that AL-1 is closer to the continental margin where the Acadian Orogeny took place in the Devonian.

The Late Devonian is known as the period of glaciation. Towards the end (Famennian Age), the climate became drier, both factors causing an eustatic fall in sea level (Becker et. al., 2020). Progradation of the clastic wedge generated during the Acadian Orogeny also occurred due to regression of the seas (Isaacson, 2008). Increased riverine delivery of nutrients promoted eutrophic conditions that may have contributed to bottom-water anoxia and preferential preservation of organic matter in the sediments and extinction (Algeo and Scheckler, 1998).

In regard to what controls the accumulation of organics in the sediments, the facies and and chemostratigraphic analysis of the Chattanooga Formation in Alabama and Tennessee suggests that high organic content (TOC>10%) is found in settings where high primary productivity coincides with bottom-water anoxia. In the studied sections, primary productivity was boosted either by riverine nutrient input and/or upwelling waters.

Chapter 6 - Conclusion

Five lithofacies were identified in the sedimentary succession of the Chattanooga Formation in TN-1 and AL-1. These facies were deposited in a wave-dominated marine environment in hemi-pelagic to pelagic settings. The integration between sedimentology and chemostratigraphy allowed the identification of key stratigraphic surfaces and the partition of the succession into three sequences in each study area. Sequence 1 at AL-1 corresponds to Sequence 2 at TN-1, based on their similarities in terms of facies associations and behavior of the chemical indices.

The stratigraphic framework shows incomplete system tracts, which can be attributed to the less preservation of sediments associated with epicontinental basins. The only sequence with a complete system tract is Sequence 1 at AL-1. The TST is the only systems tract present in all the sequences studied at both locations. This is probably due to the distal marine position where the sediments accumulated, characterized by low sedimentation rates.

The TOC in both locations ranges between 8 and 16 wt%, increasing upward at TN-1 whereas decreasing upward at AL-1. The highest amount of organic matter is found in Sequence 1 at AL-1.In both study locations, the sequences with the highest TOC were characterized by deposition in environments with anoxic bottom waters and high productivity. There is evidence of upwelling in both locations and variable riverine input.

AL-1 was deposited in deeper water conditions in relation to TN-1, deposited closer to the continent, despite the relatively deep marine setting. The allogenic controls of the stratigraphic framework are likely eustasy, overprinted by tectonics at AL-1, which may have been deposited in the foredeep resulting from thrust loading during the Arcadian Orogeny.

Integration between sedimentology and chemical proxies was useful to detect changes in the depositional conditions, with certain sequences formed in more stable environments and others in a dynamic, highly variable environment regarding detrital input, paleoproductivity and redox conditions. The highest TOC is found in Sequence 1 in Alabama and Sequence 3 in Tennessee. During the accumulation of these units, paleoproductivity was high and bottom waters were anoxic, and hence burial of organic matter in the sediments seems to be favored when there is a conjunction between production and preservation.

References

Algeo, T.J & Scheckler, S.E. 1998 Terrestrial-marine teleconnections in the Devonian: links between the evolution of land plants, weathering processes, and marine anoxic events. Phil.Trans. R. Soc. Lond. B (1998) 353, 113-130

Algeo, T. J., & Lyons, T. W. (2006). Mo–total organic carbon covariation in modern anoxic marine environments: Implications for analysis of paleoredox and paleohydrographic conditions. Paleoceanography, 21(1).

Algeo, T. J., & Maynard, J. B. (2008). Trace-metal covariation as a guide to water-mass conditions in ancient anoxic marine environments. Geosphere, 4(5), 872-887.

Arnaboldi, M., & Meyers, P. A. (2007). Trace element indicators of increased primary production and decreased water-column ventilation during deposition of latest Pliocene sapropels at five locations across the Mediterranean Sea. Palaeogeography, Palaeoclimatology, Palaeoecology, 249(3-4), 425-443.

Becker, R. T., Marshall, J. E. A., Da Silva, A. C., Agterberg, F. P., Gradstein, F. M., & Ogg, J. G. (2020). The devonian period. In Geologic time scale 2020 (pp. 733-810). Elsevier.

Benitez-Nelson, C. R. (2000). The biogeochemical cycling of phosphorus in marine systems. Earth-Science Reviews, 51(1-4), 109-135.

Bhatia, M. R., & Crook, K. A. (1986). Trace element characteristics of graywackes and tectonic setting discrimination of sedimentary basins. Contributions to mineralogy and petrology, 92(2), 181-193.

Blakey, R. C. (2013). Using paleogeographic maps to portray Phanerozoic geologic and paleotectonic history of western North America. AAPG Bulletin, 97(1), 146.

Boggs Jr, S., & Boggs, S. (2009). Petrology of sedimentary rocks. Cambridge university press, P451-455.

Bohacs, K. M. (1990). Sequence stratigraphy of the Monterey Formation, Santa Barbara County: Integration of physical, chemical, and biofacies data from outcrop and subsurface.

Miall, A. D. (2022). Facies analysis. In Stratigraphy: A modern synthesis (pp. 91-174). Cham: Springer International Publishing.

Bohacs, K. M., Lazar, O. R., & Demko, T. M. (2014). Parasequence types in shelfal mudstone strata—Quantitative observations of lithofacies and stacking patterns, and conceptual link to modern depositional regimes. Geology, 42(2), 131-134.

Catuneanu, O., Galloway, W.E., Kendall, C.G.St.C., Miall, A.D., Posamentier, H.W., Strasser, A. & Tucker, M.E. 2011. Sequence stratigraphy: methodology and nomenclature. Newsletters on Stratigraphy, 44, 173–245

Collison, J.D. (1996) Alluvial Sediments. In: Reading, H.G., Ed., Sedimentary Environments: Processes, Facies and Stratigraphy, 3rd Edition, Blackwell Science, Oxford, 37-81.

Comer, J. B., & Hinch, H. H. (1987). Recognizing and quantifying expulsion of oil from the Woodford Formation and age-equivalent rocks in Oklahoma and Arkansas. AAPG bulletin, 71(7), 844-858.

Conant, L. C., & Swanson, V. E. (1961). Chattanooga Shale and related rocks of central Tennessee and nearby areas. Geological Survey Professional Paper, 357.

Dakos, V., Carpenter, S. R., van Nes, E. H., & Scheffer, M. (2015). Resilience indicators: prospects and limitations for early warnings of regime shifts. Philosophical Transactions of the Royal Society B: Biological Sciences, 370(1659), 20130263.

Dai, L., Gao, Y., Zhang, S., Liu, S., Song, L., Wang, Y., & Wang, J. (2021). Early warning signals of critical transitions in sedimentary records: A case study from the southern North Yellow Sea. Global and Planetary Change, 202, 103483.

DeCelles, P. G., & Giles, K. A. (1996). Foreland basin systems. Basin research, 8(2), 105-123.

Dehairs, F., Chesselet, R., & Jedwab, J. (1980). Discrete suspended particles of barite and the barium cycle in the open ocean. Earth and Planetary Science Letters, 49(2), 528-550.

Dehairs, F., Lambert, C. E., Chesselet, R., & Risler, N. (1987). The biological production of marine suspended barite and the barium cycle in the Western Mediterranean Sea. Biogeochemistry, 4, 119-140.

Dehairs, F., Stroobants, N., & Goeyens, L. (1991). Suspended barite as a tracer of biological activity in the Southern Ocean. Marine Chemistry, 35(1-4), 399-410.

Dehairs, F., Baeyens, W., & Goeyens, L. (1992). Accumulation of suspended barite at mesopelagic depths and export production in the Southern Ocean. Science, 258(5086), 1332-1335.

Dehairs, F., Stroobants, N., & Goeyens, L. (1991). Suspended barite as a tracer of biological activity in the Southern Ocean. Marine Chemistry, 35(1-4), 399-410.

de Witt Jr, W. (1981). Revision of the aerial extent of the New Albany, Chattanooga, and Ohio shales in Kentucky. GSA Cincinnati, 81, 331-334.

de Witt Jr, W., Roen, J. B., & Wallace, L. G. (1993). Stratigraphy of Devonian black shales and associated rocks in the Appalachian Basin: United States Geological Survey Bulletin 1909, p. B1-B47.

Dromart, G., Monier, P., Curial, A., Moretto, R., & Guillocheau, F. (1994). Triassic

transgressive-regressive cycles in the Bresse-Jura and adjacent Basins, eastern France.

Hydrocarbon and petroleum geology of France, 347-360.

Dymond, J., Suess, E., & Lyle, M. (1992). Barium in deep-sea sediment: A geochemical proxy

for paleoproductivity. Paleoceanography, 7(2), 163-181.

Ettensohn, F. R., Woodrow, D. L., & Sevon, W. D. (1985). Controls on development of Catskill

Delta complex basin-facies. The Catskill Delta: Geological Society of America Special

Paper, 201, 65-77.

Ettensohn, F. R., Miller, M. L., Dillman, S. B., Elam, T. D., Geller, K. L., Swager, D. R., ... &

Barron, L. S. (1988). Characterization and implications of the Devonian-Mississippian

black shale sequence, eastern and central Kentucky, USA: Pycnoclines, transgression,

regression, and tectonism.

Falkner, K. K., Bowers, T. S., Todd, J. F., Lewis, B. L., Landing, W. M., & Edmond, J. M.

(1993). The behavior of barium in anoxic marine waters. Geochimica et Cosmochimica

Acta, 57(3), 537-554.

Föllmi, K. B. (1996). The phosphorus cycle, phosphogenesis and marine phosphate-rich

deposits. Earth-Science Reviews, 40(1-2), 55-124.

Goldberg, K., & Humayun, M. (2016). Geochemical paleoredox indicators in organic-rich shales

of the Irati Formation, Permian of the Paraná Basin, southern Brazil. Brazilian Journal of

Geology, 46, 377-393.

Hammes, U., & Frébourg, G. (2012). Haynesville and Bossier mudrocks: A facies and sequence

stratigraphic investigation, East Texas and Louisiana, USA. Marine and Petroleum

Geology, 31(1), 8-26.

Hansma, J., Tohver, E., Yan, M., Trinajstic, K., Roelofs, B., Peek, S., ... & Hocking, R. (2015). Late Devonian carbonate magnetostratigraphy from the Oscar and Horse Spring Ranges, Lennard Shelf, Canning Basin, Western Australia. Earth and Planetary Science Letters, 409, 232-242.

Hoppie, B., & Garrison, R. E. (2001). Miocene phosphate accumulation in the Cuyama basin, southern California. Marine Geology, 177(3-4), 353-380.

House, M. R. (2023, February 9). Devonian Period. Encyclopedia Britannica. https://www.britannica.com/science/Devonian-Period

Isaacson, P. E., Díaz-Martínez, E., Grader, G. W., Kalvoda, J., Bábek, O., & Devuyst, F. X. (2008). Late Devonian–earliest Mississippian glaciation in Gondwanaland and its biogeographic consequences. Palaeogeography, Palaeoclimatology, Palaeoecology, 268(3-4), 126-142.

James, N. P., & Dalrymple, R. W. (Eds.). (2010). Facies models 4. Canada: Geological Association of Canada.

Joachimski, M. M., Breisig, S., Buggisch, W., Talent, J. A., Mawson, R., Gereke, M., ... & Weddige, K. (2009). Devonian climate and reef evolution: insights from oxygen isotopes in apatite. Earth and Planetary Science Letters, 284(3-4), 599-609.

Reading, H. G. (Ed.). (2009). Sedimentary environments: processes, facies and stratigraphy. John Wiley & Sons.

Kidder, D. L., & Erwin, D. H. (2001). Secular distribution of biogenic silica through the Phanerozoic: comparison of silica-replaced fossils and bedded cherts at the series level. The Journal of Geology, 109(4), 509-522.

Kim, D., Schuffert, J. D., & Kastner, M. (1999). Francolite authigenesis in California continental slope sediments and its implications for the marine P cycle. Geochimica et Cosmochimica Acta, 63(19-20), 3477-3485.

Kübler, B., & Jaboyedoff, M. (2000). Illite crystallinity. Comptes Rendus de l'Académie des Sciences-Series IIA-Earth and Planetary Science, 331(2), 75-89.

Lazar, O. R., Bohacs, K. M., Macquaker, J. H. S., Schieber, J., Lazar, R., & Bohacs, K. (2010). Fine-grained rocks in outcrops: Classification and description guidelines. In Sedimentology and stratigraphy of shales: AAPG 2010 annual convention and exhibition, field guide for post-convention field trip (Vol. 10, pp. 3-14).

Lazar, O. R., Bohacs, K. M., Schieber, J., Macquaker, J. H. S., & Demko, T. M. (2015). Mudstone primer. Lithofacies Variations, Diagnostic Criteria, and Sedimentologic–Stratigraphic Implications at Lamina to Bedset Scale. SEPM (Society for Sedimentary Geology)(205 pp.).

Li, Y., & Schieber, J. (2015). On the origin of a phosphate enriched interval in the Chattanooga Shale (Upper Devonian) of Tennessee—a combined sedimentologic, petrographic, and geochemical study. Sedimentary Geology, 329, 40-61.

Loucks, R. G., & Ruppel, S. C. (2007). Mississippian Barnett Shale: Lithofacies and depositional setting of a deep-water shale-gas succession in the Fort Worth Basin, Texas. AAPG bulletin, 91(4), 579-601.

Lü, M., Chen, K., Xue, L., Yi, L., & Zhu, H. (2010). High-resolution transgressive-regressive sequence stratigraphy of Chang 8 Member of Yanchang Formation in southwestern Ordos basin, northern China. Journal of Earth Science, 21(4), 423-438.

Lu, M. (2015). Sedimentological and geochemical records of depositional environments of the

    Late Devonian Chattanooga shale (Doctoral dissertation, University of Alabama

    Libraries).

Lu, M., Lu, Y., Ikejiri, T., Hogancamp, N., Sun, Y., Wu, Q., ... & Pashin, J. (2019). Geochemical

    evidence of first forestation in the southernmost Euramerica from Upper Devonian

    (Famennian) black shales. Scientific Reports, 9(1), 7581.

Lyons, T. W., & Severmann, S. (2006). A critical look at iron paleoredox proxies: New insights

    from modern euxinic marine basins. Geochimica et Cosmochimica Acta, 70(23), 5698-

    5722.

McManus, J., Berelson, W. M., Severmann, S., Poulson, R. L., Hammond, D. E., Klinkhammer,

    G. P., & Holm, C. (2006). Molybdenum and uranium geochemistry in continental margin

    sediments: paleoproxy potential. Geochimica et Cosmochimica acta, 70(18), 4643-4662.

Miall, A. D. (2022). Facies analysis. In Stratigraphy: A modern synthesis (pp. 91-174). Cham:

    Springer International Publishing.

Milici, Robert & Ryder, R.T. & Swezey, Christopher. (2001). Appalachian Basin petroleum

    systems. U.S. Geological Survey Open-File Report. 01-406. 81-84. U.S. Geological

    Survey Open-File Report 01-406, p. 81-84.

Milici, R. C., & Swezey, C. S. (2006). Assessment of Appalachian Basin oil and gas resources:

    Devonian shale—Middle and Upper Paleozoic total petroleum system. US Geological

    Survey Open-File Report, 1237(2006), 70.

Mitchum Jr, R. M., Vail, P. R., & Thompson III, S. (1977). Seismic stratigraphy and global

    changes of sea level: Part 2. The depositional sequence as a basic unit for stratigraphic

analysis: Section 2. Application of seismic reflection configuration to stratigraphic interpretation.

Moore, D. M., & Reynolds Jr, R. C. (1989). X-ray Diffraction and the Identification and Analysis of Clay Minerals. Oxford University Press (OUP).

Moore, D. M., and Reynolds, R. C., (1997): X-ray Diffraction and the Identification and Analysis of Clay Minerals, v. 332, New York: Oxford University Press.

Morford, J. L., Emerson, S. R., Breckel, E. J., & Kim, S. H. (2005). Diagenesis of oxyanions (V, U, Re, and Mo) in pore waters and sediments from a continental margin. Geochimica et Cosmochimica Acta, 69(21), 5021-5032.

Mørk, A., Embry, A. F., & Weitschat, W. (1989). Triassic transgressive-regressive cycles in the Sverdrup Basin, Svalbard and the Barents Shelf. In Correlation in Hydrocarbon Exploration: Proceedings of the conference Correlation in Hydrocarbon Exploration organized by the Norwegian Petroleum Society and held in Bergen, Norway, 3–5 October 1988 (pp. 113-130). Springer Netherlands.

Murphy, A. E., Sageman, B. B., & Hollander, D. J. (2000). Eutrophication by decoupling of the marine biogeochemical cycles of C, N, and P: A mechanism for the Late Devonian mass extinction. Geology, 28(5), 427-430.

Murphy, A. E., Sageman, B. B., Hollander, D. J., Lyons, T. W., & Brett, C. E. (2000). Black shale deposition and faunal overturn in the Devonian Appalachian Basin: Clastic starvation, seasonal water-column mixing, and efficient biolimiting nutrient recycling. Paleoceanography, 15(3), 280-291.

Nance, H. S., & Rowe, H. (2015). Eustatic controls on stratigraphy, chemostratigraphy, and

    water mass evolution preserved in a Lower Permian mudrock succession, Delaware

    Basin, west Texas, USA. Interpretation, 3(1), SH11-SH25.

Nichols, G. (2009). Sedimentology and stratigraphy. John Wiley & Sons, 349-380

Over, D. J. (2002). The Frasnian/Famennian boundary in central and eastern United States.

    Palaeogeography, Palaeoclimatology, Palaeoecology, 181(1-3), 153-169.

Over, D. J. (2007). Conodont biostratigraphy of the Chattanooga Shale, Middle and Upper

    Devonian, southern Appalachian Basin, eastern United States. Journal of Paleontology,

    81(6), 1194-1217.

Parrish, J. T. (1987). Palaeo-upwelling and the distribution of organic-rich rocks. Geological

    Society, London, Special Publications, 26(1), 199-205.

Parrish, J. T., & Curtis, R. L. (1982). Atmospheric circulation, upwelling, and organic-rich rocks

    in the Mesozoic and Cenozoic eras. Palaeogeography, palaeoclimatology, palaeoecology,

    40(1-3), 31-66.

Pearce, T. H., & Jarvis, I. (1992). Applications of geochemical data to modelling sediment

    dispersal patterns in distal turbidites; late Quaternary of the Madeira abyssal plain.

    Journal of Sedimentary Research, 62(6), 1112-1129.

Pearce, T. J., Besly, B. M., Wray, D. S., & Wright, D. K. (1999). Chemostratigraphy: a method

    to improve interwell correlation in barren sequences—a case study using onshore

    Duckmantian/Stephanian sequences (West Midlands, UK). Sedimentary Geology, 124(1-

    4), 197-220.

Picard, M. D. (1971). Classification of fine-grained sedimentary rocks. Journal of Sedimentary

    Research, 41(1), 179-195.

Posamentier, H. W., & Vail, P. R. (1988). Eustatic controls on clastic deposition II—sequence and systems tract models.

Potter, P. E., Maynard, J. B., Pryor, W. A., Potter, P. E., Maynard, J. B., & Pryor, W. A. (1980). Question Set. Sedimentology of Shale: Study Guide and Reference Source, 85-142.

Potter, P. E., Maynard, J. B., & Pryor, W. A. (1982). Appalachian gas bearing Devonian shales-statements and discussions. Oil & Gas Journal, 80(4), 290.

Retrieved from "https://en.wikipedia.org/w/index.php?title=Geology_of_the_Appalachians&oldid=1134583161"

Robeck, R. C., & Brown, A. (1950). Black shale investigations, Block 3, Tennessee (No. 63).

Sageman, B. B., & Lyons, T. W. (2003). Geochemistry of fine-grained sediments and sedimentary rocks (Vol. 7, p. 407).

Sageman, B.B. and Lyons, T.W. 2004. Geochemistry of fine-grained sediments and sedimentary rocks. In: Mackenzie, F. (ed.) Sediments, Diagenesis, and Sedimentary Rock. Treatise on Geochemistry, 7. Elsevier, Amsterdam, 115–158

Schieber, J. (1994). Evidence for high-energy events and shallow-water deposition in the Chattanooga Shale, Devonian, central Tennessee, USA. Sedimentary Geology, 93(3-4), 193-208.

Schieber, J. (1998). Developing a sequence stratigraphic framework for the Late Devonian Chattanooga Shale of the southeastern USA: relevance for the Bakken Shale. Williston Basin Symposium.

Schieber, J. (2003). Simple gifts and buried treasures–implications of finding bioturbation and erosion surfaces in black shales. The Sedimentary Record, 1(2), 4-8.

Schieber, J. (2007). Oxidation of detrital pyrite as a cause for Marcasite Formation in marine lag

      deposits from the Devonian of the eastern US. Deep Sea Research Part II: Topical

      Studies in Oceanography, 54(11-13), 1312-1326.

Schieber, J. (2009). Discovery of agglutinated benthic foraminifera in Devonian black shales and

      their relevance for the redox state of ancient seas. Palaeogeography, Palaeoclimatology,

      Palaeoecology, 271(3-4), 292-300.

Schieber, J. (2016). Mud re-distribution in epicontinental basins–Exploring likely processes.

      Marine and Petroleum Geology, 71, 119-133.

Shaw, A.B., 1964. Time in Stratigraphy. McGraw-Hill, p. 365.

Speakman, S. A. (2012). Introduction to PANalytical X'Pert HighScore Plus v3. 0. MIT Center

      for Materials Science and Engineering, 1-19.

Stow, D. A. (1981). Fine-grained sediments: Terminology. Quarterly Journal of Engineering

      Geology, 14(4), 243-244.

Stow, D. A. V., Huc, A. Y., & Bertrand, P. (2001). Depositional processes of black shales in

      deep water. Marine and Petroleum Geology, 18(4), 491-498.

Stow, D., & Smillie, Z. (2020). Distinguishing between deep-water sediment facies: Turbidites,

      contourites and hemipelagites. Geosciences, 10(2), 68.

Tribovillard, N., Algeo, T. J., Lyons, T., & Riboulleau, A. (2006). Trace metals as paleoredox

      and paleoproductivity proxies: an update. Chemical geology, 232(1-2), 12-32.

Turner, B. W., Tréanton, J. A., & Slatt, R. M. (2015, July). The use of chemostratigraphy to

      refine ambiguous sequence stratigraphic correlations in marine shales: an Example from

      the Woodford Shale, Oklahoma. In SPE/AAPG/SEG Unconventional Resources

      Technology Conference. OnePetro.

Turner, B. W., Molinares-Blanco, C. E., & Slatt, R. M. (2015). Chemostratigraphic, palynostratigraphic, and sequence stratigraphic analysis of the Woodford Shale, Wyche Farm Quarry, Pontotoc County, Oklahoma. Interpretation, 3(1), SH1-SH9.

Turner, B. W., Tréanton, J. A., & Slatt, R. M. (2016). The use of chemostratigraphy to refine ambiguous sequence stratigraphic correlations in marine mudrocks. An example from the Woodford Shale, Oklahoma, USA. Journal of the Geological Society, 173(5), 854-868.

Robeck, R. C., & Brown, A. (1950). Black shale investigations, Block 3, Tennessee (No. 63).

Rowe, H. D., Loucks, R. G., Ruppel, S. C., & Rimmer, S. M. (2008). Mississippian Barnett Formation, Fort Worth Basin, Texas: Bulk geochemical inferences and Mo–TOC constraints on the severity of hydrographic restriction. Chemical Geology, 257(1-2), 16-25.

Rowe, H., Hughes, N., & Robinson, K. (2012). The quantification and application of handheld energy-dispersive x-ray fluorescence (ED-XRF) in mudrock chemostratigraphy and geochemistry. Chemical geology, 324, 122-131.

Ryder, R. T. (2008). Assessment of Appalachian Basin oil and gas resources: Utica-Lower Paleozoic total petroleum system. US Department of the Interior, US Geological Survey.

Tribovillard, N., Ramdani, A., & Trentesaux, A. (2005). Controls on organic accumulation in Upper Jurassic shales of northwestern Europe as inferred from trace-metal geochemistry.

Tribovillard, N., Algeo, T. J., Lyons, T., & Riboulleau, A. (2006). Trace metals as paleoredox and paleoproductivity proxies: an update. Chemical geology, 232(1-2), 12-32.

Van Wagoner, J. C., Posamentier, H. W., Mitchum, R. M. J., Vail, P. R., Sarg, J. F., Loutit, T. S., & Hardenbol, J. (1988). An overview of the fundamentals of sequence stratigraphy and key definitions.

Wang, Q., Huang, Y., Zhang, Z., Wang, C., & Li, X. (2022). Application of Chemical Sequence Stratigraphy to the Prediction of Shale Gas Sweet Spots in the Wufeng and Lower Longmaxi Formations within the Upper Yangtze Region. Minerals, 12(7), 859.

Wedepohl, K. H. (1971). Environmental influences on the chemical composition of shales and clays. Physics and Chemistry of the Earth, 8, 307-333.

Woodrow, D. L., Dennison, J. M., Ettensohn, F. R., Sevon, W. T., & Kirchgasser, W. T. (1988). Middle and Upper Devonian stratigraphy and paleogeography of the central and southern Appalachians and eastern Midcontinent, USA.

Yin, S., Zhang, Z., & Huang, Y. (2022). Geochemical Characteristics and Chemostratigraphic Analysis of Wufeng and Lower Longmaxi Shales, Southwest China. Minerals, 12(9), 1124.

Appendix A - HHXRF Results (Raw Data)

The results from the HHXRF measurements were normalized using the procedure by Rowe et al. (2012). A Woodford Standard (RTC-W-220) was analyzed after every five measurements of the sample to check for the possibility of drift from the machine. The average of these runs was used as a representative elemental concentration for each sample. Finally, the overall average of each element was calculated and divided by the values reported by Rowe et al. (2012) to get the normalization factor. The chemical indices are derived by dividing the normalized elemental concentration by normalized Al concentration. This procedure was carried out for each element in both locations (TN-1 and AL-1).

Table A.1 <u>RTC-W-220 Accepted Values by Rowe et al. (2012)</u>

Rowe et al. (2012) RTC-W_220 (Woodford Formation) Accepted Values										
Al (wt%)	Si (wt%)	P (wt%)	Ti (wt%)	Fe (wt%)	Ba (ppm)	Ni (ppm)	Cu (ppm)	Zr (ppm)	Mo (ppm)	U (ppm)
5.39	3307	0.05	0.27	2.55	1884	153	147	95	83	17

Table A.2 <u>Standard Measurements of Major Elemental Concentrations at TN-1</u>

STANDARD FOR MAJOR ELEMENTS AT TN-1					
Sample ID	Al (wt%)	Si (wt%)	P (wt%)	Ti (wt%)	Fe (wt%)
TN-1-1-Standard	5.227801	31.28142	0.10213	0.262869	1.884149
TN-1-2-Standard	5.381459	32.34646	0.087589	0.282169	1.991634
TN-1-3-Standard	5.39088	32.44569	0.097325	0.287657	2.013889
TN-1-4-Standard	5.339158	32.45303	0.10376	0.285171	2.029938
TN-1-5-Standard	5.349786	31.85668	0.092227	0.283761	2.074139
TN-1-6-Standard	5.397048	32.6699	0.090054	0.286426	2.073305
TN-1-7-Standard	5.444428	32.86222	0.098532	0.292444	2.080246
TN-1-8-Standard	5.345263	32.42645	0.093004	0.289103	2.055653
TN-1-9-Standard	5.483202	32.73507	0.090127	0.294985	2.074699
TN-1-10-Standard	5.389847	32.75233	0.098	0.2944	2.0722
TN-1-11-Standard	5.416646	32.85839	0.101	0.2752	1.9336

TN-1-12-Standard	5.398606	32.78238	0.09556	0.282989	2.003703
TN-1-13-Standard	5.376332	32.59443	0.100332	0.288662	2.068042
TN-1-14-Standard	5.362211	32.38337	0.098134	0.291346	2.056599
TN-1-15-Standard	5.392734	32.43117	0.09828	0.300446	2.183046
TN-1-16-Standard	5.412669	32.97049	0.104	0.2737	1.8776
TN-1-17-Standard	5.416629	32.77084	0.103018	0.28181	1.929694
TN-1-18-Standard	5.462674	32.98267	0.105735	0.286758	2.013636
TN-1-19-Standard	5.490765	32.92574	0.107152	0.276218	1.926667
TN-1-20-Standard	5.417315	32.62504	0.103235	0.284967	1.946621
TN-1-21-Standard	5.462189	33.17977	0.101	0.2724	1.8734
TN-1-22-Standard	5.442551	32.83403	0.10359	0.277886	1.937225
TN-1-23-Standard	5.417049	32.87428	0.100047	0.281508	1.945673
TN-1-24-Standard	5.422485	32.71921	0.085222	0.29205	2.04118
TN-1-25-Standard	5.351598	32.58064	0.107618	0.290971	2.047024
TN-1-26-Standard	5.404595	32.89016	0.101788	0.29807	2.094125
TN-1-27-Standard	5.438511	32.69655	0.110237	0.305826	2.122719
TN-1-28-Standard	5.283482	31.77842	0.100806	0.293789	2.118592
TN-1-29-Standard	5.374499	32.53797	0.095644	0.299379	2.144095
TN-1-30-Standard	5.431814	32.73369	0.108372	0.298464	2.132146
TN-1-31-Standard	5.526031	33.12042	0.103	0.2847	1.9749
TN-1-32-Standard	5.402151	32.67306	0.111461	0.293698	2.018353
TN-1-33-Standard	5.385626	32.81109	0.097647	0.27842	2.041052
TN-1-34-Standard	5.523391	32.94994	0.10979	0.279483	1.998129
TN-1-35-Standard	5.495793	32.98666	0.103793	0.294944	2.141254
TN-1-36-Standard	5.458673	33.09392	0.098712	0.276295	1.931561
TN-1-37-Standard	5.462889	32.73408	0.102286	0.29403	2.074583
TN-1-38-Standard	5.417728	32.97085	0.108016	0.280249	1.864908
TN-1-39-Standard	5.419699	32.84821	0.118918	0.281593	1.960314
TN-1-40-Standard	5.267764	31.61776	0.096728	0.283497	2.030004
TN-1-41-Standard	5.360792	32.4618	0.103	0.2963	2.0906

TN-1-42-Standard	5.482941	32.65809	0.103383	0.294982	2.08483
TN-1-43-Standard	5.435228	32.52088	0.105215	0.290111	2.095807
TN-1-44-Standard	5.448619	33.12831	0.110119	0.269752	1.840347
TN-1-45-Standard	5.467294	33.26639	0.10906	0.264722	1.795014
TN-1-46-Standard	5.492335	32.82318	0.115	0.2742	1.9714
TN-1-47-Standard	5.441705	32.96844	0.105299	0.295814	1.92822
TN-1-48-Standard	5.411666	32.80792	0.106196	0.28923	1.951965
TN-1-49-Standard	5.376424	32.82832	0.101031	0.297741	2.001111
TN-1-50-Standard	5.279724	32.76307	0.099279	0.288558	1.984462
TN-1-51-Standard	5.415363	32.55547	0.102335	0.298478	2.059252
TN-1-52-Standard	5.386957	32.81186	0.109955	0.271894	1.83951
TN-1-53-Standard	5.479971	33.01076	0.115573	0.28516	1.895632
TN-1-54-Standard	5.420069	32.73799	0.103093	0.288529	1.940236
TN-1-55-Standard	5.087728	31.37773	0.086753	0.27671	1.987362
TN-1-56-Standard	5.37899	32.62733	0.114033	0.292492	2.037473
TN-1-57-Standard	5.410848	32.73974	0.11118	0.295534	2.108589
Average (wt%)	5.40457	32.6644	0.10236	0.28646	2.00688
Standard Deviation	0.07334	0.40095	0.00716	0.00945	0.08778
Standard Error: **(Std. Dev./(#runs*0.5))**	0.00312	0.01706	0.0003	0.0004	0.00374
Normalization Factor: **(Rowe's Value/Measured** **Avg. Standard Value)**	0.997304	1.031704	0.488469	0.942524	1.270631

Table A.3 <u>Major Elemental Concentrations at TN-1</u>

ELEMENTAL CONCENTRATION OF MAJOR ELEMENTS AT TN-1					
Sample ID	Al (wt%)	Si (wt%)	P (wt%)	Ti (wt%)	Fe (wt%)
TN-1-1	10.097	29.99161	0.031909	0.527865	0.414739
TN-1-2	4.859758	31.02031	0.184614	0.469933	2.973682
TN-1-3	9.271027	27.8904	0.025458	0.560546	0.472753

TN-1-4	10.52708	27.78602	0.035938	0.549003	1.028097
TN-1-5	9.885181	26.12856	0.025007	0.56389	0.618929
TN-1-6	11.37017	29.2033	0.026152	0.529368	0.772461
TN-1-7	9.057649	25.91321	0.016365	0.557187	0.386877
TN-1-8	9.563993	27.70574	0.020345	0.5341	0.590328
TN-1-9	9.416582	26.29315	0.02401	0.582745	0.688846
TN-1-10	5.903454	26.26898	0.124946	0.507772	4.863842
TN-1-11	11.45703	31.13668	0.043536	0.600148	0.583243
TN-1-12	7.57546	24.77228	0.083515	0.451104	2.767679
TN-1-13	8.013899	25.33062	0.162406	0.457754	3.603029
TN-1-14	8.076583	26.4327	0.128969	0.473898	3.558987
TN-1-15	8.391226	29.78535	0.057951	0.544736	0.802799
TN-1-16	7.664955	25.61285	0.155857	0.475372	2.402092
TN-1-17	7.046488	26.30786	0.027625	0.557528	0.204537
TN-1-18	6.688279	29.6072	0.066177	0.524282	0.648254
TN-1-19	9.196515	31.24914	0.03602	0.545459	0.505177
TN-1-20	7.967197	27.49579	0.057458	0.544762	0.688548
TN-1-21	9.483357	30.58931	0.033715	0.521668	0.482591
TN-1-22	7.2646	26.57316	0.075502	0.50371	1.029644
TN-1-23	7.383692	26.36764	0.053227	0.519239	0.915366
TN-1-24	7.576712	26.73864	0.149108	0.472769	3.361171
TN-1-25	7.666809	29.00185	0.108877	0.521943	1.705475
TN-1-26	8.23633	28.00065	0.111773	0.484977	2.909969
TN-1-27	7.054401	27.8321	0.100093	0.532902	0.987798
TN-1-28	7.211907	28.07488	0.056715	0.536998	0.563198
TN-1-29	7.186164	25.93683	0.054122	0.526573	1.021818
TN-1-30	6.839769	27.61211	0.136887	0.503083	3.24692
TN-1-31	7.795505	28.75214	0.086721	0.540369	0.526635
TN-1-32	7.403907	26.86284	0.133174	0.460161	2.912595
TN-1-33	6.673341	25.96316	0.078312	0.502022	1.028331

TN-1-34	7.082674	26.84404	0.108378	0.505531	1.494554
TN-1-35	6.174505	26.97398	0.181699	0.505748	2.352749
TN-1-36	7.804989	27.94048	0.060521	0.517731	0.544659
TN-1-37	5.974435	25.20137	0.229763	0.414557	4.48716
TN-1-38	6.319107	22.57111	0.268972	0.397273	5.282703
TN-1-39	6.894688	23.79356	0.179978	0.410128	3.993628
TN-1-40	6.115065	22.34174	0.227419	0.404725	4.74945
TN-1-41	6.342919	24.44979	0.192651	0.437664	4.404838
TN-1-42	6.033077	24.49383	0.191016	0.428892	3.965562
TN-1-43	5.74264	27.60996	0.307704	0.473565	3.673831
TN-1-44	6.543044	22.65354	0.425318	0.3869	4.66182
TN-1-45	6.927071	24.47714	0.224796	0.404602	4.645876
TN-1-46	6.438887	24.30832	0.236471	0.401172	5.117159
TN-1-47	7.510694	27.07492	0.135815	0.452455	2.94755
TN-1-48	6.025495	23.16887	0.067625	0.422416	1.025816
TN-1-49	6.320692	26.05844	0.16399	0.489541	2.04684
TN-1-50	6.108306	23.19206	0.071672	0.428335	1.286485
TN-1-51	7.501325	27.8519	0.102477	0.473432	1.024884
TN-1-52	7.610865	27.15937	0.061064	0.444091	0.82783
TN-1-53	6.692395	22.99544	0.062262	0.400396	1.700361
TN-1-54	7.354371	25.62739	0.224396	0.484803	2.379935
TN-1-55	7.93888	26.49332	0.073889	0.463593	1.487906
TN-1-56	7.71176	29.62284	0.091372	0.503982	1.110523
TN-1-57	7.922964	28.80733	0.08149	0.489106	0.825772

Table A.4 Standard Measurements of Minor Elemental Concentrations at TN-1

STANDARD FOR MINORS ELEMENTS AT TN-1						
Sample ID	Ba (ppm)	Ni (ppm)	Cu (ppm)	Zr (ppm)	Mo (ppm)	U(ppm)
TN-1-1-Standard	3376.191	133.1837	123.1156	112.1677	70.91367	7.379036
TN-1-2-Standard	2610.927	130.7856	111.1336	113.4071	71.30491	10.19922

TN-1-3-Standard	3357.625	133.1972	109.0706	111.8356	75.19036	5.963516
TN-1-4-Standard	3276.809	133.4483	110.7435	111.1477	72.84979	9.070022
TN-1-5-Standard	3691.488	126.239	108.9922	108.9326	72.74705	10.1755
TN-1-6-Standard	2635.847	123.8128	105.7869	111.7579	67.85822	5.437451
TN-1-7-Standard	3428.819	134.7395	108.8759	112.7133	77.58412	10.54475
TN-1-8-Standard	2494.58	133.0861	111.0137	111.8037	77.06069	11.19722
TN-1-9-Standard	2036.72	127.5809	110.5808	109.5333	80.52968	20.47885
TN-1-10-Standard	2418.278	138.2871	117.8479	116.4064	79.98983	18.85704
TN-1-11-Standard	2847.3	136.4374	115.4362	111.4821	71.74073	18.98067
TN-1-12-Standard	2237.073	139.6069	113.3632	114.6595	72.81718	15.41342
TN-1-13-Standard	2302.904	137.5717	115.9973	113.5148	75.9266	13.6767
TN-1-14-Standard	2153.796	134.4824	114.0184	111.6636	70.88705	14.92809
TN-1-15-Standard	1566.766	134.66	112.0443	111.5637	76.49598	20.07872
TN-1-16-Standard	3010.088	134.9477	114.6677	112.4455	80.3825	22.27361
TN-1-17-Standard	2612.666	130.8094	114.5659	110.7266	78.04814	21.49056
TN-1-18-Standard	1766.928	140.3015	113.7642	110.9758	76.216	17.42811
TN-1-19-Standard	1604.287	133.9756	112.0747	114.193	78.3018	20.9472
TN-1-20-Standard	2046.454	132.3276	116.6207	112.2497	76.17381	12.57443
TN-1-21-Standard	3481.503	130.1415	108.2725	108.1348	72.85289	10.25986
TN-1-22-Standard	2417.612	131.1243	111.5475	111.0334	72.25391	11.79742
TN-1-23-Standard	2738.689	139.4066	115.9186	108.7667	69.70199	10.83503
TN-1-24-Standard	2818.868	135.8471	115.1757	110.5857	74.70972	15.32516
TN-1-25-Standard	2207.403	139.7322	115.9295	111.0113	80.51189	19.44723
TN-1-26-Standard	2399.621	142.3285	112.1902	112.7814	77.956	18.62359
TN-1-27-Standard	1487.801	130.8059	112.1052	113.5049	75.68037	16.0635
TN-1-28-Standard	3463.303	137.781	112.7311	112.4571	79.0997	21.75999
TN-1-29-Standard	2911.694	130.6619	112.0152	114.1801	76.98689	20.33572
TN-1-30-Standard	2011.675	139.3588	116.1953	113.8401	72.26286	18.20848
TN-1-31-Standard	3171.779	133.9721	115.9105	109.9863	75.52789	11.34124
TN-1-32-Standard	2642.082	126.2751	111.5218	112.0098	74.66274	11.69257

TN-1-33-Standard	2928.43	135.7005	108.4322	111.6558	75.42525	12.77161
TN-1-34-Standard	2985.924	127.829	118.3897	112.9812	77.18179	18.46032
TN-1-35-Standard	3357.145	133.6419	114.8142	112.6517	75.46855	20.87621
TN-1-36-Standard	2449.41	133.1372	117.7071	113.0157	76.87335	17.07679
TN-1-37-Standard	1736.423	131.2239	112.0046	111.8358	77.97923	14.45991
TN-1-38-Standard	2167.733	138.0853	114.3923	111.7326	68.96353	11.52296
TN-1-39-Standard	3362.37	138.8302	114.3971	112.6076	75.26787	17.14202
TN-1-40-Standard	2040.269	134.0585	114.5919	113.9574	78.67671	16.89753
TN-1-41-Standard	3648.907	132.9735	111.1501	107.7172	75.91393	12.18665
TN-1-42-Standard	2770.235	136.3957	106.695	110.5189	76.82128	12.14042
TN-1-43-Standard	2652.159	135.1685	114.1138	113.7828	74.16692	16.38935
TN-1-44-Standard	2208.799	138.4418	110.8561	109.948	72.05996	11.03723
TN-1-45-Standard	2228.076	124.2534	111.4154	113.7881	71.13738	13.6494
TN-1-46-Standard	2703.744	136.4366	114.1695	113.2985	81.35301	18.51987
TN-1-47-Standard	1851.785	136.382	113.8904	113.1793	72.34609	10.93905
TN-1-48-Standard	2949.292	134.3479	110.8083	111.9639	73.8564	11.80565
TN-1-49-Standard	3515.213	133.6028	113.9348	111.9218	77.74904	19.83678
TN-1-50-Standard	2657.788	135.2578	112.9915	113.3727	76.42003	17.57518
TN-1-51-Standard	3708.874	135.6463	114.0519	109.5576	71.86483	7.601937
TN-1-52-Standard	3545.883	131.6182	104.9091	110.3096	70.43751	9.65375
TN-1-53-Standard	3037.282	131.8862	113.635	110.6676	66.65593	7.337246
TN-1-54-Standard	1723.07	137.721	111.3351	111.651	76.33277	12.05801
TN-1-55-Standard	2721.002	131.3756	106.4732	110.7728	67.58774	5.986039
TN-1-56-Standard	3624.189	135.8781	112.775	111.8773	73.10079	16.86998
TN-1-57-Standard	2724.898	136.278	115.3109	112.4733	76.37137	15.03723
Average (wt%)	2675.903	134.0892	112.8504	111.9072	74.82871	14.39675
Standard Deviation	610.6449	3.98915	3.299833	1.66606	3.455099	4.5637
Standard Error: **(Std.** **Dev./(#runs*0.5))**	21.42614	0.13997	0.115784	0.058458	0.121232	0.16013

Normalization Factor: (Rowe's Value/Measured Avg. Standard Value)	0.704061	1.141031	1.30261	0.848918	1.1092	1.180822

Table A.5 <u>Minor Elemental Concentrations at TN-1</u>

ELEMENTAL CONCENTRATION OF MINOR ELEMENTS AT TN-1					
Sample ID	Ba (ppm)	Ni (ppm)	Cu (ppm)	Zr (ppm)	Mo (ppm)	U(ppm)
TN-1-1	2796.562	40.29292	43.13429	208.0689	14.24837	1.234281
TN-1-2	1804.785	114.6258	74.99813	223.1161	209.6907	36.04767
TN-1-3	2728.912	26.5677	27.17504	220.5232	17.76035	18.1812
TN-1-4	2150.235	35.49811	47.35311	214.2202	13.43603	17.68893
TN-1-5	2923.393	32.78707	69.21917	214.0559	14.01565	66.65024
TN-1-6	2086.295	12.34853	10.31099	201.733	9.731234	3.662961
TN-1-7	3246.931	45.93862	23.3264	247.6035	18.37716	3.962089
TN-1-8	2815.067	15.11225	16.53353	228.5594	14.29537	6.206006
TN-1-9	2998.768	26.8735	26.844	219.7539	15.19844	30.57471
TN-1-10	1140.455	52.81038	21.65088	240.4874	22.74577	5.712793
TN-1-11	975.4502	16.23316	13.8884	237.605	13.40738	29.12852
TN-1-12	950.8356	121.6877	115.4939	191.2118	221.3658	42.1289
TN-1-13	424.6444	148.9994	88.91751	180.4943	302.3335	51.82696
TN-1-14	1191.37	128.7473	82.03502	198.1745	239.4953	50.65087
TN-1-15	1071.944	101.3282	55.61913	211.5355	127.9627	42.17685
TN-1-16	746.1285	65.25923	36.58048	200.9494	182.1411	42.28409
TN-1-17	394.6828	82.27144	15.04581	246.576	86.27358	38.44278
TN-1-18	1030.426	53.73515	33.89324	229.7239	99.87777	28.35018
TN-1-19	1389.084	19.91244	13.24347	246.8294	16.75052	30.57297
TN-1-20	964.7298	116.8979	24.98454	262.0066	126.5287	36.16794
TN-1-21	2824.651	18.74619	16.06601	220.9412	13.64968	13.64718

TN-1-22	1878.003	140.1108	50.47841	221.3868	190.9069	27.04634
TN-1-23	1593.039	121.8097	32.15124	232.456	165.1543	28.58007
TN-1-24	887.2824	176.6434	88.46697	207.1517	210.0805	44.19606
TN-1_25	1016.674	133.7491	58.25862	231.5472	203.5263	48.04652
TN-1-26	1073.71	145.443	68.20408	208.9628	203.1018	41.75966
TN-1-27	1043.56	97.52687	29.84466	235.4287	198.257	35.80058
TN-1-28	1848.653	73.06812	13.62683	248.9989	115.0481	39.91995
TN-1-29	1341.996	79.26995	27.23574	202.9237	133.9847	54.51587
TN-1-30	1141.772	115.4268	126.2015	207.253	181.8791	55.21665
TN-1-31	2328.941	71.98425	24.19136	235.2742	83.75442	38.0505
TN-1-32	1900.424	128.9762	55.74089	190.1549	221.9963	56.37565
TN-1-33	2567.091	55.9448	13.35413	211.1936	241.5482	35.7273
TN-1-34	2172.046	64.49279	14.11395	203.7031	238.4528	35.00618
TN-1-35	2467.688	119.6798	60.32837	271.4418	284.3633	40.64211
TN-1-36	2223.177	57.91059	26.93379	223.5413	166.9531	42.8235
TN-1-37	694.9502	90.11356	41.88078	200.7566	284.3697	35.15765
TN-1-38	489.4174	108.1469	85.14933	197.0312	299.6515	74.99912
TN-1-39	374.2689	124.6805	59.44528	152.3967	260.9421	79.86228
TN-1-40	204.7439	109.7544	55.75742	170.89	254.4447	72.00595
TN-1-41	1656.344	99.57137	58.91502	167.2059	238.9822	54.60887
TN-1-42	748.7063	104.0894	50.94469	185.1084	238.2272	56.64932
TN-1-43	1178.086	101.305	71.43105	209.1229	192.9302	31.38747
TN-1-44	309.4694	113.6742	257.6864	160.8586	264.159	79.94532
TN-1-45	636.9978	97.30315	64.67896	164.7137	246.0802	31.61481
TN-1-46	1045.584	116.3192	82.27137	156.9187	261.4015	63.70587
TN-1-47	1056.883	113.1693	64.53569	186.8455	219.0854	35.31172
TN-1-48	891.3649	90.9254	26.9844	159.7108	42.92614	32.65233
TN-1-49	1462.323	62.18833	24.44456	213.2439	144.8066	41.92087
TN-1-50	988.0045	100.9903	31.87185	165.9287	44.57547	30.83125
TN-1-51	2197.92	76.02241	28.10083	182.9267	40.63756	22.11376

TN-1-52	1845.668	98.83524	28.42142	170.6288	117.4453	22.78184
TN-1-53	1948.092	225.9327	373.296	166.244	163.2396	24.21753
TN-1-54	2006.465	51.44071	155.8594	182.0061	91.34531	50.39038
TN-1-55	1459.148	130.2139	44.10069	159.5126	61.55179	23.2535
TN-1-56	2129.872	133.711	112.8677	201.3766	47.41739	24.81345
TN-1-57	1614.909	519.3616	374.6975	191.351	45.78316	22.92938

Table A.6 Standard Measurements of Major Elemental Concentrations at AL-1

STANDARD FOR MAJOR ELEMENTS AT AL-1					
Sample ID	Al (wt%)	Si (wt%)	P (wt%)	Ti (wt%)	Fe (wt%)
AL-1-1-Standard	5.503281	32.94674	0.125845	0.2764	1.861535
AL-1-2-Standard	5.369208	32.7218	0.107951	0.284045	1.934528
AL-1-3-Standard	5.442613	32.65902	0.102216	0.291796	2.066169
AL-1-4-Standard	5.373517	32.55656	0.106616	0.30104	2.107565
AL-1-5-Standard	5.363252	32.6165	0.099202	0.298712	2.153753
AL-1-6-Standard	5.477309	33.02788	0.102393	0.264508	1.835257
AL-1-7-Standard	5.438406	32.98385	0.101858	0.280176	1.890631
AL-1-8-Standard	5.406388	32.84328	0.102938	0.276841	1.958322
AL-1-9-Standard	5.409135	32.68371	0.101328	0.287283	2.018521
AL-1-10-Standard	5.486536	32.8286	0.099	0.2811	2.0478
AL-1-11-Standard	5.507712	33.04265	0.103	0.2706	1.9087
AL-1-12-Standard	5.46888	33.06325	0.102334	0.279097	1.907713
AL-1-13-Standard	5.424738	32.83694	0.090983	0.283145	1.979446
AL-1-14-Standard	5.436537	32.5921	0.111102	0.286417	2.025442
AL-1-15-Standard	5.547403	33.13976	0.100383	0.266804	1.788542
AL-1-16-Standard	5.497877	32.94894	0.097627	0.280984	1.876966
AL-1-17-Standard	5.46979	32.84463	0.114156	0.285995	1.94243
AL-1-18-Standard	5.41283	32.79874	0.105921	0.278099	2.004991
AL-1-19-Standard	5.236649	31.30093	0.082626	0.284512	2.028363
AL-1-20-Standard	5.424443	32.69082	0.096181	0.289237	2.012983

AL-1-21-Standard	5.497505	33.15812	0.103	0.2807	1.8471
AL-1-22-Standard	5.403005	32.94999	0.095681	0.290154	1.92224
AL-1-23-Standard	5.4706	32.9116	0.103991	0.284286	1.922192
AL-1-24-Standard	5.481397	32.85701	0.099298	0.288942	2.009172
AL-1-25-Standard	5.382824	32.6945	0.089629	0.292182	1.957825
AL-1-26-Standard	5.315248	32.60583	0.092832	0.302082	2.059574
AL-1-27-Standard	5.435718	32.66803	0.101703	0.295287	2.057773
AL-1-28-Standard	5.439977	32.68005	0.093574	0.300536	2.060427
AL-1-29-Standard	5.471729	33.1721	0.099844	0.275301	1.801972
AL-1-30-Standard	5.407075	32.60907	0.098563	0.28316	1.947338
AL-1-31-Standard	5.425188	32.8531	0.098	0.2923	2.0052
AL-1-32-Standard	5.487981	33.06424	0.099032	0.259165	1.801874
AL-1-33-Standard	5.426937	32.94273	0.096463	0.270874	1.858748
AL-1-34-Standard	5.412572	32.67238	0.111452	0.283986	1.912964
AL-1-35-Standard	5.455936	32.80064	0.098356	0.280195	1.874182
AL-1-36-Standard	5.437772	32.75177	0.089221	0.282069	1.936486
AL-1-37-Standard	5.407484	32.74429	0.09508	0.278352	1.931762
AL-1-38-Standard	5.406484	32.63181	0.11098	0.287912	1.911663
AL-1-39-Standard	5.399068	32.67202	0.096526	0.29568	1.967668
AL-1-40-Standard	5.319012	32.03309	0.100392	0.276572	2.000861
AL-1-41-Standard	5.510751	33.09197	0.100	0.2865	1.8911
AL-1-42-Standard	5.414392	32.68397	0.091023	0.282867	1.904376
AL-1-43-Standard	5.396444	32.61824	0.092542	0.280231	1.933321
AL-1-44-Standard	5.461884	32.5264	0.09622	0.284667	2.030327
AL-1-45-Standard	5.381956	32.62887	0.091762	0.293104	2.000324
AL-1-46-Standard	5.441302	32.82914	0.113621	0.272196	1.85673
AL-1-47-Standard	5.446825	32.717	0.091753	0.27265	1.896796
AL-1-48-Standard	5.395727	32.69049	0.097333	0.286034	1.950588
AL-1-49-Standard	5.429926	32.62361	0.100829	0.29053	1.969553
AL-1-50-Standard	5.44733	32.63393	0.107648	0.298024	1.998553

AL-1-51-Standard	5.330741	32.45343	0.092015	0.274694	1.863315
AL-1-52-Standard	5.325413	32.46538	0.099892	0.28264	1.943674
AL-1-53-Standard	5.325816	32.39472	0.099932	0.295141	2.051542
AL-1-54-Standard	5.342209	32.2675	0.10773	0.292807	2.081842
AL-1-55-Standard	5.290249	32.26796	0.105384	0.295074	2.047126
AL-1-56-Standard	5.324026	32.26659	0.102116	0.300979	2.106261
AL-1-57-Standard	5.345885	32.48013	0.109532	0.296079	2.132422
AL-1-58-Standard	5.341433	32.25969	0.096452	0.300369	2.199712
AL-1-59-Standard	5.353918	32.39702	0.089481	0.303051	2.11482
AL-1-60-Standard	5.409809	32.46864	0.094562	0.313417	2.173078
AL-1-61-Standard	5.393581	32.81491	0.100	0.2861	1.9348
AL-1-62-Standard	5.412447	32.58262	0.101848	0.290005	2.016932
AL-1-63-Standard	5.35175	32.29055	0.096142	0.308292	2.114065
AL-1-64-Standard	5.336834	32.49953	0.096715	0.298299	2.144967
AL-1-65-Standard	5.331121	32.26876	0.101788	0.296651	2.189913
AL-1-66-Standard	5.382671	32.20363	0.090961	0.300567	2.141978
AL-1-67-Standard	5.307716	32.39494	0.088684	0.305584	2.195134
AL-1-68-Standard	5.376031	32.32081	0.09739	0.31143	2.22533
AL-1-69-Standard	5.234963	31.86316	0.087984	0.305361	2.246913
AL-1-70-Standard	5.294711	31.99877	0.104272	0.304446	2.218303
AL-1-71-Standard	5.346817	32.28497	0.108922	0.314289	2.202602
AL-1-72-Standard	5.355085	32.48432	0.09446	0.288885	2.013233
AL-1-73-Standard	5.334113	32.34509	0.087712	0.306197	2.163223
AL-1-74-Standard	5.343346	32.27421	0.088701	0.303795	2.167916
AL-1-75-Standard	5.319772	32.21248	0.100814	0.31604	2.214044
AL-1-76-Standard	5.390534	32.61532	0.109545	0.29463	2.090034
AL-1-77-Standard	5.343462	32.13651	0.102503	0.307963	2.1076
AL-1-78-Standard	5.291178	32.03518	0.091298	0.305611	2.149114
AL-1-79-Standard	5.304237	32.06614	0.088731	0.315795	2.2129
AL-1-80-Standard	5.215831	31.68232	0.101428	0.311193	2.249617

AL-1-81-Standard	5.435346	32.86249	0.095046	0.290955	2.129922
AL-1-82-Standard	5.354868	32.77455	0.10313	0.303292	2.069494
AL-1-83-Standard	5.38351	32.8602	0.089221	0.302508	2.197846
AL-1-84-Standard	5.37351	32.47394	0.092891	0.309598	2.249616
AL-1-85-Standard	5.401583	32.67645	0.112738	0.314733	2.251549
AL-1-86-Standard	5.48121	32.73058	0.091499	0.311206	2.241636
AL-1-87-Standard	5.37655	32.48276	0.093751	0.318846	2.279988
AL-1-88-Standard	5.357825	32.55036	0.102679	0.320693	2.297712
AL-1-89-Standard	5.414822	32.54187	0.094243	0.321393	2.316308
AL-1-90-Standard	5.385595	32.54078	0.088232	0.319387	2.274525
AL-1-91-Standard	5.361369	32.80732	0.095107	0.294653	2.072165
AL-1-92-Standard	5.490052	32.78556	0.089191	0.30307	2.159528
AL-1-93-Standard	5.385191	32.61955	0.093783	0.316253	2.238298
AL-1-94-Standard	5.384466	32.58912	0.087306	0.317132	2.242415
AL-1-95-Standard	5.38672	32.35757	0.088422	0.321192	2.299414
AL-1-96-Standard	5.421205	32.44395	0.089424	0.326503	2.341784
AL-1-97-Standard	5.369784	32.4425	0.108548	0.326482	2.334649
AL-1-98-Standard	5.405354	32.83085	0.104088	0.292471	2.149494
AL-1-99-Standard	5.316523	32.23738	0.092945	0.306665	2.317207
AL-1-100-Standard	5.420498	32.45989	0.109	0.3237	2.3191
Average (wt%)	5.39468	32.5881	0.09869	0.29459	2.06063
Standard Deviation	0.06394	0.31942	0.00751	0.01513	0.14486
Standard Error: (Std. Dev./(#runs*0.5))	0.00128	0.00639	0.00015	0.0003	0.0029
Normalization Factor: (Rowe's Value/Measured Avg. Standard Value)	0.999132	1.034121	0.506639	0.916514	1.237483

Table A.7 <u>Major Elemental Concentrations at AL-1</u>

ELEMENTAL CONCENTRATION OF MAJOR ELEMENTS AT AL-1

Sample ID	Al (wt%)	Si (wt%)	P (wt%)	Ti (wt%)	Fe (wt%)
AL-1-1	8.056957	26.27971	0.115463	0.44431	2.143917
AL-1-2	7.574866	27.93935	0.088867	0.490699	1.824315
AL-1-3	8.149477	28.89922	0.068216	0.509576	1.411621
AL-1-4	7.569524	27.54047	0.065279	0.522298	1.21165
AL-1-5	8.228608	28.85289	0.140093	0.500035	2.36568
AL-1-6	7.540613	28.18144	0.088286	0.484646	1.652803
AL-1-7	7.480554	31.26786	0.106885	0.475534	1.422814
AL-1-8	7.317183	24.01702	0.128618	0.434323	3.836503
AL-1-9	6.832581	24.39317	0.101095	0.460498	4.190725
AL-1-10	7.790446	32.03651	0.077885	0.511174	1.219481
AL-1-11	7.66248	29.54317	0.099119	0.47502	1.487032
AL-1-12	7.502146	31.0706	0.070238	0.496503	1.134788
Al-1-13	6.6245	30.09641	0.102185	0.440242	1.927116
AL-1-14	7.515981	28.73878	0.075155	0.49131	2.108566
AL-1-15	6.215066	25.38751	0.078812	0.427546	2.285025
AL-1-16	7.348802	26.55026	0.120301	0.455703	2.132424
AL-1-17	4.914124	29.25371	0.107706	0.497485	2.021346
AL-1-18	6.604533	26.04169	0.11838	0.469049	3.548784
AL-1-19	6.590448	28.47834	0.087064	0.497153	2.172072
Al-1-20	6.008902	27.64924	0.094351	0.47993	2.379977
AL-1-21	6.111989	31.23432	0.086436	0.458506	1.840207
AL-1-22	6.411917	31.35359	0.067224	0.462112	1.415125
AL-1-23	6.590604	30.98745	0.104036	0.468744	2.23018
AL-1-24	7.171592	30.24031	0.075768	0.482182	1.336706
AL-1-25	6.205363	28.3563	0.053828	0.458212	0.937904
AL-1-26	6.487864	31.07692	0.077921	0.483748	0.780459
AL-1-27	5.206001	31.01813	0.102738	0.432635	3.034679
AL-1-28	6.008474	33.89081	0.089585	0.393984	0.736143
AL-1-29	6.712179	33.39037	0.077098	0.452496	0.413296

AL-1-30	5.911147	29.89576	0.226017	0.389063	4.693777
AL-1-31	6.399876	34.01365	0.075398	0.458297	0.528059
AL-1-32	5.382702	28.86481	0.109403	0.386062	2.391776
AL-1-33	5.89067	33.80774	0.087759	0.481523	0.975907
AL-1-34	4.236453	32.7944	0.092181	0.444708	1.757598
AL-1-35	6.725785	30.52418	0.072052	0.516094	1.311789
AL-1-36	7.052894	30.72829	0.059209	0.513332	0.822761
AL-1-37	5.768415	32.45869	0.096398	0.488938	0.976166
AL-1-38	5.486471	34.75785	0.058605	0.48903	0.610301
AL-1-39	5.949703	35.86468	0.058605	0.48903	0.610301
AL-1-40	5.079192	33.49052	0.046231	0.451943	0.160444
AL-1-41	4.606116	33.04407	0.06984	0.388706	1.585564
AL-1-42	4.459501	32.91324	0.07933	0.373361	1.630712
AL-1-43	3.659874	33.37753	0.061529	0.364625	1.589694
AL-1-44	3.905171	34.39674	0.083144	0.417619	2.407108
AL-1-45	2.433124	36.66041	0.109031	0.255618	0.488838
AL-1-46	3.238171	37.24304	0.065365	0.32887	0.546562
AL-1-47	4.210568	34.33479	0.068853	0.350854	1.875349
AL-1-48	3.195433	32.52998	0.060562	0.363502	0.867537
AL-1-49	4.218008	33.7681	0.054193	0.371597	0.716287
AL-1-50	2.332907	37.57865	0.061345	0.301532	0.472085
AL-1-51	4.09926	32.76061	0.073272	0.370039	1.050776
AL-1-52	4.153974	31.06578	0.08813	0.428005	2.706006
AL-1-53	4.619236	36.52317	0.054774	0.435487	0.224664
AL-1-54	2.874258	36.36472	0.064426	0.305895	1.280637
AL-1-55	4.301371	33.85767	0.07744	0.425926	1.338632
AL-1-56	3.286181	35.14565	0.051566	0.365016	0.337257
AL-1-57	3.148189	35.23091	0.05962	0.372699	0.571921
AL-1-58	3.388868	37.24614	0.062969	0.406191	0.035329
AL-1-59	4.198716	35.83864	0.065834	0.478311	-0.00221

AL-1-60	3.650172	30.41946	0.101766	0.41302	4.341252
AL-1-61	2.819508	37.36154	0.098333	0.363566	0.508818
AL-1-62	2.856796	34.92017	0.076782	0.344907	1.25393
AL-1-63	3.786871	36.86281	0.061061	0.435407	0.023997
AL-1-64	3.403736	30.80843	0.060981	0.418412	1.470082
AL-1-65	3.585269	28.46976	0.126091	0.442683	2.051253
AL-1-66	3.609188	31.49838	0.140505	0.427095	2.102418
AL-1-67	3.84165	31.36067	0.063694	0.45299	1.505013
AL-1-68	2.93864	35.5277	0.075128	0.364761	1.635485
AL-1-69	3.804145	33.35862	0.089317	0.425306	1.710489
AL-1-70	3.963473	33.78057	0.073549	0.457135	1.147417
AL-1-71	3.52287	34.7364	0.074567	0.412209	1.685583
AL-1-72	4.759726	32.90131	0.080861	0.444777	1.654312
AL-1-73	3.73595	33.48639	0.07108	0.403322	1.435165
AL-1-74	4.668527	34.50291	0.067998	0.474908	1.082142
AL-1-75	3.988008	29.70313	0.098186	0.435412	3.349552
AL-1-76	5.021736	32.08946	0.07179	0.473296	1.696031
AL-1-77	4.745424	31.81987	0.061637	0.474194	1.69158
AL-1-78	4.104883	28.36267	0.08113	0.464379	2.952072
AL-1-79	4.471152	31.21939	0.046644	0.480812	0.620322
AL-1-80	4.635028	29.58032	0.076132	0.488429	2.218133
AL-1-81	4.01521	35.13954	0.078658	0.413356	1.401306
AL-1-82	4.026664	30.5737	0.091413	0.441628	2.898508
AL-1-83	4.62277	33.83042	0.066187	0.468952	1.307207
AL-1-84	4.147365	35.69159	0.073304	0.433265	0.876378
AL-1-85	4.522355	34.26907	0.066845	0.455608	1.574109
AL-1-86	4.475996	31.92576	0.09231	0.468632	2.842307
AL-1-87	4.4632	27.72814	0.051111	0.471022	1.880209
AL-1-88	5.525849	34.56361	0.07383	0.521391	0.99961
AL-1-89	5.116473	32.62187	0.086342	0.500196	1.947779

AL-1-90	4.478103	33.03446	0.07591	0.46307	1.803832
AL-1-91	4.171985	33.51472	0.075446	0.388617	1.978778
AL-1-92	5.150594	33.69665	0.046997	0.487261	0.180248
AL-1-93	6.301649	30.39008	0.056524	0.562513	1.155637
AL-1-94	5.98584	30.6413	0.058135	0.54698	1.270526
AL-1-95	6.275563	32.07274	0.057412	0.596295	0.906637
AL-1-96	5.845313	32.53322	0.093911	0.573544	1.08818
AL-1-97	4.913779	32.84696	0.060726	0.57001	0.476822
AL-1-98	5.717703	32.64258	0.134612	0.569324	1.456861
AL-1-99	4.921844	30.58204	0.059158	0.585215	0.862134
AL-1-100	6.056022	32.658	0.110616	0.594052	1.105863

Table A.8 Standard Measurements of Minor Elemental Concentrations at AL-1

Sample ID	Ba (ppm)	Ni (ppm)	Cu (ppm)	Zr (ppm)	Mo (ppm)	U(ppm)
AL-1-1-Standard	2856.85	134.4783	112.4638	113.5909	76.47336	11.71960658
AL-1-2-Standard	2951.266	134.2366	114.624	111.3843	74.29277	17.52561501
AL-1-3-Standard	2306.264	135.7144	120.6667	113.0191	72.35757	11.62417889
AL-1-4-Standard	2699.611	138.5218	116.6817	113.8027	71.28753	11.18828839
AL-1-5-Standard	1657.914	138.5428	114.1429	112.822	78.55832	19.0998211
AL-1-6-Standard	2100.087	131.522	111.569	114.2126	76.64381	15.77676695
AL-1-7-Standard	3194.534	134.4599	110.013	113.9247	80.8899	14.8626126

AL-1-8-Standard	3556.402	135.5531	113.7327	108.7662	70.09522	7.138117704
AL-1-9-Standard	2654.877	124.6831	104.0174	111.7991	73.41483	12.22140888
AL-1-10-Standard	2478.293	137.0415	110.2357	111.6857	71.97025	10.80461669
AL-1-11-Standard	3206.02	135.5704	113.3373	111.8327	75.82205	13.5193813
AL-1-12-Standard	3264.63	136.3285	110.8987	110.6383	75.41306	13.38280977
AL-1-13-Standard	2995.291	136.1192	110.1156	110.2182	68.58221	2.313827189
AL-1-14-Standard	1705.821	133.8053	112.9212	113.2382	75.39557	22.90773617
AL-1-15-Standard	3155.43	131.3338	108.0451	109.9631	70.69206	8.347751776
AL-1-16-Standard	2629.645	129.9983	106.6353	113.1822	75.2872	7.048553171
AL-1-17-Standard	2611.133	132.1691	113.626	109.7364	75.35234	15.54880196
AL-1-18-Standard	2571.268	137.1623	114.3839	111.2873	71.04501	12.99771682
AL-1-19-Standard	3572.865	132.0304	107.1147	111.1947	71.66178	8.560276693
AL-1-20-Standard	3212.251	134.5308	109.6241	109.0681	68.45288	5.240781614
AL-1-21-Standard	3354.735	135.0629	112.6237	111.3051	72.79482	9.038113003
AL-1-22-Standard	3210.488	131.5736	112.3738	111.1674	75.7315	15.81870651

AL-1-23-Standard	2058.32	138.4829	110.3233	111.51	71.65325	9.647527755
AL-1-24-Standard	2670.858	134.9522	113.6931	109.845	79.03115	13.58379508
AL-1-25-Standard	2772.637	130.4588	109.1501	111.4231	75.92327	8.889420625
AL-1-26-Standard	2155.579	134.4309	113.3632	111.5046	74.01396	9.965989802
AL-1-27-Standard	2826.441	135.1598	111.2534	112.1354	74.45755	12.82873841
AL-1-28-Standard	2440.828	131.7025	107.1958	112.1525	76.78169	13.38958577
AL-1-29-Standard	3553.235	140.7256	115.9874	113.5698	70.32554	12.84206447
AL-1-30-Standard	2233.891	136.1433	107.9757	111.1073	75.53802	14.01013174
AL-1-31-Standard	3373.866	133.7126	110.0704	108.7592	73.85517	12.00112191
AL-1-32-Standard	2236.693	134.1196	105.5501	107.4017	69.92091	9.408226017
AL-1-33-Standard	3487.431	134.3657	110.4845	111.441	74.50886	14.8795913
AL-1-34-Standard	1646.627	133.5981	110.7624	110.5076	72.79873	6.244183052
AL-1-35-Standard	2934.885	136.3524	115.6096	109.0371	77.33521	20.29457161
AL-1-36-Standard	2191.081	134.7082	110.7742	111.9436	78.37837	16.50273739
AL-1-37-Standard	3068.357	135.8137	113.3005	112.7349	74.7015	16.06212887

AL-1-38-Standard	2289.224	137.0891	108.7466	111.7639	74.43504	17.24745651
AL-1-39-Standard	2476.648	137.2655	110.0434	111.5184	74.39283	13.54611411
AL-1-40-Standard	2434.904	129.8537	109.4602	112.2959	76.64017	22.51872742
AL-1-41-Standard	4117.667	134.2583	111.911	108.7956	67.6746	1.712253704
AL-1-42-Standard	3363.957	132.106	108.571	110.236	73.20181	8.132344234
AL-1-43-Standard	2436.587	128.7778	105.2239	111.8157	76.51465	11.53166927
AL-1-44-Standard	3713.368	131.3965	107.7168	109.7676	72.45604	5.833069606
AL-1-45-Standard	3298.803	130.3414	111.5424	111.6532	78.33384	10.04528627
AL-1-46-Standard	2986.824	130.6693	112.8455	110.3456	76.22383	14.84366107
AL-1-47-Standard	2884.32	135.9119	113.2778	111.2956	76.37254	15.6172494
AL-1-48-Standard	2512.344	137.0934	111.5585	108.6121	76.31781	13.29273774
AL-1-49-Standard	3206.286	140.7324	110.6282	109.3454	75.90997	13.94229177
AL-1-50-Standard	2648.441	136.5977	108.6101	113.2267	69.99536	5.921528939
AL-1-51-Standard	2340.907	129.9886	115.4878	111.8319	69.30152	12.32535636
AL-1-52-Standard	3292.385	129.8134	113.417	110.6932	76.53883	12.71656434

AL-1-53-Standard	2542.385	132.5505	110.3658	113.6745	75.85676	15.88967133
AL-1-54-Standard	3682.17	133.3162	111.7116	111.3856	76.3361	5.956048904
AL-1-55-Standard	2731.933	134.6486	112.9337	113.7235	71.44508	5.140899664
AL-1-56-Standard	2836.654	130.9883	112.5414	113.8512	79.66822	14.47486613
AL-1-57-Standard	3119.568	134.5353	115.4869	112.9361	72.0571	13.10112478
AL-1-58-Standard	2758.969	131.7473	114.5734	113.3806	72.5251	10.82319272
AL-1-59-Standard	4353.573	128.3484	108.4998	108.7822	80.35161	11.07085086
AL-1-60-Standard	2408.057	137.475	113.5644	109.3454	72.15858	9.069786138
AL-1-61-Standard	3889.429	133.4965	109.9439	108.6296	76.35085	12.61380053
AL-1-62-Standard	3434.429	142.3265	112.9513	110.1389	74.2766	6.96187517
AL-1-63-Standard	2950.528	129.1902	111.9226	111.4785	74.90829	10.76193495
AL-1-64-Standard	3041.258	131.1656	114.3028	110.8737	73.85114	10.73809984
AL-1-65-Standard	3761.749	130.9682	108.5136	112.8191	71.4157	7.188241918
AL-1-66-Standard	2699.381	132.89	109.5425	110.8147	77.17631	17.4409042
AL-1-67-Standard	3069.113	130.8995	113.841	112.6634	76.12123	10.76119421

AL-1-68-Standard	3578.389	133.8157	111.5575	114.5289	74.15314	9.995936247
AL-1-69-Standard	2356.024	131.3028	114.3351	111.4714	68.76251	8.148396735
AL-1-70-Standard	2624.085	133.9768	108.5112	112.3878	71.8256	10.04570148
AL-1-71-Standard	2612.054	128.9466	112.5344	110.5635	72.65074	15.40595932
AL-1-72-Standard	2966.578	133.4851	112.8645	112.1663	66.97815	6.00467796
AL-1-73-Standard	2910.38	131.0377	109.769	109.7847	71.1048	6.895072748
AL-1-74-Standard	2886.322	134.3957	113.0901	110.2237	72.37694	4.17855654
AL-1-75-Standard	1749.298	127.221	107.6187	110.2633	73.48485	12.94393966
AL-1-76-Standard	1758.642	133.6432	113.9704	111.4059	77.36235	11.39915373
AL-1-77-Standard	2384.301	127.311	107.0722	112.3037	75.44788	12.36839877
AL-1-78-Standard	2823.733	130.7119	111.9066	112.8306	80.30733	23.26203271
AL-1-79-Standard	1990.595	137.4345	109.6746	110.0578	70.03439	4.131740774
AL-1-80-Standard	3209.661	132.1454	111.5832	110.4933	72.02271	9.578445087
AL-1-81-Standard	3487.992	134.8477	105.8259	108.0635	69.82851	2.355255368
AL-1-82-Standard	5011.077	127.8496	113.5537	108.6107	75.22598	4.774605636

AL-1-83-Standard	3502.733	136.8477	113.4229	110.7492	74.86624	8.01105646
AL-1-84-Standard	2704.162	136.3055	116.987	110.6033	77.44836	9.428783618
AL-1-85-Standard	3446.803	130.8272	106.751	112.0385	75.49811	13.03790525
AL-1-86-Standard	2848.93	130.5141	113.4385	110.5707	75.64626	12.10858284
AL-1-87-Standard	2211.001	130.8362	112.7742	113.3912	74.00916	14.0048073
AL-1-88-Standard	2274.128	135.42	111.929	108.511	75.01163	6.194793306
AL-1-89-Standard	2272.71	129.5052	110.7755	108.7684	77.31297	12.75936674
AL-1-90-Standard	3704.505	133.2164	114.4275	110.8736	73.65547	8.183553764
AL-1-91-Standard	2108.794	131.0789	114.5463	113.654	73.79205	10.4130235
AL-1-92-Standard	1697.524	131.0345	112.9734	113.863	69.7905	8.580660903
AL-1-93-Standard	3183.057	135.2531	117.859	112.8851	74.63626	7.976954419
AL-1-94-Standard	3140.425	133.3215	114.9824	113.5288	78.96222	14.53415129
AL-1-95-Standard	2853.505	131.3021	108.3843	110.4597	73.81911	7.693699915
AL-1-96-Standard	2428.92	131.6667	108.7997	111.298	73.453	10.98661782
AL-1-97-Standard	3884.852	131.2456	108.0926	114.3052	71.19893	5.536334673

AL-1-98-Standard	2354.269	135.2727	112.5398	113.5493	73.49452	10.89145759
AL-1-99-Standard	3758.347	136.1852	114.9813	112.7457	72.97133	8.030755025
AL-1-100-Standard	3418.418	133.5707	114.7603	111.8485	71.65509	7.456001158
Average (wt%)	2870.205	133.4313	111.5737	111.394	74.09032	11.15770483
Standard Deviation	620.0418	3.129647	2.976567	1.649521	2.941716	4.345370368
Standard Error: (Std. Dev./(#runs*0.5))	12.40084	0.062593	0.059531	0.03299	0.058834	0.086907407
Normalization Factor: (Rowe's Value/Measured Avg. Standard Value)	0.656399	1.146657	1.317515	0.852828	1.120254	1.523610837

Table A.9 Minor Elemental Concentrations at AL-1

ELEMENTAL CONCENTRATION OF MINORS ELEMENTS AT AL-1							
Sample ID	Ba (ppm)	Fe (ppm)	Ni (ppm)	Cu (ppm)	Zr (ppm)	Mo (ppm)	U(ppm)
AL-1-1	1562.4	44833.0	119.5	71.4	195.1	398.8	54.29312
AL-1-2	1871.2	27728.3	97.5	46.53659	214.3015	218.0086	89.5503
AL-1-3	1321.2	21222.3	75.2	21.6	203.2	219.2	44.0715
AL-1-4	1894.0	22658.6	76.7	18.9	215.3	227.6	37.3550
AL-1-5	2082.9	40925.4	131.8	82.5	208.6	189.3	59.3551
AL-1-6	1608.2	30987.0	90.0	37.3	224.5	161.7	45.7664
AL-1-7	1566.0	22628.5	75.1	62.3	263.3	102.3	34.3116
AL-1-8	2075.4	59361.6	96.4	47.0	174.8	227.8	48.8701
AL-1-9	1766.7	57775.7	76.7	25.3	207.2	193.1	36.3215

AL-1-10	2209.9	24747.3	79.2	63.3	245.0	60.2	35.5955
AL-1-11	1809.0	32827.9	88.2	44.4	219.8	192.6	42.4929
AL-1-12	1547.1	22435.1	58.2	50.1	225.8	35.1	79.2387
Al-1-13	1851.9	29561.7	120.8	68.0	230.5	59.6	57.2011
AL-1-14	1529.6	38788.3	90.3	53.5	212.4	161.3	215.5357
AL-1-15	2385.7	40703.0	73.6	20.7	215.1	194.6	35.8564
AL-1-16	1911.8	51098.9	101.7	50.9	180.5	263.1	49.3802
AL-1-17	2108.9	24165.6	64.8	10.3	374.2	187.8	33.9802
AL-1-18	1472.0	49101.6	83.2	14.0	204.1	248.6	21.5948
AL-1-19	1764.3	41138.0	83.5	13.5	209.4	204.5	15.9397
Al-1-20	2524.9	28825.9	71.5	12.4	211.8	158.5	17.6919
AL-1-21	1612.8	28762.5	63.5	12.0	239.2	114.9	18.6172
AL-1-22	2089.2	30354.8	63.0	14.9	204.7	113.6	21.3975
AL-1-23	1794.7	32948.9	82.2	10.1	212.4	193.6	20.1154
AL-1-24	1950.6	19973.7	66.9	16.5	208.9	141.7	24.7899
AL-1-25	1450.2	18319.5	54.0	11.4	192.5	134.3	14.3246
AL-1-26	2124.7	13750.6	58.1	12.0	209.2	115.9	22.6648
AL-1-27	1357.5	25314.0	50.6	9.4	204.6	154.0	22.7979
AL-1-28	1996.4	14386.6	64.2	15.6	146.7	145.4	81.4829
AL-1-29	1769.1	12628.8	42.1	11.3	196.8	114.4	19.5427
AL-1-30	1439.4	61717.0	77.5	50.8	182.9	184.8	38.1888
AL-1-31	2189.3	12214.9	37.5	7.2	202.2	140.3	12.5186
AL-1-32	2096.4	43863.6	131.9	84.3	188.2	219.2	59.2544
AL-1-33	2579.7	24366.0	65.2	14.6	247.0	151.0	9.2743
AL-1-34	1501.0	28033.1	59.7	8.9	301.5	168.0	4.8700
AL-1-35	1943.2	22417.2	51.4	9.4	241.2	101.1	10.9404
AL-1-36	1374.9	15718.1	46.3	7.4	244.8	56.0	11.8128
AL-1-37	2194.0	23477.8	67.4	60.5	271.1	24.1	9.0386
AL-1-38	1397.8	12731.7	20.1	7.4	286.5	34.2	6.4128
AL-1-39	1865.1	9004.0	14.9	7.0	257.2	36.0	11.5755

AL-1-40	1197.9	8399.1	47.7	12.0	216.2	109.6	12.3150
AL-1-41	1783.3	21295.3	46.2	6.2	167.1	84.6	5.4303
AL-1-42	1461.9	21398.5	49.7	6.6	168.9	112.6	9.5466
AL-1-43	1445.2	20660.1	44.2	14.9	187.4	92.1	6.5674
AL-1-44	1578.9	31290.8	49.3	10.5	189.2	117.3	9.9013
AL-1-45	813.1	9775.0	33.8	14.9	82.7	37.7	9.4052
AL-1-46	977.0	10835.7	39.9	9.1	95.0	34.4	13.5380
AL-1-47	1029.8	22059.9	46.7	8.9	158.9	117.8	10.8955
AL-1-48	1372.5	13010.0	41.7	13.0	139.8	62.6	12.0299
AL-1-49	954.5	28540.0	47.8	12.8	174.0	112.4	10.4795
AL-1-50	800.1	9813.1	34.4	4.9	121.5	63.9	7.9433
AL-1-51	899.9	24919.1	47.4	11.2	161.1	73.8	10.5986
AL-1-52	1374.5	16387.4	36.8	8.9	234.5	61.7	8.6233
AL-1-53	1484.2	10905.3	37.5	10.4	202.0	5.0	14.0351
AL-1-54	1070.4	14602.7	30.3	15.2	78.9	28.8	11.0166
AL-1-55	876.9	17718.0	38.5	11.3	199.6	72.8	14.4675
AL-1-56	827.8	9409.3	26.7	2.6	183.9	63.3	13.3716
AL-1-57	1028.1	9769.8	31.6	6.0	193.6	74.7	13.1146
AL-1-58	953.0	13833.1	36.0	5.7	194.0	104.5	11.7890
AL-1-59	2462.2	7344.8	35.4	5.7	199.7	60.3	3.8184
AL-1-60	1538.5	54597.1	59.2	16.4	196.4	134.6	11.0176
AL-1-61	1445.7	10375.2	35.5	3.9	148.8	70.2	11.9698
AL-1-62	1081.7	18121.0	32.4	5.0	206.0	88.7	12.3156
AL-1-63	1851.7	7470.8	39.9	7.1	234.6	107.6	12.9778
AL-1-64	1658.0	18119.7	56.1	15.9	119.8	62.5	13.4017
AL-1-65	1666.8	20926.4	46.9	5.7	246.9	105.0	11.0514
AL-1-66	1509.0	24371.1	41.3	29.5	212.0	72.8	14.6471
AL-1-67	1893.2	18556.8	41.7	8.6	198.0	97.4	11.8756
AL-1-68	1674.5	14107.7	37.4	9.3	201.0	103.2	10.0610
AL-1-69	1515.0	16785.7	57.0	8.1	213.8	183.3	11.2601

AL-1-70	1913.1	16158.6	39.7	8.1	247.9	120.0	7.0512
AL-1-71	1040.2	24871.0	40.4	11.5	205.1	62.2	9.1159
AL-1-72	1803.6	21320.7	42.6	13.0	214.5	52.1	9.5198
AL-1-73	2014.0	15671.1	38.6	8.7	190.5	73.2	6.9922
AL-1-74	2476.9	13613.4	45.4	8.7	227.9	73.3	7.4346
AL-1-75	1830.8	39964.2	56.9	32.0	200.8	115.4	9.6239
AL-1-76	1941.5	20386.2	45.2	14.2	234.8	49.7	7.3887
AL-1-77	2095.2	19053.1	41.0	20.1	231.6	29.1	4.5774
AL-1-78	1582.9	39356.3	39.5	12.5	277.2	36.3	5.2274
AL-1-79	1676.4	11145.6	32.8	8.8	256.8	67.0	9.2920
AL-1-80	1555.0	28388.8	49.8	81.1	213.5	99.4	7.3199
AL-1-81	1786.5	17486.2	37.4	14.0	212.9	83.7	4.9188
AL-1-82	1949.6	29883.2	55.3	15.2	201.1	145.7	9.9234
AL-1-83	2429.8	17437.9	51.8	11.4	228.4	141.8	8.2614
AL-1-84	1899.6	14694.0	51.8	9.3	211.5	105.2	7.1680
AL-1-85	1809.5	21783.2	46.6	15.9	192.6	95.1	7.8511
AL-1-86	1742.5	29549.9	226.5	13.1	218.0	61.6	6.8383
AL-1-87	1982.9	22290.1	47.3	22.2	209.5	52.9	11.3920
AL-1-88	2158.4	16890.6	51.2	25.5	209.3	40.5	8.0789
AL-1-89	1532.7	23965.9	54.5	19.1	215.9	47.0	7.3808
AL-1-90	1556.4	20227.5	38.5	19.9	225.8	55.3	7.9181
AL-1-91	991.8	27826.5	41.2	19.5	231.3	69.1	7.3405
AL-1-92	1752.3	7234.1	37.1	7.9	223.0	37.5	6.8475
AL-1-93	2217.1	16271.4	65.3	17.2	248.6	189.5	12.2753
AL-1-94	2133.7	26310.7	53.9	19.4	239.1	173.5	11.3892
AL-1-95	2357.3	15571.8	30.6	9.4	282.9	41.4	6.7736
AL-1-96	2169.7	18048.2	44.8	23.8	248.0	35.8	6.7808
AL-1-97	2253.5	11292.6	28.6	9.4	276.3	33.1	4.8922
AL-1-98	1982.0	21583.5	39.4	20.6	291.1	34.2	5.6624
AL-1-99	2107.5	16431.4	36.4	10.8	331.3	44.1	6.7882

AL-1-100	2077.8	16841.5	51.9	20.1	290.0	36.5	6.4176

Difference between chapters and appendices:

1. Chapters contain essential information, including tables and figures. Appendices are for supplemental data. There's no limit on the number of chapters or appendices.

2. From Chapter 1 on, the content and format of your research is up to you, your adviser(s), and your graduate committee. You have many choices on fonts, headings, paragraph style, tables, captions, etc. Consistency is essential.

3. For details, see the Graduate School Requirements and Guidelines for Electronic Theses, Dissertations, and Reports at k-state.edu/grad/etdr/create/guidelines.html.

Appendix B - ICPMS RESULTS

Table B.1 Result from ICPMS Analysis for TN-1

	La ppm	Ce ppm	Pr ppm	Nd ppm	Sm ppm	Eu ppm	Gd ppm	Tb ppm	Dy ppm	Ho ppm	Er ppm	Tm ppm	Yb ppm	Lu ppm
					ICPMS RESULTS FOR TN-1									
Sample ID	La ppm	Ce ppm	Pr ppm	Nd ppm	Sm ppm	Eu ppm	Gd ppm	Tb ppm	Dy ppm	Ho ppm	Er ppm	Tm ppm	Yb ppm	Lu ppm
KGO TN-1-5	46.39	96.00	11.69	44.33	8.88	1.68	6.71	1.07	6.22	1.26	3.57	0.55	3.60	0.55
KGO TN-1-7	45.74	91.71	10.83	39.96	7.75	1.52	6.73	1.16	7.04	1.43	4.07	0.63	4.00	0.63
KGO TN-1-14	34.19	70.76	8.80	35.44	7.52	1.61	7.07	1.09	6.16	1.22	3.31	0.50	3.09	0.48
KGO TN-1-20	39.34	80.29	10.01	39.61	8.43	1.70	7.33	1.15	6.56	1.29	3.53	0.53	3.19	0.49
KGO TN-1-26	39.28	77.18	9.57	37.05	7.32	1.50	6.86	1.12	6.53	1.33	3.61	0.56	3.46	0.52
KGO TN-1-33	37.64	70.89	8.58	32.14	6.13	1.24	5.46	0.87	5.14	1.06	3.03	0.46	2.90	0.46

KGO TN-1-39	39.35	73.98	9.14	35.57	7.09	1.45	6.92	1.03	5.99	1.23	3.37	0.49	2.97	0.46
KGO TN-1-44	47.82	100.25	13.07	54.36	11.78	2.58	12.27	1.82	10.39	2.08	5.55	0.76	4.33	0.65
KGO TN-1-53	33.91	56.04	7.95	30.38	5.99	1.23	5.52	0.92	5.75	1.22	3.60	0.60	3.81	0.61
KGO TN-1-55	35.25	58.37	8.60	33.10	6.49	1.30	5.88	0.98	5.74	1.19	3.45	0.56	3.45	0.53

Table B.2 Result from ICPMS Analysis for TN-1

ICPMS RESULTS FOR TN-1														
Sample ID	Ba ppm	Th ppm	Nb ppm	Y ppm	Hf ppm	Ta ppm	U ppm	Pb ppm	Rb ppm	Cs ppm	Sr ppm	Sc ppm	Zr ppm	Mo ppm
KGO TN-1-5	460	15.61	18.82	33.89	6.10	1.26	21.20	29.01	185.5	10.95	82	20.0	221	11
KGO TN-1-7	479	16.21	19.77	38.87	7.23	1.39	17.63	16.48	178.5	10.08	89	19.4	260	8

KGO TN-1-14	355	9.70	12.83	34.38	3.53	0.86	50.61	4.80	117.2	6.87	72	12.7	135	244
KGO TN-1-20	409	11.69	15.34	34.18	4.78	1.09	36.08	3.49	131.1	7.43	77	13.8	183	208
KGO TN-1-26	420	11.25	15.37	37.05	4.84	1.07	45.56	1.20	131.0	7.15	84	13.7	186	208
KGO TN-1-33	357	9.53	13.84	30.41	4.13	0.94	58.27	0.87	112.7	6.20	69	11.5	156	237
KGO TN-1-39	309	8.47	12.79	38.15	3.58	0.85	68.36	2.25	104.8	5.76	52	10.8	129	257
KGO TN-1-44	47.82	100.25	13.07	54.36	11.78	2.58	12.27	1.82	10.39	2.08	5.55	0.76	4.33	0.65
KGO TN-1-53	33.91	56.04	7.95	30.38	5.99	1.23	5.52	0.92	5.75	1.22	3.60	0.60	3.81	0.61

Sample ID	La ppm	Ce ppm	Pr ppm	Nd ppm	Sm ppm	Eu ppm	Gd ppm	Tb ppm	Dy ppm	Ho ppm	Er ppm	Tm ppm	Yb ppm	Lu ppm
KGO TN-1-55	35.25	58.37	8.60	33.10	6.49	1.30	5.88	0.98	5.74	1.19	3.45	0.56	3.45	0.53

Table B.3 Result from ICPMS Analysis for AL-1

ICPMS RESULTS FOR AL-1														
Sample ID	La ppm	Ce ppm	Pr ppm	Nd ppm	Sm ppm	Eu ppm	Gd ppm	Tb ppm	Dy ppm	Ho ppm	Er ppm	Tm ppm	Yb ppm	Lu ppm
KGO AL-1-11	40.15	78.18	9.40	35.47	6.20	1.08	4.79	0.76	4.48	0.93	2.61	0.41	2.55	0.39
KGO AL-1-20	36.94	70.70	8.61	32.33	6.09	1.19	5.31	0.86	5.20	1.11	3.05	0.47	2.99	0.46
KGO AL-1-28	6.59	12.06	1.47	5.63	1.39	0.44	2.18	0.46	3.32	0.74	2.08	0.30	1.71	0.28
KGO AL-1-34	36.29	64.00	7.94	28.79	5.14	0.92	4.22	0.72	4.46	0.96	2.83	0.45	2.95	0.47

Sample ID	La ppm	Ce ppm	Pr ppm	Nd ppm	Sm ppm	Eu ppm	Gd ppm	Tb ppm	Dy ppm	Ho ppm	Er ppm	Tm ppm	Yb ppm	Lu ppm
KGOAL-1-42	31.89	55.07	7.21	26.27	4.57	0.81	3.86	0.67	4.27	0.92	2.71	0.42	2.71	0.42
KGOAL-1-57	29.39	50.87	6.85	24.83	4.30	0.81	3.59	0.59	3.92	0.84	2.43	0.39	2.43	0.39
KGOAL-1-64	9.45	16.35	2.22	8.69	1.71	0.34	1.54	0.25	1.47	0.32	0.91	0.14	0.80	0.13
KGOAL-1-71	30.16	53.36	7.13	26.52	4.68	0.89	4.05	0.67	4.25	0.91	2.67	0.40	2.62	0.43
KGOAL-1-86	34.63	58.95	7.87	28.82	5.16	0.93	4.27	0.70	4.26	0.94	2.61	0.41	2.59	0.41
KGOAL-1-98	50.27	83.48	12.03	46.33	8.96	1.78	8.46	1.33	8.05	1.70	4.85	0.72	4.46	0.71

KGO AL-1-11	40.15	78.18	9.40	35.47	6.20	1.08	4.79	0.76	4.48	0.93	2.61	0.41	2.55	0.39
KGO AL-1-20	36.94	70.70	8.61	32.33	6.09	1.19	5.31	0.86	5.20	1.11	3.05	0.47	2.99	0.46
KGO AL-1-28	6.59	12.06	1.47	5.63	1.39	0.44	2.18	0.46	3.32	0.74	2.08	0.30	1.71	0.28
KGO AL-1-34	36.29	64.00	7.94	28.79	5.14	0.92	4.22	0.72	4.46	0.96	2.83	0.45	2.95	0.47
KGO AL-1-42	31.89	55.07	7.21	26.27	4.57	0.81	3.86	0.67	4.27	0.92	2.71	0.42	2.71	0.42
KGO AL-1-57	29.39	50.87	6.85	24.83	4.30	0.81	3.59	0.59	3.92	0.84	2.43	0.39	2.43	0.39
KGO AL-1-64	9.45	16.35	2.22	8.69	1.71	0.34	1.54	0.25	1.47	0.32	0.91	0.14	0.80	0.13

KGO AL-1-71	30.16	53.36	7.13	26.52	4.68	0.89	4.05	0.67	4.25	0.91	2.67	0.40	2.62	0.43
KGO AL-1-86	34.63	58.95	7.87	28.82	5.16	0.93	4.27	0.70	4.26	0.94	2.61	0.41	2.59	0.41

Table B.4 Result from ICPMS Analysis for AL-1

ICPMS RESULTS FOR AL-1													
Sample ID	Ba ppm	Th ppm	Nb ppm	Y ppm	Hf ppm	Ta ppm	U ppm	Pb ppm	Rb ppm	Cs ppm	Sr ppm	Sc ppm	Zr ppm	Mo ppm
KGO AL-1-11	376	8.96	15.79	26.83	5.24	1.07	36.70	8.28	127.6	6.88	75	11.6	194	124
KGO AL-1-20	343	9.32	14.64	31.13	5.08	0.98	48.87	5.91	109.9	5.78	69	11.1	191	167
KGO AL-1-28	247	1.29	2.36	25.47	0.81	0.15	118.35	7.31	15.0	0.75	100	1.6	31	22

KGO AL-1-34	281	9.00	15.65	28.82	6.45	1.07	17.63	7.16	95.9	5.23	58	8.7	240	123
KGO AL-1-42	246	7.04	13.34	28.35	5.71	0.91	14.88	10.03	80.7	4.38	52	7.7	207	78
KGO AL-1-57	251	6.88	12.43	25.58	4.08	0.86	14.27	9.90	91.9	5.12	51	9.1	152	90
KGO AL-1-64	88	2.26	3.69	9.72	1.44	0.26	13.20	3.90	21.0	1.11	44	2.1	54	28
KGO AL-1-71	241	7.74	12.57	26.54	4.68	0.89	13.69	7.25	81.4	4.61	57	8.1	169	52
KGO AL-1-86	261	7.86	13.96	26.94	5.24	0.97	10.25	6.60	92.8	5.30	60	8.4	191	33
KGO AL-1-98	300	11.94	17.72	50.55	7.33	1.24	15.53	6.23	110.5	6.42	68	10.8	268	8

Sample ID	Ba ppm	Th ppm	Nb ppm	Y ppm	Hf ppm	Ta ppm	U ppm	Pb ppm	Rb ppm	Cs ppm	Sr ppm	Sc ppm	Zr ppm	Mo ppm
KGO AL-1-11	376	8.96	15.79	26.83	5.24	1.07	36.70	8.28	127.6	6.88	75	11.6	194	124
KGO AL-1-20	343	9.32	14.64	31.13	5.08	0.98	48.87	5.91	109.9	5.78	69	11.1	191	167
KGO AL-1-28	247	1.29	2.36	25.47	0.81	0.15	118.35	7.31	15.0	0.75	100	1.6	31	22
KGO AL-1-34	281	9.00	15.65	28.82	6.45	1.07	17.63	7.16	95.9	5.23	58	8.7	240	123
KGO AL-1-42	246	7.04	13.34	28.35	5.71	0.91	14.88	10.03	80.7	4.38	52	7.7	207	78
KGO AL-1-57	251	6.88	12.43	25.58	4.08	0.86	14.27	9.90	91.9	5.12	51	9.1	152	90

KGOAL-1-64	88	2.26	3.69	9.72	1.44	0.26	13.20	3.90	21.0	1.11	44	2.1	54	28
KGOAL-1-71	241	7.74	12.57	26.54	4.68	0.89	13.69	7.25	81.4	4.61	57	8.1	169	52
KGOAL-1-86	261	7.86	13.96	26.94	5.24	0.97	10.25	6.60	92.8	5.30	60	8.4	191	33

Appendix C - XRD

This procedure for clay fraction is described in this section after Kübler et. al. (2000). This is widely accepted procedure for XRD analysis of clay fraction, which requires a separation of the fractions into the 2-16 µm and <2µm (supposed authigenic).

The six samples from the two locations were prepared by gently crushing them without letting them turn into powder. This ensures that the clay texture and crystallinity is not destroyed. After this step is the decarbonation procedure which must be conducted in a fume cupboard. It involves the following apparatus: 6 boiling flask; batch of 10% HCl (200 ml per sample). Mix 240 ml of 37% HCl with 760 ml of distilled water; six pieces of 400 ml centrifuge bottles; magnetic or glass stirrer and a balance (digital scale).

Firstly, in each boiling flask, about 3 tablespoon of the crushed sample were added in boiling flasks; and 100ml of HCl was added to each flask and a timer was set for twenty (20) minutes. During these 20 minutes, the flask was stirred periodically to ensure an even distribution of the samples in the flask. Upon completion of the time, the supernatant liquid (acid solution + suspended particles) is poured into the 400 ml centrifuge bottles with the solid left over disposed and the flask rinsed immediately to avoid leaving residue. Each centrifuge bottle is weighed, and the weight is adjusted with distilled water to be the same. This was set aside.

The next step after this is the acid wash, which involves washing each sample until it reaches a pH of 7 (via dilution with distilled water) to avoid reaction with the acid. These diluted samples are placed in a centrifuge bottle with equal weights and allowed to spin in the centrifuge for 10 minutes. This procedure is repeated until the samples starts to be cloudy.

Next step involves labelling slides (sample <2 and 2-16), then preparing vials for each sample. With the supernatant cloudy liquid, the water contained is disposed in the tube and 1/3 of the content in the bottle is mixed with distilled water and shaken vigorously. The vigorous shaking enabled the dislodging of the sediments platted to the walls of the bottle. Finally, the solution is poured into the labelled vials and in a 50ml centrifuge tubes up to the upper 45ml reference line.

For the <2µm clay size separation, the centrifuge tubes were covered tightly and shaken vigorously and then put into the centrifuge which was set up to rotate for 58seconds at 1000rpm. After this, the clay fraction is collected using a 50ml syringe until the solution reaches the lower

reference line of 35ml. The samples collected with the syringe is dropped on the labelled glass slide using a pipette. The remaining samples from each syringe in then poured into a clean vial labelled <2. The 50ml tubes are filled back with distilled water up till the reference line. The procedure in this paragraph is repeated 2-3 times to ensure that enough sample is collected. For every time the procedure is repeated, the solution is collected up to the reference line and disposed to ensure that no <2µm fraction is remaining.

To separate the 2-16µm clay size, the centrifuged tubes is filled to the upper reference line (45 ml) with distilled water and covered with a lid. This mixture is shaken vigorously and allowed to settle for 97seconds using a timer. It is important to note that gravity is the major means of separating the 2-16µm clay size. Upon completion of the time lapse, the clay fraction is collected using the syringe up to the lower reference line (35ml) and dropped onto the appropriate glass slide labelled 2-16. Rinsing the syringe in between samples lowers chances of cross contamination between samples.

This process is repeated for each sample, and they are allowed to air dry at room temperature in the laboratory. When dry, a cloudy stain is seen on the glass then it is dry. Should you want more smear on the slide, the clay solution stored in the vials can be used to improve the size of the smear.

Bulk Analysis

The results from the bulk analysis conducted on the eight samples is represented below
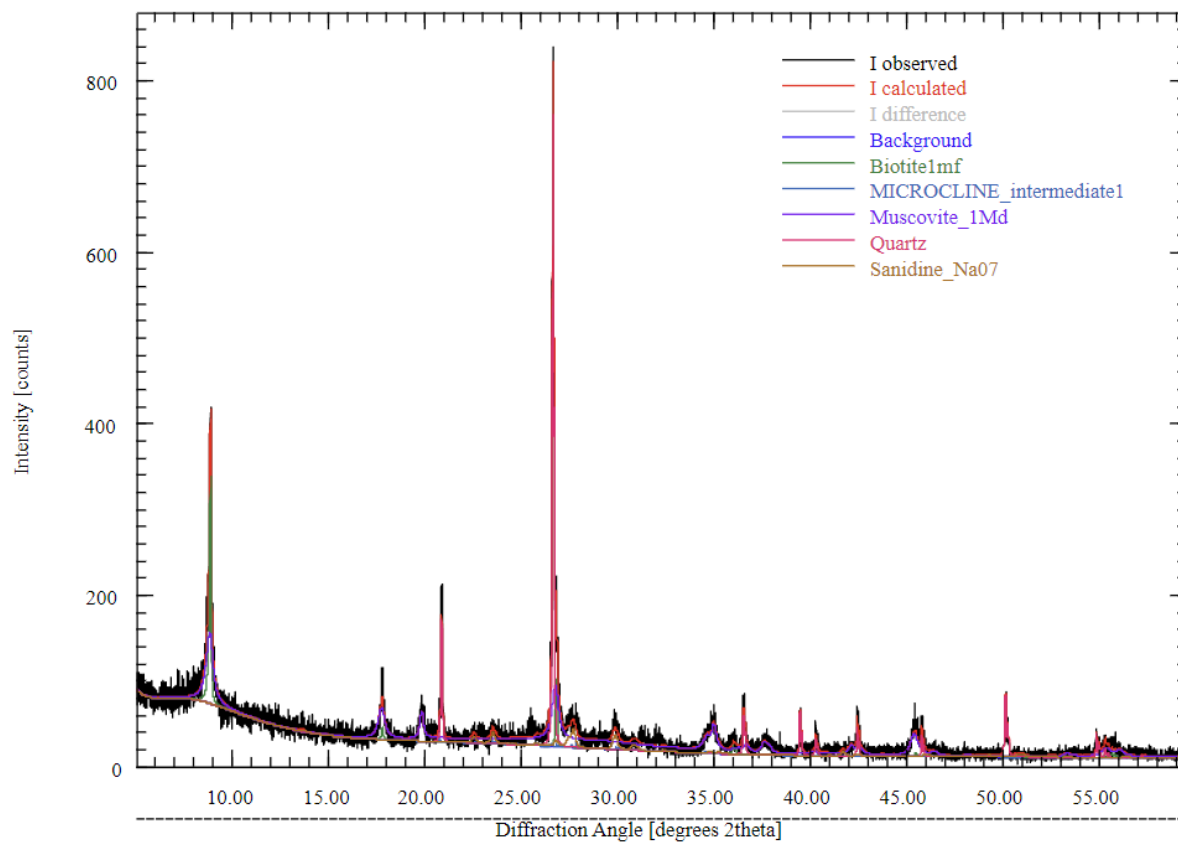
Figure C.6.1 Diffractogram (bulk analysis) for sample TN-1-6. Major peaks include biotite, microcline, muscovite, and quartz.
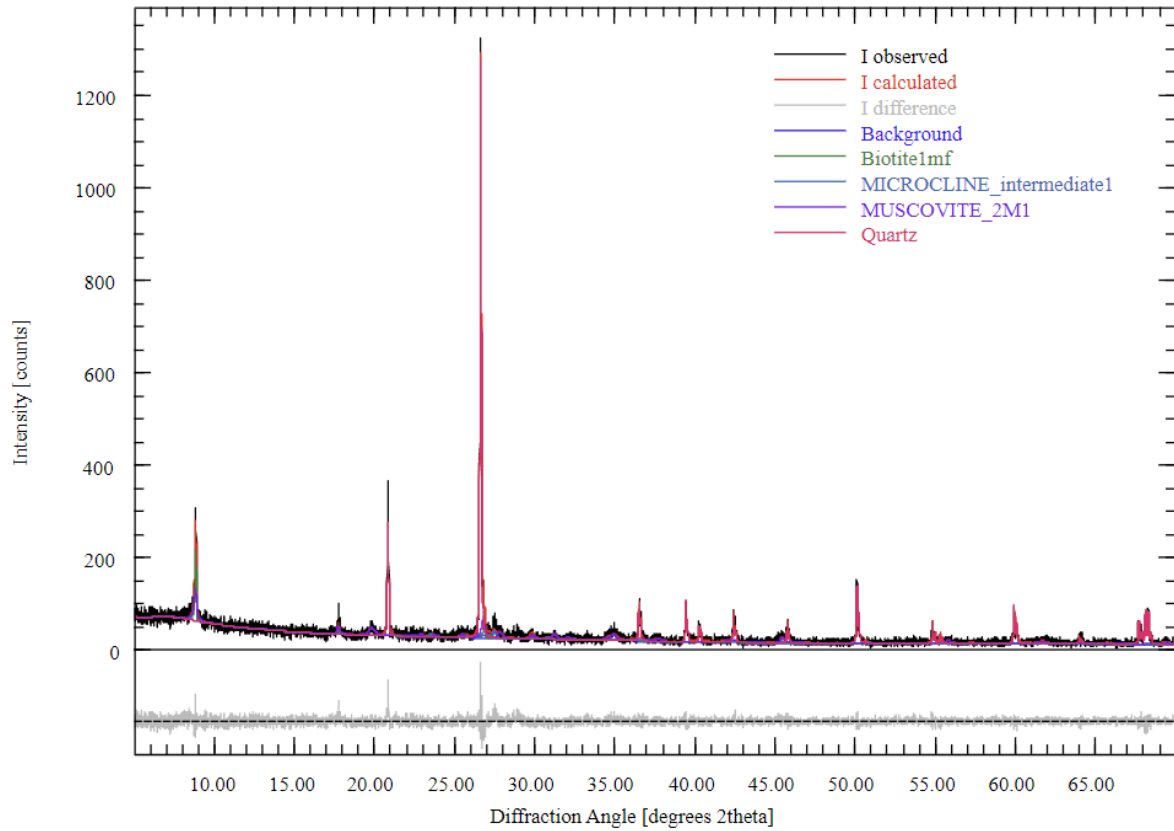
Figure C.6.2 Diffractogram (bulk analysis) for sample TN-1-10. Major peaks include biotite, microcline, muscovite, and quartz.
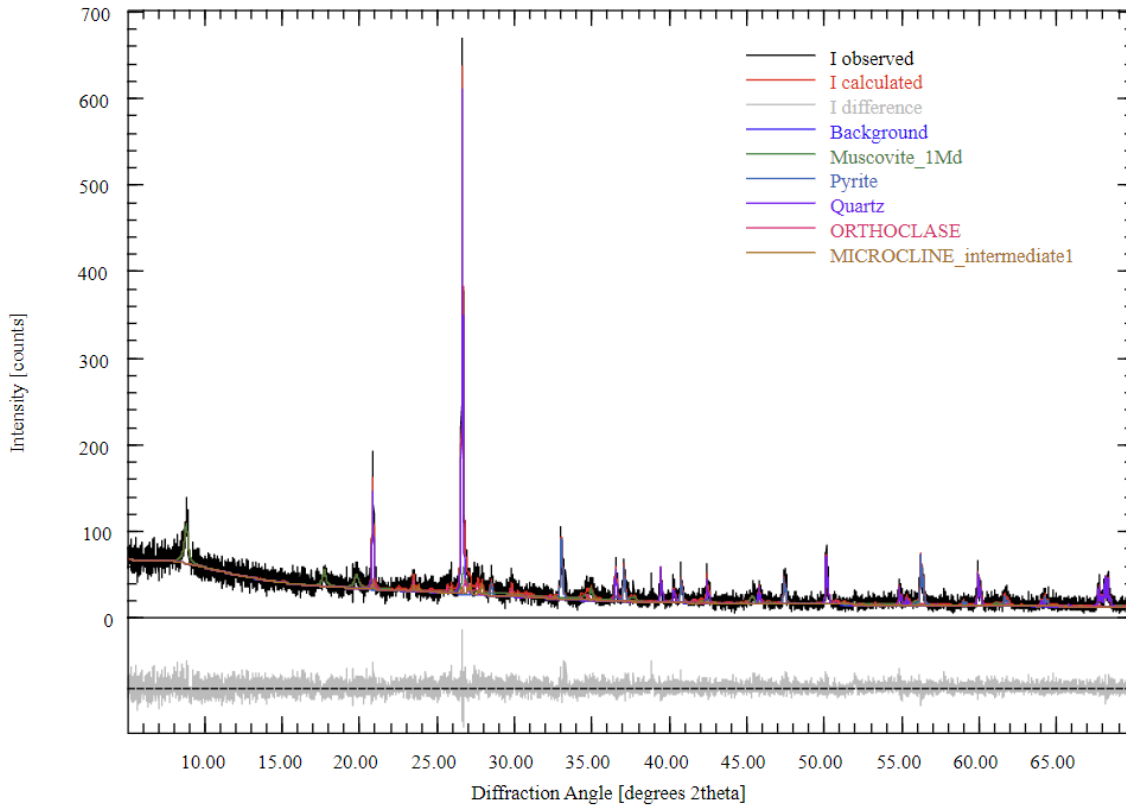
Figure C.6.3 Diffractogram (bulk analysis) for sample TN-1-46. Major peaks include biotite, microcline, muscovite, and quartz.
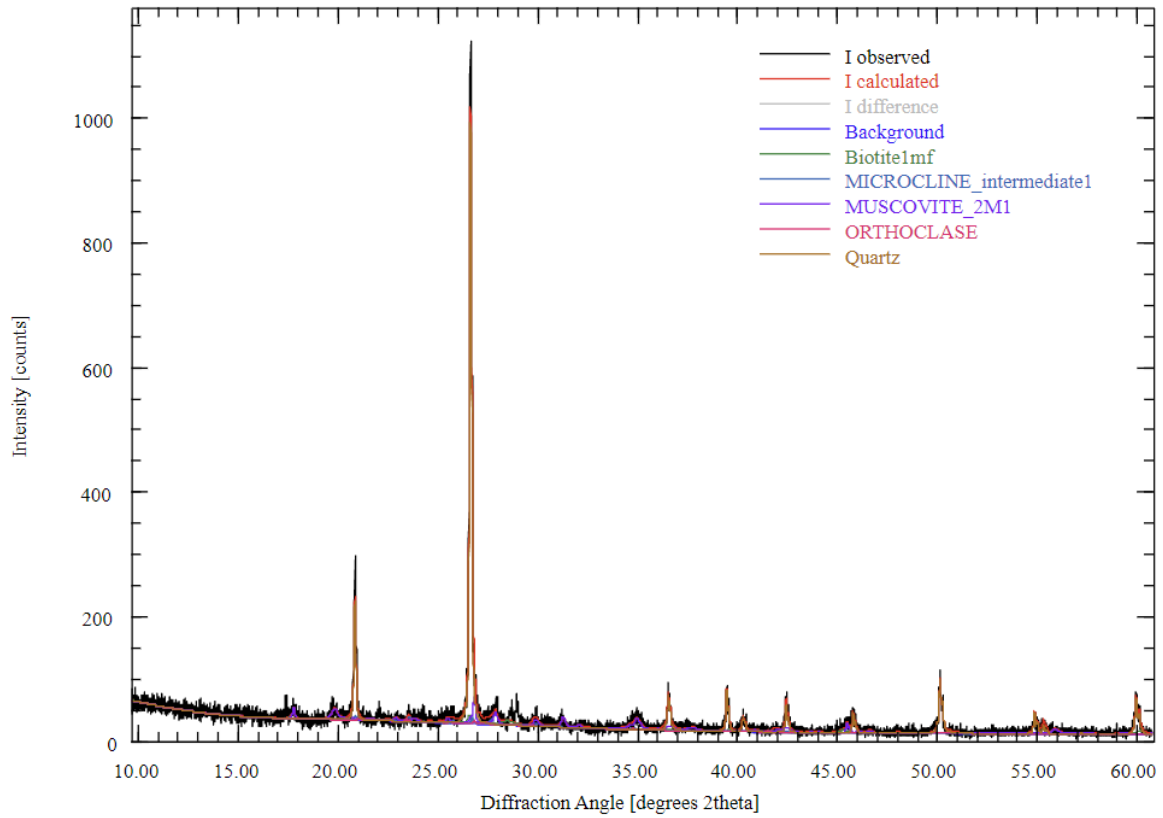
Figure C.6.4 Diffractogram (bulk analysis) for sample AL-1-22. Major peaks include biotite, microcline, muscovite, and quartz.
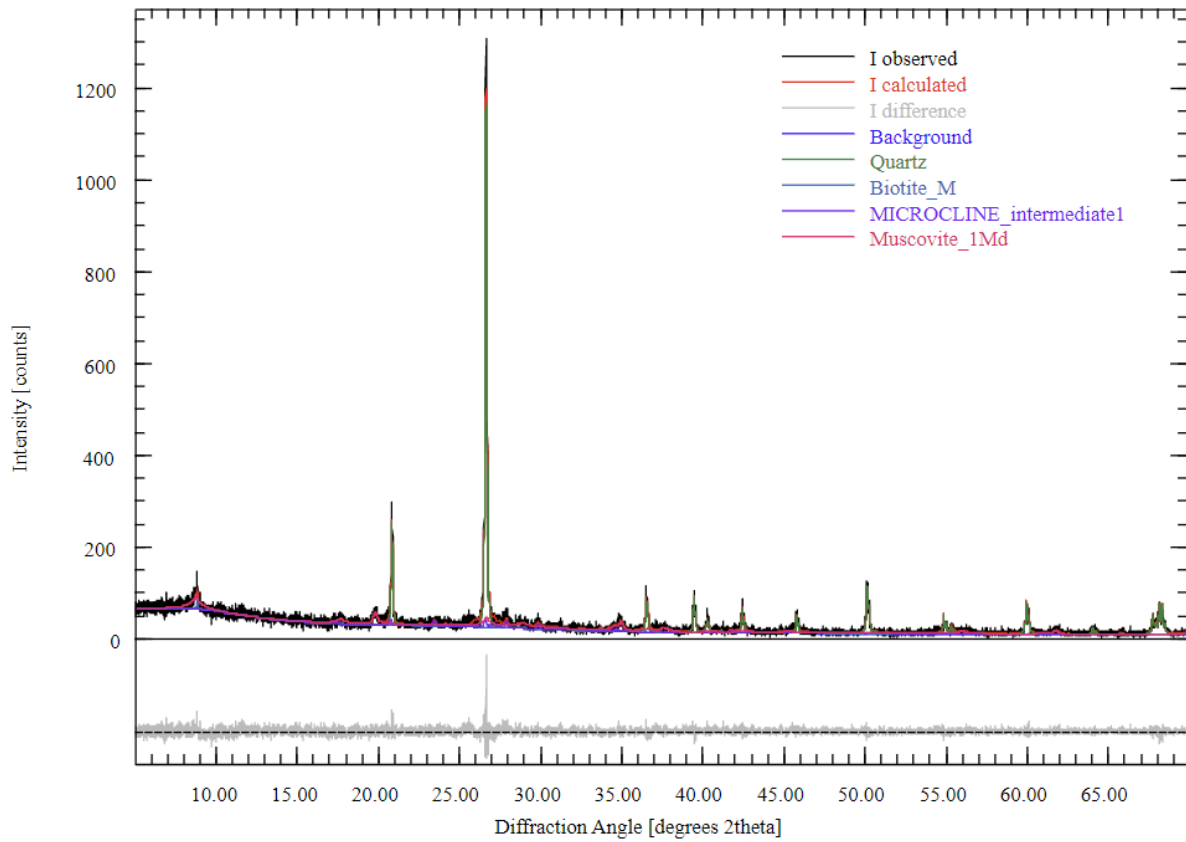
FigureC.5 Diffractogram (bulk analysis) for sample AL-1-86. Major peaks include biotite, microcline, muscovite, and quartz.

Appendix D - Tipping Point Analysis

The chemical indices used for the calculation of the individual statistical values are listed below. The python code for the analysis of the skewness, auto correlation factor (ACF) and variance are also shown below.

Table D.1 Chemical Indices for TN-1

CHEMICAL INDICES FOR TN-1									
Sample ID	Height (ft)	Si/Al	Ti/Al	Zr/Al	P/Al	Fe/Al	Ba/Al	Ni/Al	Cu/Al
TN-1-1	0.3333	3.0728	0.0494	0.0018	0.0015	0.0523	0.0196	0.0005	0.0006
TN-1-2	0.6667	6.6033	0.0914	0.0039	0.0186	0.7796	0.0262	0.0027	0.0020
TN-1-3	2.5000	3.1121	0.0571	0.0020	0.0013	0.0650	0.0208	0.0003	0.0004
TN-1-4	2.8300	2.7305	0.0493	0.0017	0.0017	0.1244	0.0144	0.0004	0.0006
TN-1-5	3.1600	2.7344	0.0539	0.0018	0.0012	0.0798	0.0209	0.0004	0.0009
TN-1-6	3.4900	2.6570	0.0440	0.0015	0.0011	0.0866	0.0130	0.0001	0.0001
TN-1-7	4.4800	2.9596	0.0581	0.0023	0.0009	0.0544	0.0253	0.0006	0.0003
TN-1-8	5.4700	2.9968	0.0528	0.0020	0.0010	0.0786	0.0208	0.0002	0.0002
TN-1-9	6.1300	2.8885	0.0585	0.0020	0.0012	0.0932	0.0225	0.0003	0.0004
TN-1-10	6.4600	4.6033	0.0813	0.0035	0.0104	1.0497	0.0136	0.0010	0.0005
TN-1-11	6.7900	2.8114	0.0495	0.0018	0.0019	0.0649	0.0060	0.0002	0.0002
TN-1-12	7.1200	3.3829	0.0563	0.0021	0.0054	0.4655	0.0089	0.0018	0.0020
TN-1-13	7.4500	3.2699	0.0540	0.0019	0.0099	0.5728	0.0037	0.0021	0.0014
TN-1-14	7.7922	3.3856	0.0555	0.0021	0.0078	0.5614	0.0104	0.0018	0.0013
TN-1-15	8.1344	3.6720	0.0614	0.0021	0.0034	0.1219	0.0090	0.0014	0.0009
TN-1-16	8.4766	3.4568	0.0586	0.0022	0.0100	0.3993	0.0069	0.0010	0.0006
TN-1-17	8.8188	3.8622	0.0748	0.0030	0.0019	0.0370	0.0040	0.0013	0.0003
TN-1-18	9.1610	4.5794	0.0741	0.0029	0.0048	0.1235	0.0109	0.0009	0.0007
TN-1-19	9.5032	3.5151	0.0561	0.0023	0.0019	0.0700	0.0107	0.0002	0.0002
TN-1-20	9.8454	3.5702	0.0646	0.0028	0.0035	0.1101	0.0085	0.0017	0.0004
TN-1-21	10.1876	3.3368	0.0520	0.0020	0.0017	0.0648	0.0210	0.0002	0.0002

TN-1-22	10.5298	3.7841	0.0655	0.0026	0.0051	0.1806	0.0183	0.0022	0.0009
TN-1-23	10.8720	3.6942	0.0665	0.0027	0.0035	0.1579	0.0152	0.0019	0.0006
TN-1-24	11.2142	3.6508	0.0590	0.0023	0.0096	0.5652	0.0083	0.0027	0.0015
TN-1_25	11.5564	3.9133	0.0643	0.0026	0.0070	0.2834	0.0094	0.0020	0.0010
TN-1-26	11.8986	3.5169	0.0556	0.0022	0.0066	0.4501	0.0092	0.0020	0.0011
TN-1-27	12.2408	4.0814	0.0714	0.0028	0.0069	0.1784	0.0104	0.0016	0.0006
TN-1-28	12.5830	4.0271	0.0704	0.0029	0.0039	0.0995	0.0181	0.0012	0.0002
TN-1-29	12.9252	3.7338	0.0693	0.0024	0.0037	0.1812	0.0132	0.0013	0.0005
TN-1-30	13.2673	4.1762	0.0695	0.0026	0.0098	0.6048	0.0118	0.0019	0.0024
TN-1-31	13.6095	3.8155	0.0655	0.0026	0.0054	0.0861	0.0211	0.0011	0.0004
TN-1-32	13.9517	3.7533	0.0587	0.0022	0.0088	0.5012	0.0181	0.0020	0.0010
TN-1-33	14.2939	4.0248	0.0711	0.0027	0.0057	0.1963	0.0272	0.0010	0.0003
TN-1-34	14.6361	3.9208	0.0675	0.0024	0.0075	0.2688	0.0216	0.0010	0.0003
TN-1-35	14.9783	4.5193	0.0774	0.0037	0.0144	0.4855	0.0282	0.0022	0.0013
TN-1-36	15.3205	3.7033	0.0627	0.0024	0.0038	0.0889	0.0201	0.0008	0.0005
TN-1-37	15.6627	4.3637	0.0656	0.0029	0.0188	0.9569	0.0082	0.0017	0.0009
TN-1-38	16.0049	3.6951	0.0594	0.0027	0.0208	1.0651	0.0055	0.0020	0.0018
TN-1-39	16.3471	3.5700	0.0562	0.0019	0.0128	0.7380	0.0038	0.0021	0.0011
TN-1-40	16.6893	3.7796	0.0625	0.0024	0.0182	0.9895	0.0024	0.0021	0.0012
TN-1-41	17.0315	3.9876	0.0652	0.0022	0.0149	0.8848	0.0184	0.0018	0.0012
TN-1-42	17.3737	4.2000	0.0672	0.0026	0.0155	0.8374	0.0088	0.0020	0.0011
TN-1-43	17.7159	4.9737	0.0779	0.0031	0.0262	0.8151	0.0145	0.0020	0.0016
TN-1-44	18.0581	3.5817	0.0559	0.0021	0.0318	0.9078	0.0033	0.0020	0.0051
TN-1-45	18.4003	3.6554	0.0552	0.0020	0.0159	0.8545	0.0065	0.0016	0.0012
TN-1-46	18.7425	3.9055	0.0589	0.0021	0.0180	1.0125	0.0115	0.0021	0.0017
TN-1-47	19.0847	3.7292	0.0569	0.0021	0.0089	0.5000	0.0099	0.0017	0.0011
TN-1-48	19.4269	3.9778	0.0663	0.0023	0.0055	0.2169	0.0104	0.0017	0.0006
TN-1-49	19.7691	4.2649	0.0732	0.0029	0.0127	0.4126	0.0163	0.0011	0.0005
TN-1-50	20.1113	3.9278	0.0663	0.0023	0.0057	0.2683	0.0114	0.0019	0.0007
TN-1-51	20.4535	3.8410	0.0596	0.0021	0.0067	0.1741	0.0207	0.0012	0.0005

TN-1-52	20.7957	3.6916	0.0551	0.0019	0.0039	0.1386	0.0171	0.0015	0.0005
TN-1-53	21.1379	3.5546	0.0565	0.0021	0.0046	0.3237	0.0205	0.0039	0.0073
TN-1-54	21.4801	3.6048	0.0623	0.0021	0.0149	0.4123	0.0193	0.0008	0.0028
TN-1-55	21.8223	3.4523	0.0552	0.0017	0.0046	0.2388	0.0130	0.0019	0.0007
TN-1-56	22.1645	3.9738	0.0618	0.0022	0.0058	0.1835	0.0195	0.0020	0.0019
TN-1-57	22.5067	3.7613	0.0583	0.0021	0.0050	0.1328	0.0144	0.0075	0.0062

Table D.2 Chemical Indices for TN-1

CHEMICAL INDICES FOR TN-1										
Sample ID	Height (ft)	Mo/Al	U/Al	Mo/Al (ICP MS)	U/Al (ICP MS)	EF Ni	EF Cu	EF Mo	EF U	EF Mo (ICP MS)	EF U (ICP MS)
TN-1-1	0.3333	0.0002	0.0000	0.0000	0.0000	1.8365	1.7955	8.4172	0.4158	0.0000	0.0000
TN-1-2	0.6667	0.0048	0.0009	0.0000	0.0000	10.8546	6.4862	257.3713	25.2328	0.0000	0.0000
TN-1-3	2.5000	0.0002	0.0002	0.0000	0.0000	1.3188	1.2320	11.4267	6.6711	0.0000	0.0000
TN-1-4	2.8300	0.0001	0.0002	0.0000	0.0000	1.5518	1.8906	7.6131	5.7161	0.0000	0.0000
TN-1-5	3.1600	0.0002	0.0008	0.0001	0.0002	1.5264	2.9430	8.4572	22.9361	5.9946	6.1769
TN-1-6	3.4900	0.0001	0.0000	0.0000	0.0000	0.4998	0.3811	5.1050	1.0959	0.0000	0.0000
TN-1-7	4.4800	0.0002	0.0001	0.0001	0.0002	2.3340	1.0824	12.1020	1.4880	4.8926	5.6080
TN-1-8	5.4700	0.0002	0.0001	0.0000	0.0000	0.7272	0.7266	8.9156	2.2074	0.0000	0.0000

110

TN-1-9	6.1300	0.0002	0.0004	0.0000	0.0000	1.3133	1.1981	9.6272	11.0452	0.0000	0.0000
TN-1-10	6.4600	0.0004	0.0001	0.0000	0.0000	4.1168	1.5414	22.9821	3.2919	0.0000	0.0000
TN-1-11	6.7900	0.0001	0.0003	0.0000	0.0000	0.6520	0.5095	6.9802	8.6487	0.0000	0.0000
TN-1-12	7.1200	0.0033	0.0007	0.0000	0.0000	7.3923	6.4077	174.2999	18.9180	0.0000	0.0000
TN-1-13	7.4500	0.0042	0.0008	0.0000	0.0000	8.5563	4.6633	225.0287	21.9996	0.0000	0.0000
TN-1-14	7.7922	0.0033	0.0007	0.0030	0.0006	7.3359	4.2690	176.8744	21.3335	162.6494	18.0515
TN-1-15	8.1344	0.0017	0.0006	0.0000	0.0000	5.5571	2.7858	90.9606	17.0983	0.0000	0.0000
TN-1-16	8.4766	0.0026	0.0007	0.0000	0.0000	3.9181	2.0058	141.7405	18.7660	0.0000	0.0000
TN-1-17	8.8188	0.0014	0.0006	0.0000	0.0000	5.3731	0.8974	73.0299	18.5586	0.0000	0.0000
TN-1-18	9.1610	0.0017	0.0005	0.0000	0.0000	3.6973	2.1299	89.0738	14.4193	0.0000	0.0000
TN-1-19	9.5032	0.0002	0.0004	0.0000	0.0000	0.9964	0.6052	10.8643	11.3088	0.0000	0.0000
TN-1-20	9.8454	0.0018	0.0005	0.0026	0.0005	6.7522	1.3180	94.7282	15.4426	140.4552	13.0457
TN-1-21	10.1876	0.0002	0.0002	0.0000	0.0000	0.9097	0.7120	8.5853	4.8954	0.0000	0.0000
TN-1-22	10.5298	0.0029	0.0004	0.0000	0.0000	8.8757	2.9204	156.7493	12.6649	0.0000	0.0000
TN-1-23	10.8720	0.0025	0.0005	0.0000	0.0000	7.5919	1.8301	133.4173	13.1672	0.0000	0.0000

TN-1-24	11.2142	0.0031	0.0007	0.0000	0.0000	10.7291	4.9074	165.3867	19.8429	0.0000	0.0000
TN-1_25	11.5564	0.0030	0.0007	0.0000	0.0000	8.0283	3.1937	158.3439	21.3182	0.0000	0.0000
TN-1-26	11.8986	0.0027	0.0006	0.0025	0.0006	8.1265	3.4804	147.0875	17.2475	135.7576	15.9367
TN-1-27	12.2408	0.0031	0.0006	0.0000	0.0000	6.3622	1.7781	167.6347	17.2637	0.0000	0.0000
TN-1-28	12.5830	0.0018	0.0007	0.0000	0.0000	4.6625	0.7941	95.1536	18.8297	0.0000	0.0000
TN-1-29	12.9252	0.0021	0.0009	0.0000	0.0000	5.0764	1.5929	111.2125	25.8065	0.0000	0.0000
TN-1-30	13.2673	0.0030	0.0010	0.0000	0.0000	7.7662	7.7549	158.6123	27.4620	0.0000	0.0000
TN-1-31	13.6095	0.0012	0.0006	0.0000	0.0000	4.2495	1.3043	64.0854	16.6043	0.0000	0.0000
TN-1-32	13.9517	0.0033	0.0009	0.0000	0.0000	8.0167	3.1642	178.8464	25.9020	0.0000	0.0000
TN-1-33	14.2939	0.0040	0.0006	0.0036	0.0009	3.8580	0.8411	215.9018	18.2121	191.1103	25.1527
TN-1-34	14.6361	0.0037	0.0006	0.0000	0.0000	4.1904	0.8375	200.8171	16.8132	0.0000	0.0000
TN-1-35	14.9783	0.0051	0.0008	0.0000	0.0000	8.9200	4.1065	274.7052	22.3912	0.0000	0.0000
TN-1-36	15.3205	0.0024	0.0006	0.0000	0.0000	3.4145	1.4504	127.5904	18.6644	0.0000	0.0000
TN-1-37	15.6627	0.0053	0.0007	0.0000	0.0000	6.9413	2.9462	283.9109	20.0183	0.0000	0.0000
TN-1-38	16.0049	0.0053	0.0014	0.0000	0.0000	7.8760	5.6634	282.8502	40.3742	0.0000	0.0000

TN-1-39	16.3471	0.0042	0.0014	0.0037	0.0010	8.3220	3.6237	225.7486	39.4031	200.5868	28.5627
TN-1-40	16.6893	0.0046	0.0014	0.0000	0.0000	8.2597	3.8322	248.1921	40.0563	0.0000	0.0000
TN-1-41	17.0315	0.0042	0.0010	0.0000	0.0000	7.2242	3.9038	224.7357	29.2872	0.0000	0.0000
TN-1-42	17.3737	0.0044	0.0011	0.0000	0.0000	7.9398	3.5490	235.5310	31.9418	0.0000	0.0000
TN-1-43	17.7159	0.0037	0.0006	0.0000	0.0000	8.1183	5.2279	200.3938	18.5929	0.0000	0.0000
TN-1-44	18.0581	0.0045	0.0014	0.0050	0.0013	7.9952	16.5525	240.8138	41.5639	270.5530	36.0949
TN-1-45	18.4003	0.0040	0.0005	0.0000	0.0000	6.4643	3.9243	211.8959	15.5255	0.0000	0.0000
TN-1-46	18.7425	0.0045	0.0012	0.0000	0.0000	8.3135	5.3702	242.1547	33.6567	0.0000	0.0000
TN-1-47	19.0847	0.0032	0.0006	0.0000	0.0000	6.9341	3.6114	173.9919	15.9935	0.0000	0.0000
TN-1-48	19.4269	0.0008	0.0006	0.0000	0.0000	6.9444	1.8822	42.4937	18.4342	0.0000	0.0000
TN-1-49	19.7691	0.0025	0.0008	0.0000	0.0000	4.5278	1.6254	136.6531	22.5616	0.0000	0.0000
TN-1-50	20.1113	0.0008	0.0006	0.0000	0.0000	7.6086	2.1930	43.5282	17.1701	0.0000	0.0000
TN-1-51	20.4535	0.0006	0.0003	0.0000	0.0000	4.6639	1.5745	32.3136	10.0283	0.0000	0.0000
TN-1-52	20.7957	0.0017	0.0004	0.0000	0.0000	5.9762	1.5695	92.0444	10.1826	0.0000	0.0000
TN-1-53	21.1379	0.0027	0.0004	0.0023	0.0005	15.5361	23.4435	145.4922	12.3098	124.2210	13.4074

TN-1-54	21.4801	0.0014	0.0008	0.0000	0.0000	3.2189	8.9072	74.0860	23.3080	0.0000	0.0000
TN-1-55	21.8223	0.0009	0.0003	0.0008	0.0004	7.5482	2.3347	46.2463	9.9640	42.4951	10.5245
TN-1-56	22.1645	0.0007	0.0004	0.0000	0.0000	7.9792	6.1513	36.6758	10.9455	0.0000	0.0000
TN-1-57	22.5067	0.0006	0.0003	0.0000	0.0000	30.1666	19.8767	34.4678	9.8448	0.0000	0.0000

Table D.3 Chemical Indices for AL-1

CHEMICAL INDICES FOR AL-1									
Sample ID	Height (ft)	Si/Al	Ti/Al	Zr/Al	P/Al	Fe/Al	Ba/Al	Ni/Al	Cu/Al
AL-1-1	0.3565	3.3760	0.0506	0.0021	0.0073	0.3296	0.0127	0.0017	0.0012
AL-1-2	0.7131	3.8176	0.0594	0.0024	0.0059	0.2983	0.0162	0.0015	0.0008
AL-1-3	1.0696	3.6703	0.0574	0.0021	0.0042	0.2145	0.0107	0.0011	0.0003
AL-1-4	1.4261	3.7657	0.0633	0.0024	0.0044	0.1983	0.0164	0.0012	0.0003
AL-1-5	1.7827	3.6292	0.0557	0.0022	0.0086	0.3561	0.0166	0.0018	0.0013
AL-1-6	2.1392	3.8682	0.0590	0.0025	0.0059	0.2715	0.0140	0.0014	0.0007
AL-1-7	2.4957	4.3263	0.0583	0.0030	0.0072	0.2356	0.0138	0.0012	0.0011
AL-1-8	2.8523	3.3972	0.0544	0.0020	0.0089	0.6494	0.0186	0.0015	0.0008
AL-1-9	3.2088	3.6951	0.0618	0.0026	0.0075	0.7597	0.0170	0.0013	0.0005
AL-1-10	3.5653	4.2563	0.0602	0.0027	0.0051	0.1939	0.0186	0.0012	0.0011
AL-1-11	3.9219	3.9906	0.0569	0.0024	0.0066	0.2404	0.0155	0.0013	0.0008
AL-1-12	4.2784	4.2866	0.0607	0.0026	0.0047	0.1873	0.0135	0.0009	0.0009
Al-1-13	4.6349	4.7023	0.0610	0.0030	0.0078	0.3603	0.0184	0.0021	0.0014
AL-1-14	4.9915	3.9576	0.0600	0.0024	0.0051	0.3475	0.0134	0.0014	0.0009
AL-1-15	5.3480	4.2279	0.0631	0.0030	0.0064	0.4554	0.0252	0.0014	0.0004
AL-1-16	5.7045	3.7394	0.0569	0.0021	0.0083	0.3594	0.0171	0.0016	0.0009
AL-1-17	6.0611	6.1615	0.0929	0.0065	0.0111	0.5095	0.0282	0.0015	0.0003

AL-1-18	6.4176	4.0811	0.0651	0.0026	0.0091	0.6655	0.0146	0.0014	0.0003
AL-1-19	6.7741	4.4725	0.0692	0.0027	0.0067	0.4082	0.0176	0.0015	0.0003
Al-1-20	7.1307	4.7625	0.0733	0.0030	0.0080	0.4906	0.0276	0.0014	0.0003
AL-1-21	7.4872	5.2893	0.0688	0.0033	0.0072	0.3729	0.0173	0.0012	0.0003
AL-1-22	7.8437	5.0611	0.0661	0.0027	0.0053	0.2734	0.0214	0.0011	0.0003
AL-1-23	8.2003	4.8664	0.0652	0.0028	0.0080	0.4191	0.0179	0.0014	0.0002
AL-1-24	8.5568	4.3643	0.0617	0.0025	0.0054	0.2309	0.0179	0.0011	0.0003
AL-1-25	8.9133	4.7297	0.0677	0.0026	0.0044	0.1872	0.0154	0.0010	0.0002
AL-1-26	9.2699	4.9578	0.0684	0.0028	0.0061	0.1490	0.0215	0.0010	0.0002
AL-1-27	9.6264	6.1668	0.0762	0.0034	0.0100	0.7220	0.0171	0.0011	0.0002
AL-1-28	9.9829	5.8380	0.0601	0.0021	0.0076	0.1517	0.0218	0.0012	0.0003
AL-1-29	10.3395	5.1488	0.0618	0.0025	0.0058	0.0763	0.0173	0.0007	0.0002
AL-1-30	10.6960	5.2346	0.0604	0.0026	0.0194	0.9835	0.0160	0.0015	0.0011
AL-1-31	11.0525	5.5009	0.0657	0.0027	0.0060	0.1022	0.0225	0.0007	0.0001
AL-1-32	11.4091	5.5503	0.0658	0.0030	0.0103	0.5503	0.0256	0.0028	0.0021
AL-1-33	11.7656	5.9402	0.0750	0.0036	0.0076	0.2052	0.0288	0.0013	0.0003
AL-1-34	12.1221	8.0121	0.0963	0.0061	0.0110	0.5138	0.0233	0.0016	0.0003
AL-1-35	12.4787	4.6973	0.0704	0.0031	0.0054	0.2416	0.0190	0.0009	0.0002
AL-1-36	12.8352	4.5094	0.0668	0.0030	0.0043	0.1445	0.0128	0.0008	0.0001
AL-1-37	13.1917	5.8240	0.0778	0.0040	0.0085	0.2096	0.0250	0.0013	0.0014
AL-1-38	13.5483	6.5570	0.0818	0.0045	0.0054	0.1378	0.0167	0.0004	0.0002
AL-1-39	13.9048	6.2391	0.0754	0.0037	0.0050	0.1270	0.0206	0.0003	0.0002
AL-1-40	14.2613	6.8246	0.0816	0.0036	0.0046	0.0391	0.0155	0.0011	0.0003
AL-1-41	14.6179	7.4252	0.0774	0.0031	0.0077	0.4263	0.0254	0.0012	0.0002
AL-1-42	14.9744	7.6389	0.0768	0.0032	0.0090	0.4529	0.0215	0.0013	0.0002
AL-1-43	15.3309	9.4392	0.0914	0.0044	0.0085	0.5380	0.0259	0.0014	0.0005
AL-1-44	15.6875	9.1165	0.0981	0.0041	0.0108	0.7634	0.0266	0.0014	0.0004
AL-1-45	16.0440	15.5949	0.0964	0.0029	0.0227	0.2488	0.0220	0.0016	0.0008
AL-1-46	16.4005	11.9040	0.0932	0.0025	0.0102	0.2091	0.0198	0.0014	0.0004
AL-1-47	16.7571	8.4400	0.0764	0.0032	0.0083	0.5516	0.0161	0.0013	0.0003

AL-1-48	17.1136	10.5367	0.1044	0.0037	0.0096	0.3363	0.0282	0.0015	0.0005
AL-1-49	17.4701	8.2861	0.0808	0.0035	0.0065	0.2103	0.0149	0.0013	0.0004
AL-1-50	17.8267	16.6722	0.1186	0.0044	0.0133	0.2506	0.0225	0.0017	0.0003
AL-1-51	18.1832	8.2717	0.0828	0.0034	0.0091	0.3175	0.0144	0.0013	0.0004
AL-1-52	18.5397	7.7405	0.0945	0.0048	0.0108	0.8068	0.0217	0.0010	0.0003
AL-1-53	18.8963	8.1836	0.0865	0.0037	0.0060	0.0602	0.0211	0.0009	0.0003
AL-1-54	19.2528	13.0949	0.0976	0.0023	0.0114	0.5518	0.0245	0.0012	0.0007
AL-1-55	19.6093	8.1470	0.0908	0.0040	0.0091	0.3855	0.0134	0.0010	0.0003
AL-1-56	19.9659	11.0695	0.1019	0.0048	0.0080	0.1271	0.0165	0.0009	0.0001
AL-1-57	20.3224	11.5827	0.1086	0.0052	0.0096	0.2250	0.0215	0.0012	0.0003
AL-1-58	20.6789	11.3756	0.1099	0.0049	0.0094	0.0129	0.0185	0.0012	0.0002
AL-1-59	21.0355	8.8345	0.1045	0.0041	0.0080	-0.0007	0.0385	0.0010	0.0002
AL-1-60	21.3920	8.6255	0.1038	0.0046	0.0141	1.4731	0.0277	0.0019	0.0006
AL-1-61	21.7485	13.7151	0.1183	0.0045	0.0177	0.2235	0.0337	0.0014	0.0002
AL-1-62	22.1051	12.6516	0.1107	0.0062	0.0136	0.5436	0.0249	0.0013	0.0002
AL-1-63	22.4616	10.0753	0.1055	0.0053	0.0082	0.0078	0.0321	0.0012	0.0002
AL-1-64	22.8181	9.3683	0.1128	0.0030	0.0091	0.5349	0.0320	0.0019	0.0006
AL-1-65	23.1747	8.2188	0.1133	0.0059	0.0178	0.7086	0.0305	0.0015	0.0002
AL-1-66	23.5312	9.0329	0.1086	0.0050	0.0197	0.7215	0.0275	0.0013	0.0011
AL-1-67	23.8877	8.4492	0.1082	0.0044	0.0084	0.4852	0.0324	0.0012	0.0003
AL-1-68	24.2443	12.5132	0.1139	0.0058	0.0130	0.6893	0.0374	0.0015	0.0004
AL-1-69	24.6008	9.0761	0.1026	0.0048	0.0119	0.5569	0.0262	0.0017	0.0003
AL-1-70	24.9573	8.8214	0.1058	0.0053	0.0094	0.3586	0.0317	0.0011	0.0003
AL-1-71	25.3139	10.2056	0.1073	0.0050	0.0107	0.5926	0.0194	0.0013	0.0004
AL-1-72	25.6704	7.1545	0.0857	0.0038	0.0086	0.4305	0.0249	0.0010	0.0004
AL-1-73	26.0269	9.2772	0.0990	0.0044	0.0096	0.4758	0.0354	0.0012	0.0003
AL-1-74	26.3835	7.6493	0.0933	0.0042	0.0074	0.2871	0.0349	0.0011	0.0002
AL-1-75	26.7400	7.7089	0.1002	0.0043	0.0125	1.0403	0.0302	0.0016	0.0011
AL-1-76	27.0965	6.6139	0.0865	0.0040	0.0072	0.4183	0.0254	0.0010	0.0004
AL-1-77	27.4531	6.9402	0.0917	0.0042	0.0066	0.4415	0.0290	0.0010	0.0006

AL-1-78	27.8096	7.1515	0.1038	0.0058	0.0100	0.8907	0.0253	0.0011	0.0004
AL-1-79	28.1661	7.2269	0.0986	0.0049	0.0053	0.1718	0.0246	0.0008	0.0003
AL-1-80	28.5227	6.6054	0.0967	0.0039	0.0083	0.5927	0.0220	0.0012	0.0023
AL-1-81	28.8792	9.0581	0.0944	0.0045	0.0099	0.4323	0.0292	0.0011	0.0005
AL-1-82	29.2357	7.8587	0.1006	0.0043	0.0115	0.8915	0.0318	0.0016	0.0005
AL-1-83	29.5923	7.5745	0.0931	0.0042	0.0073	0.3502	0.0345	0.0013	0.0003
AL-1-84	29.9488	8.9072	0.0958	0.0044	0.0090	0.2617	0.0301	0.0014	0.0003
AL-1-85	30.3053	7.8431	0.0924	0.0036	0.0075	0.4311	0.0263	0.0012	0.0005
AL-1-86	30.6619	7.3824	0.0960	0.0042	0.0105	0.7865	0.0256	0.0058	0.0004
AL-1-87	31.0184	6.4302	0.0968	0.0040	0.0058	0.5218	0.0292	0.0012	0.0007
AL-1-88	31.3749	6.4739	0.0866	0.0032	0.0068	0.2241	0.0257	0.0011	0.0006
AL-1-89	31.7315	6.5991	0.0897	0.0036	0.0086	0.4715	0.0197	0.0012	0.0005
AL-1-90	32.0880	7.6352	0.0949	0.0043	0.0086	0.4989	0.0228	0.0010	0.0006
AL-1-91	32.4445	8.3146	0.0854	0.0047	0.0092	0.5874	0.0156	0.0011	0.0006
AL-1-92	32.8011	6.7714	0.0868	0.0037	0.0046	0.0433	0.0224	0.0008	0.0002
AL-1-93	33.1576	4.9914	0.0819	0.0034	0.0045	0.2271	0.0231	0.0012	0.0004
AL-1-94	33.5141	5.2982	0.0838	0.0034	0.0049	0.2629	0.0234	0.0010	0.0004
AL-1-95	33.8707	5.2897	0.0872	0.0038	0.0046	0.1789	0.0247	0.0006	0.0002
AL-1-96	34.2272	5.7606	0.0900	0.0036	0.0081	0.2306	0.0244	0.0009	0.0005
AL-1-97	34.5837	6.9188	0.1064	0.0048	0.0063	0.1202	0.0301	0.0007	0.0003
AL-1-98	34.9403	5.9090	0.0913	0.0043	0.0119	0.3156	0.0228	0.0008	0.0005
AL-1-99	35.2968	6.4311	0.1091	0.0057	0.0061	0.2170	0.0281	0.0008	0.0003
AL-1-100	35.6533	5.5815	0.0900	0.0041	0.0093	0.2262	0.0225	0.0010	0.0004

Table D.4 Chemical Indices for AL-1

CHEMICAL INDICES FOR AL-1										
Sample ID	Height (ft)	Mo/Al	U/Al	Mo/Al	U/Al (ICP MS)	EF Ni	EF Cu	EF U	EF Mo	EF Mo	EF U (ICP MS)

			(ICP MS)						(ICP MS)	
AL-1-1	0.3565	0.0056	0.0010	0.0000	0.0000	6.8444	3.7609	29.5237	297.6522	0.0000	0.0000
AL-1-2	0.7131	0.0032	0.0018	0.0000	0.0000	5.9411	2.6069	51.7952	173.0636	0.0000	0.0000
AL-1-3	1.0696	0.0030	0.0008	0.0000	0.0000	4.2594	1.1233	23.6933	161.7656	0.0000	0.0000
AL-1-4	1.4261	0.0034	0.0008	0.0000	0.0000	4.6782	1.0575	21.6211	180.7710	0.0000	0.0000
AL-1-5	1.7827	0.0026	0.0011	0.0000	0.0000	7.3959	4.2527	31.6031	138.3215	0.0000	0.0000
AL-1-6	2.1392	0.0024	0.0009	0.0000	0.0000	5.5115	2.0979	26.5912	128.9860	0.0000	0.0000
AL-1-7	2.4957	0.0015	0.0007	0.0000	0.0000	4.6339	3.5361	20.0958	82.2507	0.0000	0.0000
AL-1-8	2.8523	0.0035	0.0010	0.0000	0.0000	6.0808	2.7252	29.2615	187.2400	0.0000	0.0000
AL-1-9	3.2088	0.0032	0.0008	0.0000	0.0000	5.1813	1.5699	23.2904	169.9514	0.0000	0.0000
AL-1-10	3.5653	0.0009	0.0007	0.0000	0.0000	4.6951	3.4470	20.0184	46.4434	0.0000	0.0000
AL-1-11	3.9219	0.0028	0.0008	0.0016	0.0005	5.3127	2.4590	24.2966	151.1312	86.5759	13.7729
AL-1-12	4.2784	0.0005	0.0016	0.0000	0.0000	3.5818	2.8342	46.2753	28.1288	0.0000	0.0000
Al-1-13	4.6349	0.0010	0.0013	0.0000	0.0000	8.4160	4.3544	37.8311	54.1432	0.0000	0.0000
AL-1-14	4.9915	0.0024	0.0044	0.0000	0.0000	5.5434	3.0187	125.6409	129.0782	0.0000	0.0000

AL-1-15	5.3480	0.0035	0.0009	0.0000	0.0000	5.4667	1.4122	25.2766	188.2608	0.0000	0.0000
AL-1-16	5.7045	0.0040	0.0010	0.0000	0.0000	6.3875	2.9383	29.4397	215.2559	0.0000	0.0000
AL-1-17	6.0611	0.0043	0.0011	0.0000	0.0000	6.0899	0.8923	30.2955	229.7809	0.0000	0.0000
AL-1-18	6.4176	0.0042	0.0005	0.0000	0.0000	5.8129	0.8997	14.3253	226.3621	0.0000	0.0000
AL-1-19	6.7741	0.0035	0.0004	0.0000	0.0000	5.8465	0.8723	10.5965	186.6157	0.0000	0.0000
Al-1-20	7.1307	0.0030	0.0004	0.0028	0.0008	5.4921	0.8760	12.8996	158.6013	149.2705	23.3877
AL-1-21	7.4872	0.0021	0.0005	0.0000	0.0000	4.7934	0.8358	13.3453	113.0188	0.0000	0.0000
AL-1-22	7.8437	0.0020	0.0005	0.0000	0.0000	4.5354	0.9873	14.6209	106.5754	0.0000	0.0000
AL-1-23	8.2003	0.0033	0.0005	0.0000	0.0000	5.7552	0.6499	13.3721	176.6393	0.0000	0.0000
AL-1-24	8.5568	0.0022	0.0005	0.0000	0.0000	4.3079	0.9764	15.1446	118.7965	0.0000	0.0000
AL-1-25	8.9133	0.0024	0.0004	0.0000	0.0000	4.0143	0.7807	10.1138	130.1150	0.0000	0.0000
AL-1-26	9.2699	0.0020	0.0005	0.0000	0.0000	4.1324	0.7869	15.3055	107.4480	0.0000	0.0000
AL-1-27	9.6264	0.0033	0.0007	0.0000	0.0000	4.4863	0.7656	19.1862	177.8975	0.0000	0.0000
AL-1-28	9.9829	0.0027	0.0021	0.0004	0.0020	4.9319	1.0991	59.4155	145.4656	19.8494	56.6406
AL-1-29	10.3395	0.0019	0.0004	0.0000	0.0000	2.8934	0.7135	12.7561	102.4941	0.0000	0.0000

AL-1-30	10.6960	0.0035	0.0010	0.0000	0.0000	6.0484	3.6474	28.3049	187.9663	0.0000	0.0000
AL-1-31	11.0525	0.0025	0.0003	0.0000	0.0000	2.7058	0.4796	8.5700	131.8660	0.0000	0.0000
AL-1-32	11.4091	0.0046	0.0017	0.0000	0.0000	11.3160	6.6441	48.2301	244.9239	0.0000	0.0000
AL-1-33	11.7656	0.0029	0.0002	0.0000	0.0000	5.1116	1.0507	6.8978	154.1584	0.0000	0.0000
AL-1-34	12.1221	0.0044	0.0002	0.0029	0.0004	6.5038	0.8884	5.0364	238.3987	155.2444	11.9651
AL-1-35	12.4787	0.0017	0.0002	0.0000	0.0000	3.5250	0.5961	7.1267	90.4074	0.0000	0.0000
AL-1-36	12.8352	0.0009	0.0003	0.0000	0.0000	3.0331	0.4440	7.3381	47.7041	0.0000	0.0000
AL-1-37	13.1917	0.0005	0.0002	0.0000	0.0000	5.3929	4.4500	6.8650	25.1294	0.0000	0.0000
AL-1-38	13.5483	0.0007	0.0002	0.0000	0.0000	1.6912	0.5707	5.1210	37.5282	0.0000	0.0000
AL-1-39	13.9048	0.0007	0.0003	0.0000	0.0000	1.1532	0.4997	8.5239	36.3712	0.0000	0.0000
AL-1-40	14.2613	0.0024	0.0004	0.0000	0.0000	4.3350	1.0017	10.6228	129.7408	0.0000	0.0000
AL-1-41	14.6179	0.0021	0.0002	0.0000	0.0000	4.6313	0.5697	5.1652	110.3938	0.0000	0.0000
AL-1-42	14.9744	0.0028	0.0003	0.0017	0.0003	5.1439	0.6268	9.3791	151.8503	93.2984	9.5974
AL-1-43	15.3309	0.0028	0.0003	0.0000	0.0000	5.5809	1.7285	7.8619	151.3457	0.0000	0.0000
AL-1-44	15.6875	0.0034	0.0004	0.0000	0.0000	5.8321	1.1396	11.1083	180.6965	0.0000	0.0000

AL-1-45	16.0440	0.0017	0.0006	0.0000	0.0000	6.4076	2.6057	16.9356	93.1003	0.0000	0.0000
AL-1-46	16.4005	0.0012	0.0006	0.0000	0.0000	5.6860	1.1983	18.3170	63.8511	0.0000	0.0000
AL-1-47	16.7571	0.0031	0.0004	0.0000	0.0000	5.1231	0.8971	11.3372	168.2857	0.0000	0.0000
AL-1-48	17.1136	0.0022	0.0006	0.0000	0.0000	6.0212	1.7220	16.4941	117.7850	0.0000	0.0000
AL-1-49	17.4701	0.0030	0.0004	0.0000	0.0000	5.2331	1.2891	10.8850	160.2107	0.0000	0.0000
AL-1-50	17.8267	0.0031	0.0005	0.0000	0.0000	6.8058	0.8897	14.9176	164.6730	0.0000	0.0000
AL-1-51	18.1832	0.0020	0.0004	0.0000	0.0000	5.3354	1.1550	11.3276	108.2246	0.0000	0.0000
AL-1-52	18.5397	0.0017	0.0003	0.0000	0.0000	4.0887	0.9058	9.0951	89.2551	0.0000	0.0000
AL-1-53	18.8963	0.0001	0.0005	0.0000	0.0000	3.7479	0.9555	13.3120	6.5089	0.0000	0.0000
AL-1-54	19.2528	0.0011	0.0006	0.0000	0.0000	4.8614	2.2423	16.7927	60.3379	0.0000	0.0000
AL-1-55	19.6093	0.0019	0.0005	0.0000	0.0000	4.1272	1.1186	14.7361	101.7048	0.0000	0.0000
AL-1-56	19.9659	0.0022	0.0006	0.0000	0.0000	3.7465	0.3356	17.8275	115.7810	0.0000	0.0000
AL-1-57	20.3224	0.0027	0.0006	0.0029	0.0005	4.6304	0.8097	18.2512	142.7599	153.5370	13.0297
AL-1-58	20.6789	0.0035	0.0005	0.0000	0.0000	4.9010	0.7121	15.2413	185.4426	0.0000	0.0000
AL-1-59	21.0355	0.0016	0.0001	0.0000	0.0000	3.8926	0.5745	3.9844	86.4005	0.0000	0.0000

AL-1-60	21.3920	0.0041	0.0005	0.0000	0.0000	7.4915	1.9058	13.2242	221.7838	0.0000	0.0000
AL-1-61	21.7485	0.0028	0.0006	0.0000	0.0000	5.8049	0.5930	18.6000	149.6699	0.0000	0.0000
AL-1-62	22.1051	0.0035	0.0007	0.0000	0.0000	5.2298	0.7426	18.8875	186.7614	0.0000	0.0000
AL-1-63	22.4616	0.0032	0.0005	0.0000	0.0000	4.8595	0.7939	15.0147	170.8282	0.0000	0.0000
AL-1-64	22.8181	0.0021	0.0006	0.0008	0.0004	7.6150	1.9810	17.2505	110.4525	44.2066	11.1558
AL-1-65	23.1747	0.0033	0.0005	0.0000	0.0000	6.0331	0.6693	13.5049	176.1371	0.0000	0.0000
AL-1-66	23.5312	0.0023	0.0006	0.0000	0.0000	5.2885	3.4720	17.7804	121.3245	0.0000	0.0000
AL-1-67	23.8877	0.0028	0.0005	0.0000	0.0000	5.0145	0.9455	13.5436	152.5007	0.0000	0.0000
AL-1-68	24.2443	0.0039	0.0005	0.0000	0.0000	5.8770	1.3391	15.0000	211.1134	0.0000	0.0000
AL-1-69	24.6008	0.0054	0.0005	0.0000	0.0000	6.9125	0.8993	12.9683	289.7457	0.0000	0.0000
AL-1-70	24.9573	0.0034	0.0003	0.0000	0.0000	4.6222	0.8651	7.7944	182.0928	0.0000	0.0000
AL-1-71	25.3139	0.0020	0.0004	0.0015	0.0004	5.2876	1.3861	11.3371	106.1280	78.7542	11.1714
AL-1-72	25.6704	0.0012	0.0003	0.0000	0.0000	4.1298	1.1548	8.7628	65.8292	0.0000	0.0000
AL-1-73	26.0269	0.0022	0.0003	0.0000	0.0000	4.7651	0.9828	8.1999	117.8947	0.0000	0.0000
AL-1-74	26.3835	0.0018	0.0002	0.0000	0.0000	4.4862	0.7887	6.9771	94.4253	0.0000	0.0000

AL-1-75	26.7400	0.0032	0.0004	0.0000	0.0000	6.5875	3.4027	10.5728	173.9435	0.0000	0.0000
AL-1-76	27.0965	0.0011	0.0002	0.0000	0.0000	4.1551	1.1958	6.4464	59.5501	0.0000	0.0000
AL-1-77	27.4531	0.0007	0.0001	0.0000	0.0000	3.9855	1.7974	4.2262	36.8895	0.0000	0.0000
AL-1-78	27.8096	0.0010	0.0002	0.0000	0.0000	4.4413	1.2893	5.5794	53.1751	0.0000	0.0000
AL-1-79	28.1661	0.0017	0.0003	0.0000	0.0000	3.3886	0.8364	9.1051	90.1041	0.0000	0.0000
AL-1-80	28.5227	0.0024	0.0002	0.0000	0.0000	4.9566	7.4269	6.9191	128.9793	0.0000	0.0000
AL-1-81	28.8792	0.0023	0.0002	0.0000	0.0000	4.2977	1.4783	5.3672	125.3460	0.0000	0.0000
AL-1-82	29.2357	0.0041	0.0004	0.0000	0.0000	6.3360	1.6003	10.7972	217.6053	0.0000	0.0000
AL-1-83	29.5923	0.0034	0.0003	0.0000	0.0000	5.1702	1.0440	7.8298	184.5061	0.0000	0.0000
AL-1-84	29.9488	0.0028	0.0003	0.0000	0.0000	5.7603	0.9559	7.5722	152.4963	0.0000	0.0000
AL-1-85	30.3053	0.0024	0.0003	0.0000	0.0000	4.7570	1.4914	7.6061	126.5139	0.0000	0.0000
AL-1-86	30.6619	0.0015	0.0002	0.0007	0.0002	23.3641	1.2422	6.6936	82.7541	39.1789	6.5860
AL-1-87	31.0184	0.0013	0.0004	0.0000	0.0000	4.8886	2.1086	11.1828	71.3004	0.0000	0.0000
AL-1-88	31.3749	0.0008	0.0002	0.0000	0.0000	4.2771	1.9569	6.4055	44.0982	0.0000	0.0000
AL-1-89	31.7315	0.0010	0.0002	0.0000	0.0000	4.9197	1.5860	6.3202	55.1871	0.0000	0.0000

|										
AL-1-90	32.0880	0.0014	0.0003	0.0000	0.0000	3.9733	1.8893	7.7468	74.1928	0.0000	0.0000
AL-1-91	32.4445	0.0019	0.0003	0.0000	0.0000	4.5572	1.9782	7.7087	99.6389	0.0000	0.0000
AL-1-92	32.8011	0.0008	0.0002	0.0000	0.0000	3.3240	0.6541	5.8247	43.7226	0.0000	0.0000
AL-1-93	33.1576	0.0034	0.0003	0.0000	0.0000	4.7809	1.1615	8.5345	180.7943	0.0000	0.0000
AL-1-94	33.5141	0.0033	0.0003	0.0000	0.0000	4.1563	1.3728	8.3361	174.3437	0.0000	0.0000
AL-1-95	33.8707	0.0007	0.0002	0.0000	0.0000	2.2494	0.6378	4.7289	39.6307	0.0000	0.0000
AL-1-96	34.2272	0.0007	0.0002	0.0000	0.0000	3.5355	1.7252	5.0824	36.8787	0.0000	0.0000
AL-1-97	34.5837	0.0008	0.0002	0.0000	0.0000	2.6828	0.8119	4.3620	40.5135	0.0000	0.0000
AL-1-98	34.9403	0.0007	0.0002	0.0001	0.0003	3.1816	1.5279	4.3388	35.9593	7.9550	7.8086
AL-1-99	35.2968	0.0010	0.0002	0.0000	0.0000	3.4123	0.9332	6.0426	53.9214	0.0000	0.0000
AL-1-100	35.6533	0.0007	0.0002	0.0000	0.0000	3.9566	1.4063	4.6429	36.2046	0.0000	0.0000

Results from Tipping Point Analysis
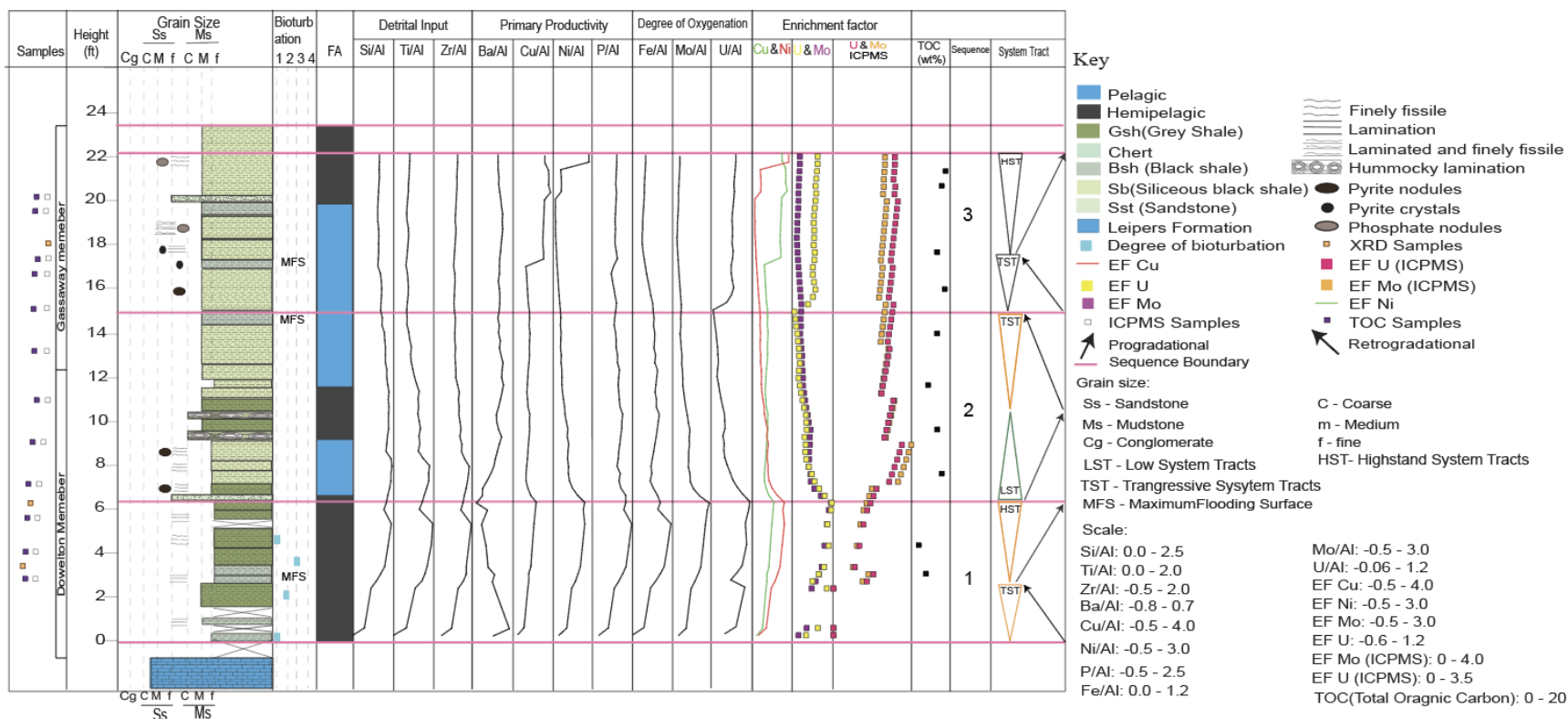
Figure D.1 Integration between facies analysis and chemostratigraphy of outcrop section at TN-1, showing the stratigraphic framework and system tracts from tipping point analysis using skewness.
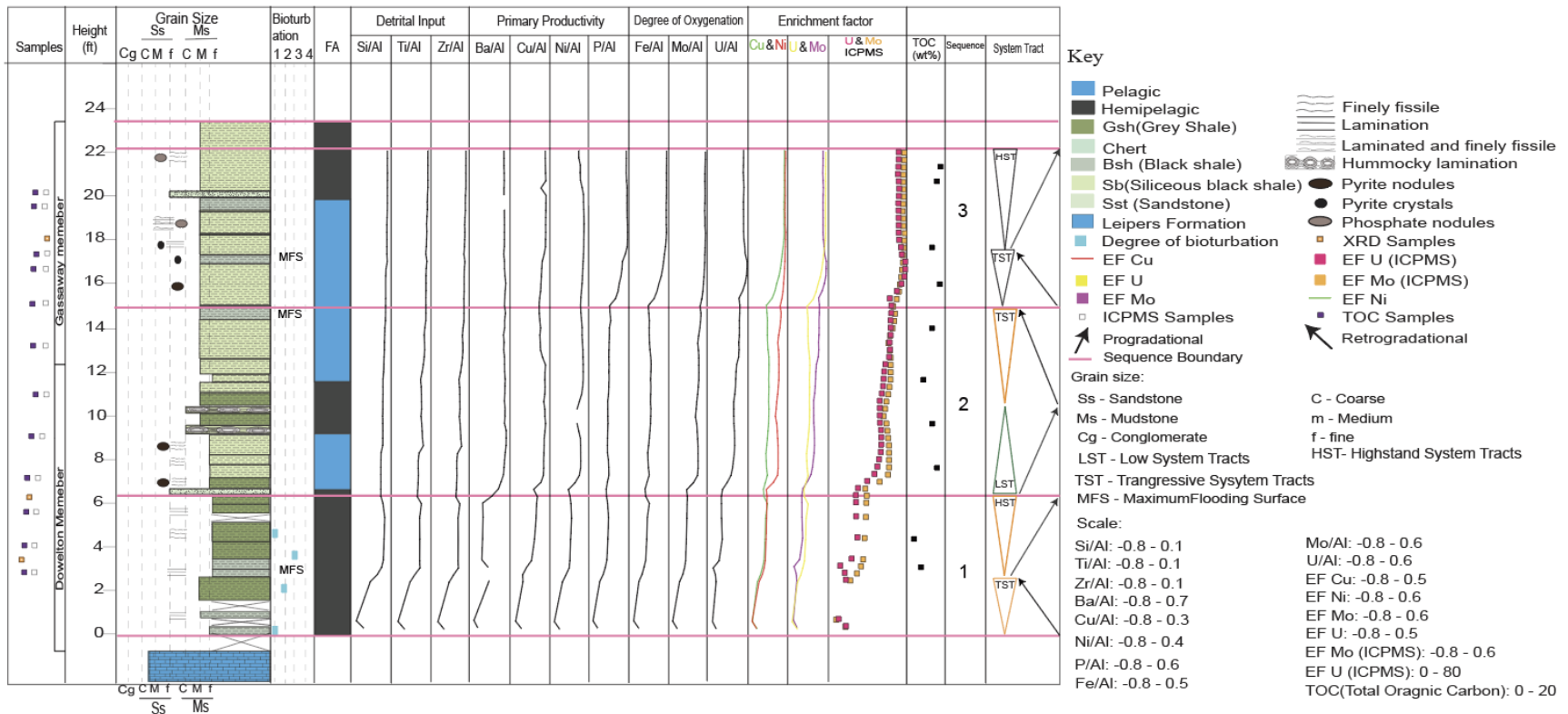
Figure D.2 Integration between facies analysis and chemostratigraphy of outcrop section at TN-1, showing the stratigraphic framework and system tracts from tipping point analysis using ACF.
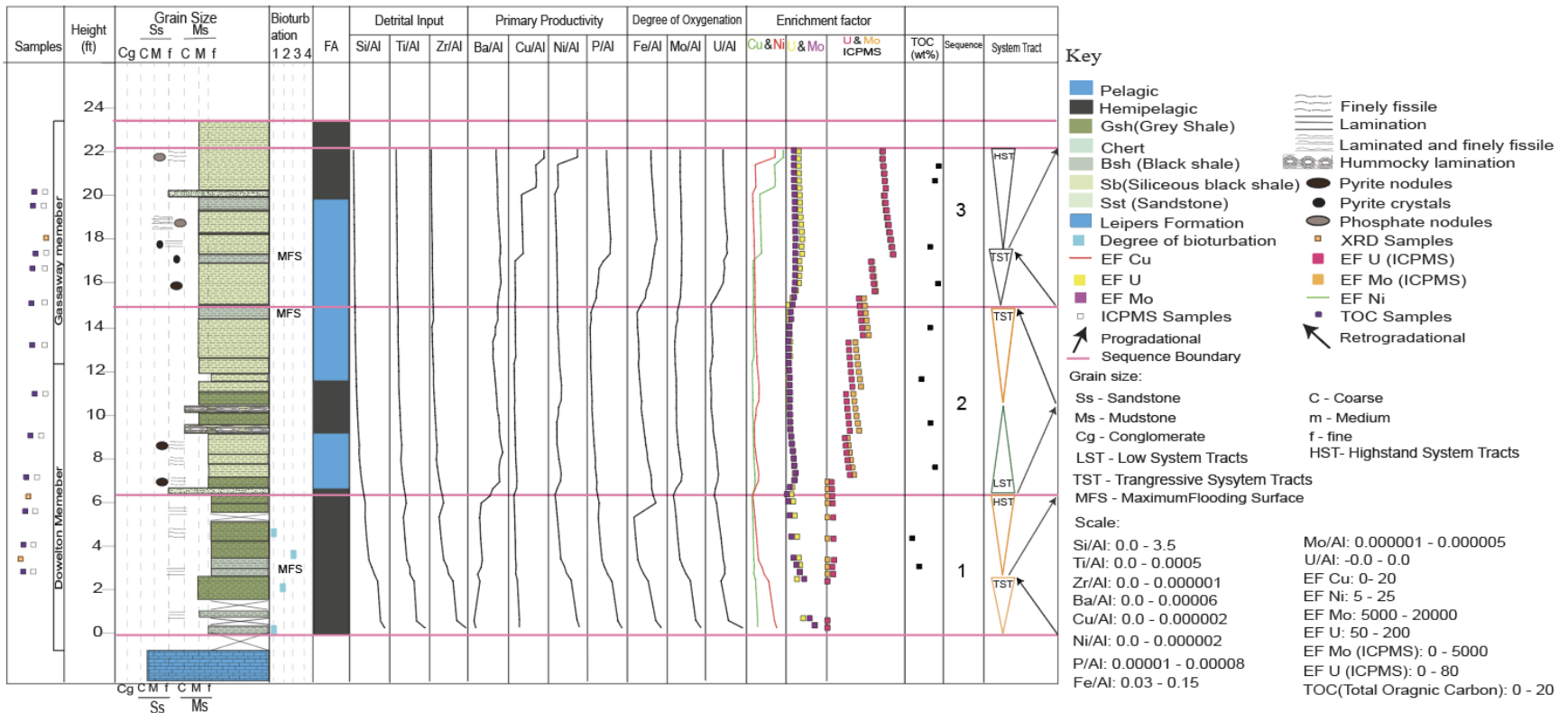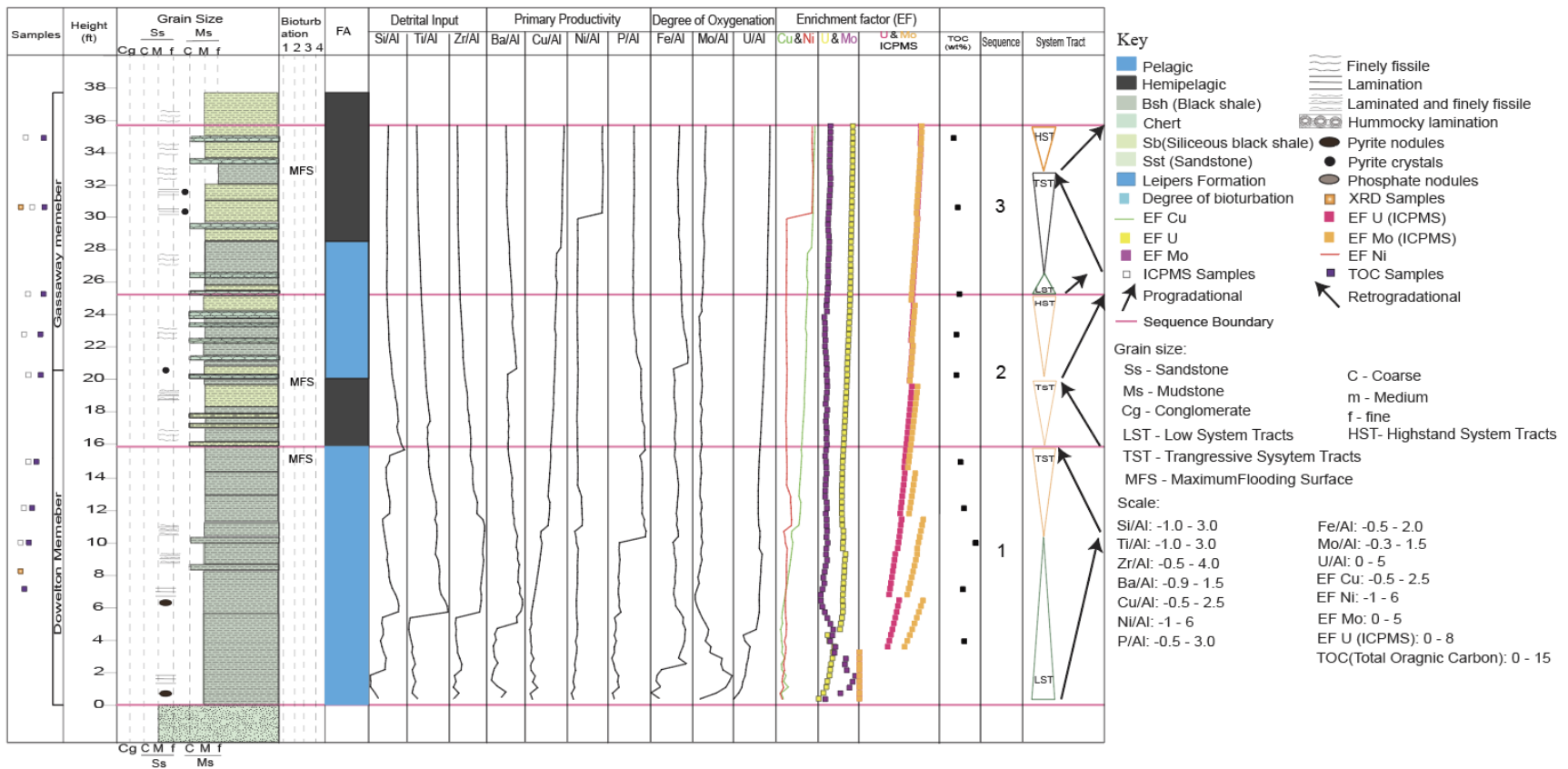
Figure D.3 Integration between facies analysis and chemostratigraphy of outcrop section at TN-1, showing the stratigraphic framework and system tracts from tipping point analysis using variance

Figure D.4 Integration between facies analysis and chemostratigraphy of outcrop section at AL-1, showing the stratigraphic framework and system tracts from tipping point analysis using skewness.
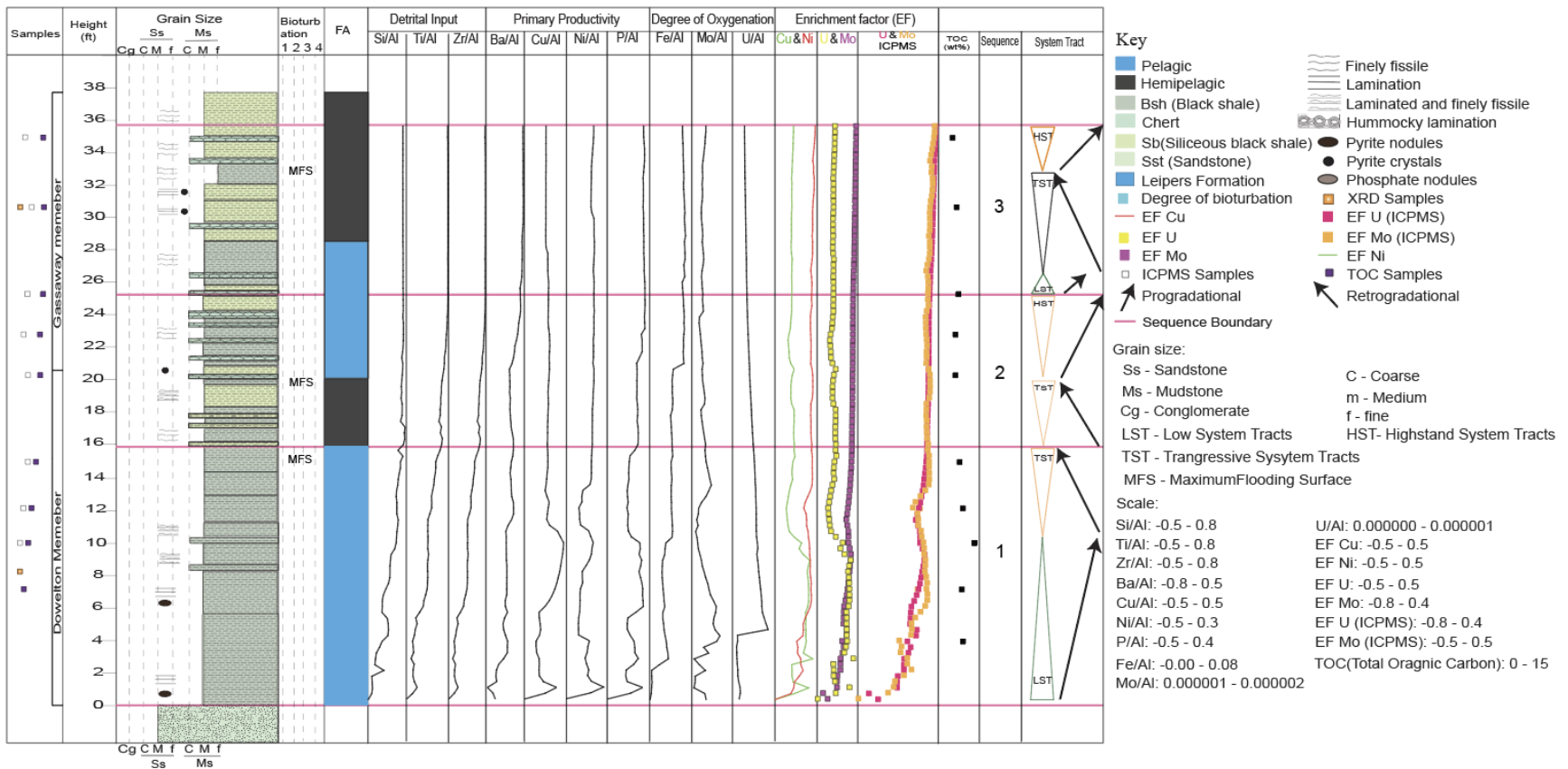
Figure D.5 Integration between facies analysis and chemostratigraphy of outcrop section at AL-1, showing the stratigraphic framework and system tracts from tipping point analysis using ACF.
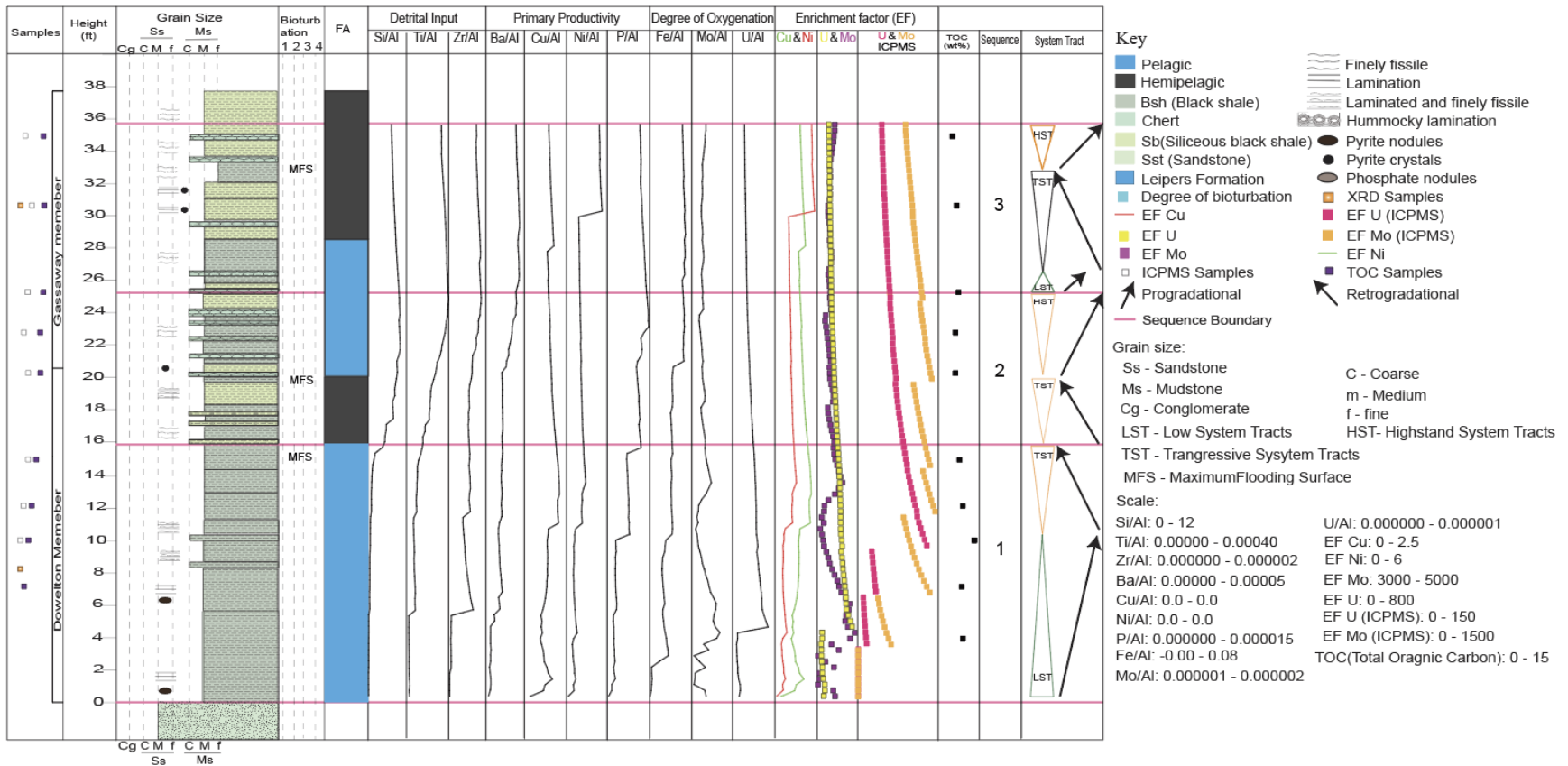
129

Figure D.6 Integration between facies analysis and chemostratigraphy of outcrop section at AL-1, showing the stratigraphic framework and system tracts from tipping point analysis using variance.

Python Script for Tipping Point Analysis

```python
import numpy as np
import pandas as pd
import seaborn as sns
import matplotlib.pyplot as plt
df = pd.read_csv("TN_Ind.csv")
detrital = df[['Depth/Height (ft)','Si/Al', 'Ti/Al', 'Zr/Al']]
from scipy.stats import skew
skewness_si = []
for i in range (57):
        sk = skew(detrital['Si/Al'][0:i+2])
        skewness_si.append(sk)
        skewness_Ti = []
for i in range (57):
        sk = skew(detrital['Ti/Al'][0:i+2])
        skewness_Ti.append(sk)
        skewness_Zr = []
for i in range (57):
        sk = skew(detrital['Zr/Al'][0:i+2])
        skewness_Zr.append(sk)
```

Repeat procedure above for primary productivity, degree of oxygenation and enrichment factor proxies.

```python
#Calculation of Auto Correlation Factor
from statsmodels.tsa.stattools import acf
from statsmodels.graphics.tsaplots import plot_acf
import numpy as np
from statsmodels.tsa.stattools import acf
from statsmodels.graphics.tsaplots import plot_acf
```

```
ACF_Si = []
for i in range (57):
        acf_result = acf(detrital['Si/Al'][0:i+2], nlags=1, fft=True)
        ACF_Si.append(acf_result)
        ACF_Ti = []
for i in range (57):
        acf_result = acf(detrital['Ti/Al'][0:i+2], nlags=1, fft=True)
        ACF_Ti.append(acf_result)
        ACF_Zr = []
for i in range (57):
        acf_result = acf(detrital['Zr/Al'][0:i+2], nlags=1, fft=True)
        ACF_Zr.append(acf_result)
        detrital['AC_Si'] = ACF_Si
        detrital['AC_Ti'] = ACF_Ti
        detrital['AC_Zr'] = ACF_Zr
```

Repeat procedure above for primary productivity, degree of oxygenation and enrichment factor proxies.

```
#Calculate of Variance
detrital = df[['Location','Depth/Height (ft)','Si/Al', 'Ti/Al', 'Zr/Al']]
variance_Si = []
for i in range (57):
        var = np.var(detrital['Si/Al'][0:i+2])
        variance_Si.append(var)
        variance_Ti = []
for i in range (57):
        var = np.var(detrital['Ti/Al'][0:i+2])
        variance_Ti.append(var)
        variance_Zr = []
for i in range (57):
        var = np.var(detrital['Zr/Al'][0:i+2])
```

variance_Zr.append(var)

    detrital['VAR_Si'] = variance_Si

    detrital['VAR_Ti'] = variance_Ti

    detrital['VAR_Zr'] = variance_Zr

    Repeat procedure above for primary productivity, degree of oxygenation and enrichment factor proxies

    Repeat the procedure for AL-1